CHARACTERIZATION OF HEAT TRANSFER IN THE SECONDARY COOLING SYSTEM OF A CONTINUOUS SLAB CASTER

by

STEPHEN GEORGE HIBBINS
B.A.Sc., The University of Toronto, 1979

A THESIS SUBMITTED IN PARTIAL FULFILLMENT OF
THE REQUIREMENTS FOR THE DEGREE OF
MASTER OF APPLIED SCIENCE

in

THE FACULTY OF GRADUATE STUDIES
Department of Metallurgical Engineering

We accept this thesis as conforming
to the required standard

THE UNIVERSITY OF BRITISH COLUMBIA
January, 1982

In presenting this thesis in partial fulfilment of the requirements for an advanced degree at the University of British Columbia, I agree that the Library shall make it freely available for reference and study. I further agree that permission for extensive copying of this thesis for scholarly purposes may be granted by the head of my department or by his or her representatives. It is understood that copying or publication of this thesis for financial gain shall not be allowed without my written permission.

Department of Metallurgical Engineering

The University of British Columbia
2075 Wesbrook Place
Vancouver, Canada
V6T 1W5

Date February 26/82

ABSTRACT

Air-purged radiation pyrometers have been installed at several locations below the mould of a continuous slab-casting machine. In each secondary cooling zone, slab surface temperatures have been measured under normal and modified water spray cooling practices.

A one-dimensional heat-transfer model of the casting process has been developed, based on the implicit finite-difference method, and used to convert the measured temperature profiles into overall heat-transfer coefficients which incorporate the effects of both the sprays and rolls. Regression equations have been determined for each secondary cooling zone which relate the overall coefficients to the spray water fluxes obtained.

The results of this study indicate that unstable film-boiling heat transfer occurs in parts of the secondary cooling system of the machine which was studied. This behaviour results in a large scatter in the spray heat-transfer coefficients and slab surface temperatures. The results also indicate that current spray cooling practices may exacerbate surface cracking problems. Modifications to the present secondary cooling system are suggested so that better control of slab surface temperatures and better slab quality will be obtained.

TABLE OF CONTENTS

LIST OF TABLES

LIST OF FIGURES

NOMENCLATURE

Symbol	Definition
a, b, n, α	constants
c_1	3.74×10^{12} W cm^2
c_2	1.41 cm K
C_p	specific heat capacity, J/g°C
CSP	casting speed, in/min (m/min otherwise)
d_n	nozzle to nozzle spacing, cm
d_s	spray nozzle distance, cm
E_λ	radiant intensity at wavelength λ, $cm^{-2}cm^{-1}$
F	spray water flowrate, gal/min (l/min if indicated)
F_c	spray water flow set point, gal/min
h	heat transfer coefficient, kW/m^2K, $kW/m^2°C$
h_{av}	average heat transfer coefficient
h_{loc}	local heat transfer coefficient
K	thermal conductivity, kW/m°C
Q	heat flux, kW/m^2 (MW/m^2 if indicated)
$\dot{q}$	rate of heat removal, kW
r^2	multiple correlation coefficient
t	time, sec
T	temperature, °C, K
T_a	ambient temparature, °C
T_{in}	slab surface temperature at zone entrance, °C
T_{out}	slab surface temperature at zone exit, °C
T_s	surface temperature, °C
T_w	spray water temperature, °C

Symbol	Definition
v	spray droplet velocity, m/s
$\dot{W}$	specific water flux, ℓ/m^2s
$\dot{W}_{av}$	average spray water flux
$\dot{W}_{loc}$	local spray water flux
x	distance, cm
ε	emmissivity
λ	wavelength of emmitted radiation, cm
σ	Stefan-Boltzmann constant, 5.6697×10^{-12} W/cm^2K^4
ρ	density, kg/m^3

ACKNOWLEDGEMENTS

I would like to sincerely thank Dr. Keith Brimacombe for his guidance and encouragement throughout the course of this project. I am indebted to Dr. Alan Cramb for the role which he played in the experimental part of this work. I would also like to extend a personal note of thanks to Alan for his friendship and influence during the time I stayed with him in Indiana. The input of Mr. N. T. Mills, Mr. W. Edgar, Mr. C. R. Jackson and Mr. A. J. Bindokas of Inland Steel Research Laboratories is gratefully acknowledged. I am also grateful for the co-operation and assistance of the technical support personnel of Inland Steel Research, and the Instrument Service and Production Departments of the Inland Steel No. 1 Slab Caster Shop.

The financial support of the Steel Company of Canada in the form of a Stelco Graduate Fellowship, and of Inland Steel Company is greatly appreciated.

Finally, I am thankful to have had the opportunity to know and associate with many of the people at Inland Steel Co. and the U. B. C. Department of Metallurgy.

Chapter 1

INTRODUCTION

The continuous casting process is now recognized as the preferred route for production of many grades of steel slabs. The rapid acceptance of the process in the past ten years has been due to the improvements in yield, energy consumption, product quality, and operating and capital costs which result from its use. The level of success which has been attained in the implementation of the process may be attributed to a considerable amount of engineering work by production, quality control, and research departments. This has resulted in reliable standard operating procedures which are now used successfully in daily operations.

The trend now in process development of continuous casting can be seen in two areas. Firstly, an increasing effort is being made to improve automation of the process. This may involve implementation of innovations such as extended sequence casting techniques or automatic metal level control. Secondly, there is a strong desire to make further quality improvements in grades currently being cast, and to increase the number of grades which can be continuously cast successfully.

The second objective can only be attained with a knowledge of how process variables affect the quality of the steel being cast. The secondary cooling system is one particular area in which certain process variables can have a significant effect on quality.

1.1 Secondary Cooling in Continuous Slab Casting

Heat removal from the strand surface in a continuous slab casting machine is accomplished in three main stages, as illustrated schematically in Figure 1. Molten steel passes first into a water cooled copper mould, in which a thin skin of solidified steel forms and subsequently contains the core of liquid metal. Upon exiting the mould, or primary cooling area, the solidifying strand passes into the secondary cooling system, or "spray chamber," in which further solidification and cooling of the strand surface is promoted by a combination of direct spraying with water, contact with supporting rolls, and radiation. Further heat removal occurs in the tertiary cooling area by a combination of radiation and contact with containment rolls.

The secondary cooling system of a slab casting machine comprises several secondary cooling "zones," the number and length of which will vary with the particular installation. The overall water flow rate to each zone is usually controlled

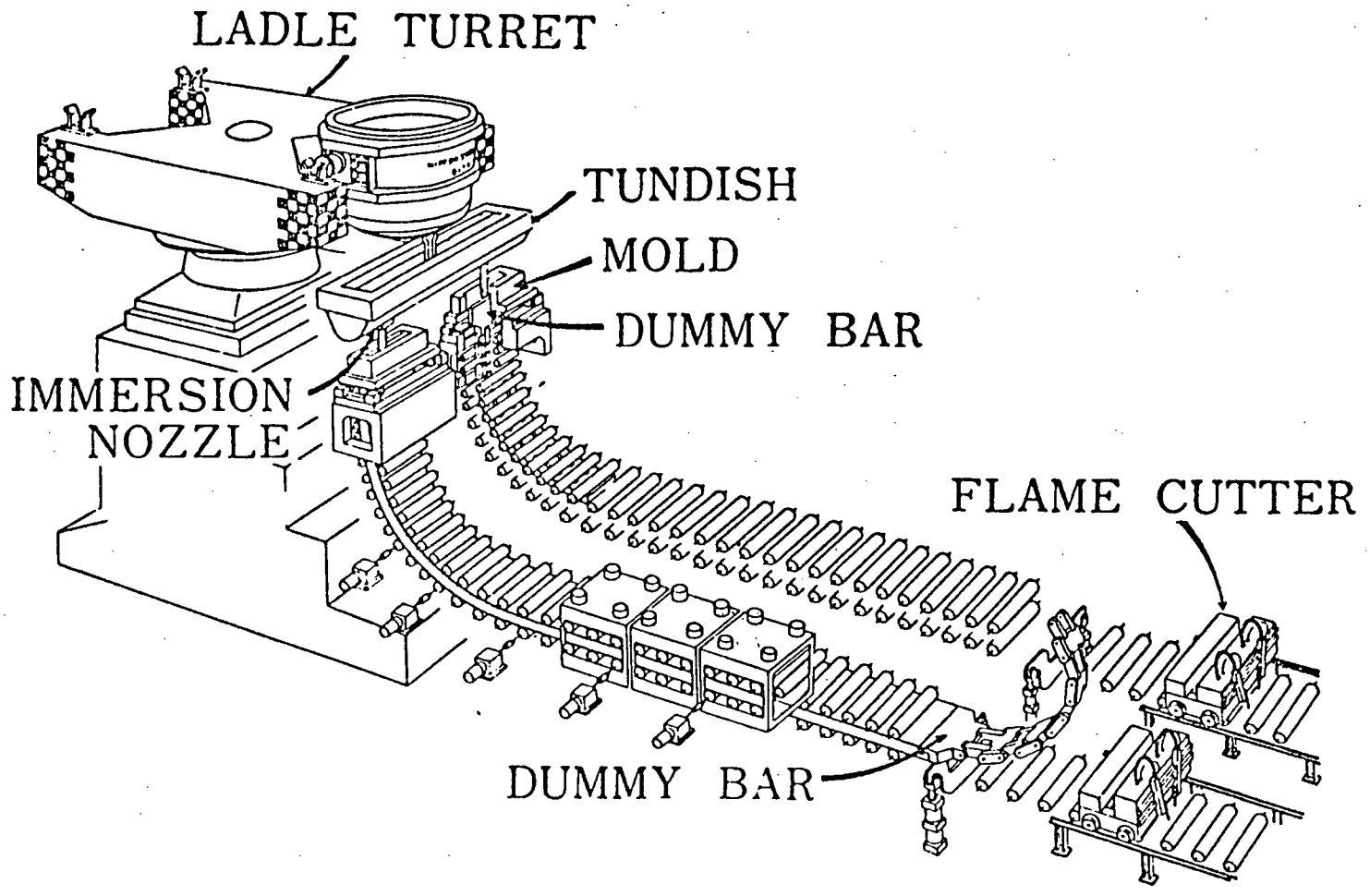

Figure 1 Schematic diagram of the main parts of a continuous slab casting machine.

as a function of casting speed, and will vary between minimum and maximum values according to a particular control equation and a "set point" which can be selected by the operator. Continuous slab casting machines usually employ square or conical spray nozzles to cool the broad and narrow faces of the slab high in the machine, but over the majority of the length of the secondary cooling system spray cooling is normally accomplished with wide angle fan spray nozzles which are directed on the broad faces only.

The spray chamber is of a modular construction, in which sets of containment rolls and the spray nozzles are attached to "segments." This facilitates removal of a particular segment which, for example, may have a broken or bent roll, and require replacement by a recently maintained module. Depending on the particular installation, and the location in the machine, the support rolls may or may not be internally cooled by flowing water.

The main functions of the secondary cooling system are to complete the solidification and cooling of the slab which began in the mould, and to ensure adequate containment of the slab by the support rolls. However, spray chamber design and operation must also take into account the relationships between secondary cooling practices and the formation of defects. In particular, crack formation in continuous casting is often

attributable to events which occur in the secondary cooling system.

1.2 Secondary Cooling and Crack Formation

Continuously-cast slabs are known to be subject to a variety of types of cracks, which are shown in Figure 2. In the broadest sense, in order for a crack to form a stress must exist at a particular location in the slab. Whether or not a crack will form will be determined by the magnitude of the stress and by the local mechanical properties of the steel at that location. Thus in order to obtain a reasonable insight into the tendency of a cast slab to crack, a knowledge and understanding of stress-inducing actions and the high temperature mechanical properties of steel must be combined.

Lankford[1] has reviewed the sources of stresses and strains in solidifying continuous-cast sections. These are:

i) mould friction forces
ii) thermal stresses
iii) ferrostatic pressure in and beneath the mould
iv) weight of the casting
v) bending forces.

In addition, other factors such as roll misalignment or mould distortion can interact with those mentioned to cause cracking.

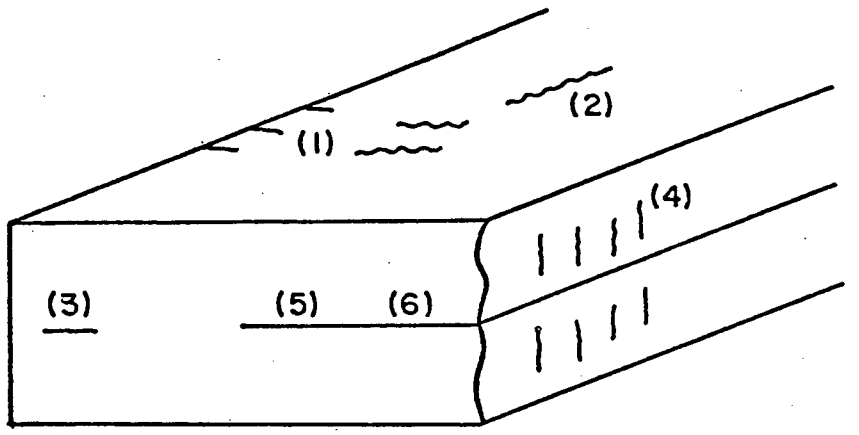

Defects in continuously cast slabs

(1) Transverse, surface

(2) Longitudinal, mid-face

(3) Triple-point

(4) Midway

(5) Centreline cracks

(6) Centreline segregation

Figure 2 Schematic drawing of slab section showing different types of defects.

Factors ii), iii), and indirectly, v), are recognized as areas in which control may be exercised in the secondary cooling system. Thermal stresses exist due to the nature of the process, in that steep temperature gradients exist through the thickness of the solidifying skin, and along the axis of the casting. Non-uniform cooling can result in surface reheating below the mould, between successive spray zones or nozzles, and cause increased local tensile stresses. The stresses are caused by differential thermal expansion when an expanding reheating region is constrained by a neighbouring colder region. Ferrostatic pressure tends to cause bulging of the broad face of the slab between rolls which causes a transverse tensile stress at the surface. Mechanical problems such as roll misalignment can aggravate this problem by causing increased bulging. Unbending of the slab at the straightening point in curved machines results in longitudinal stresses on the upper surface of the slab.

The high temperature mechanical properties of steel have been studied in several works.[1-5] It has been shown that at temperature within 40 to 70°C of the solidus temperature, steel fails in a "brittle" manner. In this region the strain to fracture is only about 0.2 to 0.3 per cent due to the presence of liquid films enriched with positively-segregated elements such as phosphorous and sulphur which separate adjacent dendrites. The studies have also shown a decrease in

ductility below about 1200 to 1250°C. The amount of decrease and temperature range over which the change occurs depends on the composition, cast structure, and previous thermal history.

Recent work[6,7] has also revealed the existence of a low ductility region in aluminum-killed and microalloyed steels at temperatures between 700 and 900°C. This is believed due to the formation of A&N at grain boundaries, but Nb and V, if present, may also form nitrides or carbides. Cracks in continuously-cast sections of these steels also have been related to the existence of a coarse-grained zone which extended a few millimetres below the surface.[8]

In several papers,[9-11] Brimacombe et al. have assessed the operating and metallurgical factors that are known to influence crack formation in light of the high-temperature mechanical properties of steel and a knowledge of the stresses generated in the solidifying shell. Those defects attributable to secondary-cooling practices in continuous slab casting have been summarized,[11] and are presented in Table I.

Table I shows that, with the exception of transverse surface cracks, all defects found in continuously-cast slabs may be caused by bulging due to ferrostatic pressure. In particular, triple-point cracks,[12,13] centreline cracks,[12,13] radial streaks,[1,15] and centreline segregation[14,16] may be

TABLE I Defects Related to Secondary Cooling Practice in Continuous Slab Casting

Defect Type	Cause	Other Factors	Corrective Action
INTERNAL DEFECTS			
Midway cracks	Bulging	High casting speed Increasing S, C.	Check roll gaps. Increase spray cooling. Reduce casting speed.
Triple-point cracks	Bulging	See Ref. 9	Regap rolls.
Centreline cracks	Bulging	High casting speed	Check roll gaps, reduce casting speed or increase spray cooling.
Centreline segregation	Bulging	High casting speed	As above.
SURFACE DEFECTS			
Transverse cracks	AlN precipitation and straightening between 700 and 900°C.	Steel composition >.02% Al, >1% Mn, Nb, V	Adjust sprays to avoid reheating from below 700°C, maintain surface outside 700-900°C range at straightener.
Longitudinal, midface cracks	Overcooling in upper spray zones. Bulging	See Ref. 9	Reduce cooling in upper spray zones. Check for bulging.

attributed to bulging. Although these defects are best controlled by proper containment of the strand, an increase in spray cooling has been reported to decrease their severity.[14,17] Spray cooling affects bulging because it alters the temperature distribution in the shell and thus the resistance of the shell to ferrostatic pressure. Recent theoretical work[18] has shown that reduction of the spray heat-transfer coefficient by about a factor of three increases bulging four-fold near the bottom of the liquid pool. However, it should be emphasized that roll pitch and roll gaps are of primary importance in controlling bulging. Within reasonable limits, the use of sprays solely to limit bulging is an indication of defects in the machine design or poor maintenance.[11] The sprays provide an important degree of freedom in the prevention of defects such as transverse cracks and this is lost if the sprays must be tied to bulging control. Thus both aspects must be kept in mind because inadequate spray cooling can result in excessive bulging which can accelerate wear of rolls and bearings and thus cause maintenance difficulties.

Events in the secondary cooling system are not the major cause of longitudinal, mid-face cracks, but spraying conditions in the upper spray zones are known to exacerbate the cracking problem. Brimacombe et al.[10] have postulated that longitudinal, mid-face cracks form when tensile strains in

the solid shell, resulting from rapid surface cooling or inadequate end-plate taper in the mould, concentrate in local regions of high temperature near the meniscus or at the level of nozzle-stream impingement on the broad face. This results in the formation of subsurface cracks close to the solidification front. These subsurface cracks may break through to the surface in the mould or upper sprays if the tensile strains are sufficiently high. Overcooling in the upper spray regions can give rise to excessive tensile stresses at the slab surface owing to its larger themal contraction relative to interior regions of the shell which are cooling less rapidly. Undercooling results in a hotter, and weaker, shell that is less able to withstand the bulging effect due to the ferrostatic pressure, and again large tensile stresses are generated at the slab surface. Steels in the 0.1 percent C range appear to be particularly susceptible to longitudinal, mid-face cracks.[9]

The low-ductility region in microalloyed steels, which has been mentioned, can result in transverse cracks on the surface if improper spray practice is employed.[6,7,8,17] The cracks appear in slabs containing >0.02% Aℓ, >1.0% Mn or Nb and V, and are often near the corners in oscillation marks on the upper face. The formation of these cracks has been attributed to axial tension on the upper broad face when unbending occurs with the surface temperature in the low-ductility range,

700 to 900°C. A&N precipitation has been found to be enhanced by cooling-reheating cycles in the same temperature range.[6] The approach to avoiding this kind of transverse-cracking problem has been to ensure that the slab surface temperature is either above[7] or below[17,19] the low-ductility range during unbending. Schmidt and Joseffson[8] found that increased spray cooling reduced the problem, but attributed their success to the formation of fine-grained austenite at the slab surface. Nozaki et al.[6] found that their "plateau" cooling pattern, which employed a lower cooling rate in the upper part of the machine, was effective in reducing longitudinal midface cracks, in addition to minimizing transverse cracking.

1.3 Design and Control of Secondary Cooling

From the preceding discussion, it is apparent that the design of the secondary cooling system is an important consideration for the continuous casting of products containing a minimum of defects. The objective of high slab quality is preferably achieved without compromising productivity or ease of operation. The proper design and operation of a secondary cooling system is essentially a problem of choosing and implementing the desired spray design and maintaining mechanical tolerances of roll gap and roll pitch. At the same time, the effects of casting speed and section size must be taken into consideration.

Brimacombe[20] has provided an example of spray-chamber design for a continuous billet caster. The design technique has been summarized,[11] and consists of the following steps:

i) Determination of the strand surface temperature distribution, or cooling rate, that minimizes the formation of a given defect.

ii) Based on the thermal requirements of i), calculation of the heat-transfer-coefficient distribution required in the secondary cooling system. This is usually accomplished with the aid of a heat-flow computer model of the continuous casting process.

iii) Determination of the optimum spray configuration and water flux based on empirical relationships.

Once mechanical tolerances for the machine have been specified, steady-state spray practices may be designed which reasonably approximate those desired. Examples of attainment of desired cooling rates have been given in the previous section, for the case of prevention of transverse surface cracks. An illustration of one of these practices is shown in Figure 3.[17]

Although the design procedures outlined above are based on the assumption of steady-state operation of the continuous casting machine, development of appropriate control models allows the same principles to be applied to unsteady-state

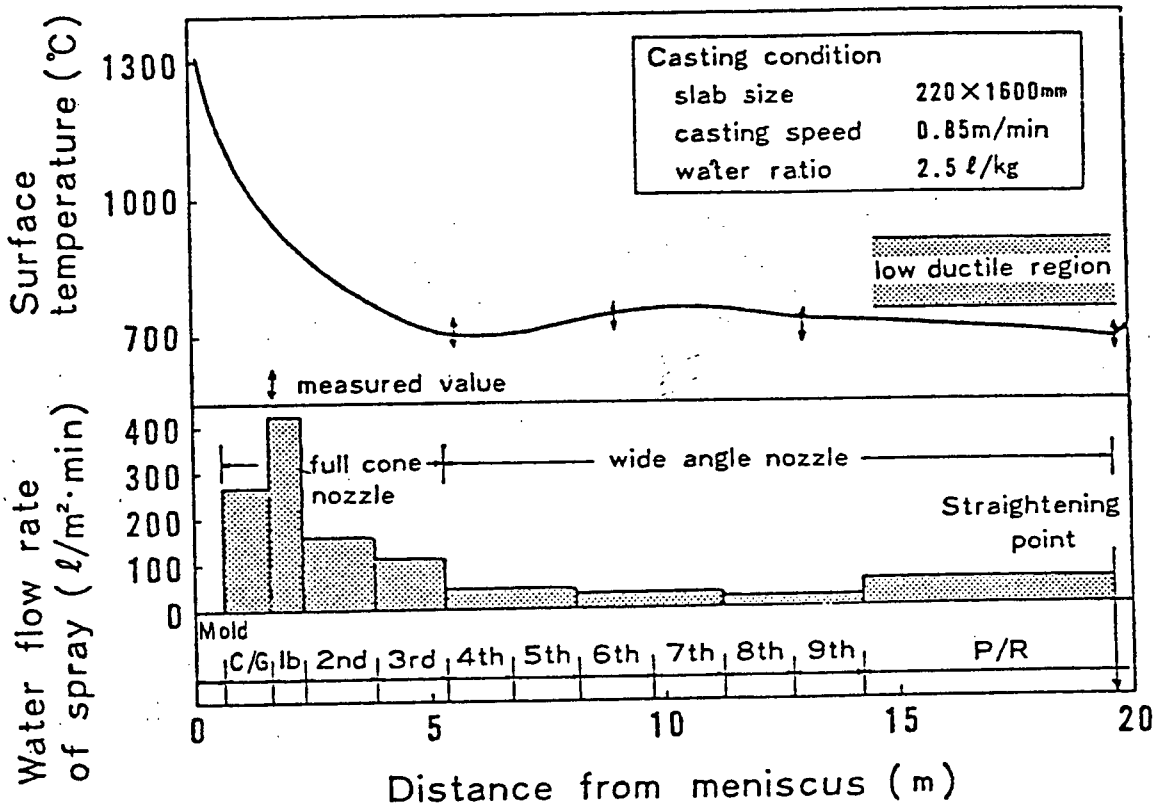

Figure 3 An example of secondary cooling system design for the avoidance of transverse, surface cracks. From Ichikawa et. al.[17]

situations. In a high-productivity operation, normal incidents such as start of cast, ladle or tundish charge, end of cast, or nozzle blockage make variations in casting speed unavoidable. If the desired temperature profile is related to time below the meniscus, rather than distance, it should, in theory, be possible to provide homogenous cooling of the strand regardless of process transients. Control models which have been developed in this regard[21-23] indicate that spray cooling should be altered, not in proportion to the casting speed, but according to the time that a given slice of steel has spent in the machine prior to reaching a given location. Thus if the desired relationship between spray heat-transfer coefficient and time is specified, calculation of the age, or residence time of a slice passing a particular point will define the desired spray water flux at that location. Baptista[23] has determined spray adjustments to be made to a slab caster during transients caused by casting speed changes, based on such residence time calculations.

With the application of such models, automatic control systems may be developed. Several publications[21,22,24,25] describe implementation of these systems, and the resulting uniformity of temperature profiles and improvements in product quality. Control is performed by a process control computer which monitors operating conditions and automatically controls water flows in the secondary cooling system in

response to changes in the operating conditions. In practice this usually requires on-line surface-temperature monitoring in order to adjust for any deviations from the temperature profiles predicted by a heat-transfer model.[24,25,26]

1.4 Scope of the Present Work

From the preceding sections it is clear that the ability to design and control the secondary cooling system of a continuous slab caster is useful, if not essential, for the production of steel slabs of high quality. Though such action may be accomplished through logical application of fundamental scientific principles, the usefulness of any design work is limited by a lack of knowledge of the real behaviour of the secondary cooling system under operating conditions. Of particular concern is the relationship between the spray heat-transfer coefficients obtained in the operating system and the spray/casting variables. As shall be shown in the next chapter, there has been a considerable amount of laboratory work done in an effort to characterize the behaviour of spray cooling systems. This work is necessarily idealized, and though useful as an aid in design and understanding of spray cooling systems, is limited in its range of applicability to industrial systems where there are combined spray and roll-contact cooling mechanisms. The amount of industrial test work which has been performed is limited, and only has been

applicable to the particular operation on which the measurements have been made.

It was therefore the objective of this work to determine empirical relationships for, and an understanding of, the heat transfer occurring in the secondary cooling system of an operating continuous slab casting machine. The experimental part of this work has involved measurement of slab surface temperatures with optical pyrometers. This work was carried out, under standard and modified operating conditions, at the No. 1 Slab Caster of Inland Steel Co.'s Indiana Harbor Works. A heat-flow mathematical model was used to convert the measured temperature profiles into average heat-transfer coefficients, incorporating the effects of both sprays and rolls, for the secondary cooling zones. These coefficients have been related to the spray and casting variables, which were also monitored.

Chapter 2

LITERATURE REVIEW

Because a significant amount of the heat removed in the secondary cooling system is by spray cooling of the slab surface, and because control of the sprays is the primary means of surface-temperature control in an operating slab caster, it is important to have an understanding of possible heat-transfer mechanisms in the spray chamber. Heat transfer occurs with boiling, of course, in this situation, and it is therefore useful to know about fundamental boiling phenomena and the complications that can result during spray cooling by multiple nozzles under continuous-casting conditions. It is in this context that a review is now given of boiling heat-transfer phenomena and laboratory studies of spray heat extraction. In addition, a survey of previous industrial studies of the heat transfer in the secondary cooling systems of continuous casting machines is included.

2.1 Fundamentals of Boiling Heat Transfer

Though boiling heat transfer is complex, considerable progress has been made in recent years in gaining a physical understanding of the boiling mechanism from experimental

observations. These experiments are usually performed under simplistic conditions in which a heated flat plate or wire is submerged in a stagnant pool of water. Depending on the temperature of the heated surface, various boiling phenomena may result which influence the heat transfer from the solid to the water. In the case of a surface of increasing temperature, the heat flux may be expected to change with surface temperature as shown in Figure 4.[27] At low temperatures, as long as the temperature of the surface does not exceed the boiling point of the liquid by more than a few degrees, heat is transferred to the adjacent liquid by free convection. The convection currents circulate the superheated liquid, and evaporation takes place at the free surface of the liquid.

As the temperature of the surface increases, vapour bubbles are formed at various nucleation sites on the surface. The bubbles become larger and more numerous as the temperature is raised further, until they finally rise to the free surface. In these regimes (regions 2 and 3 in Figure 4), the heat flux increases rapidly with increasing surface temperature. The process in these two regimes is called "nucleate boiling." Intense convection currents are set up in this region due to the motion of the vapour bubbles which is responsible for the increase in heat flux. In region 3, the bubbles begin to coalesce and evaporation becomes more important. A maximum

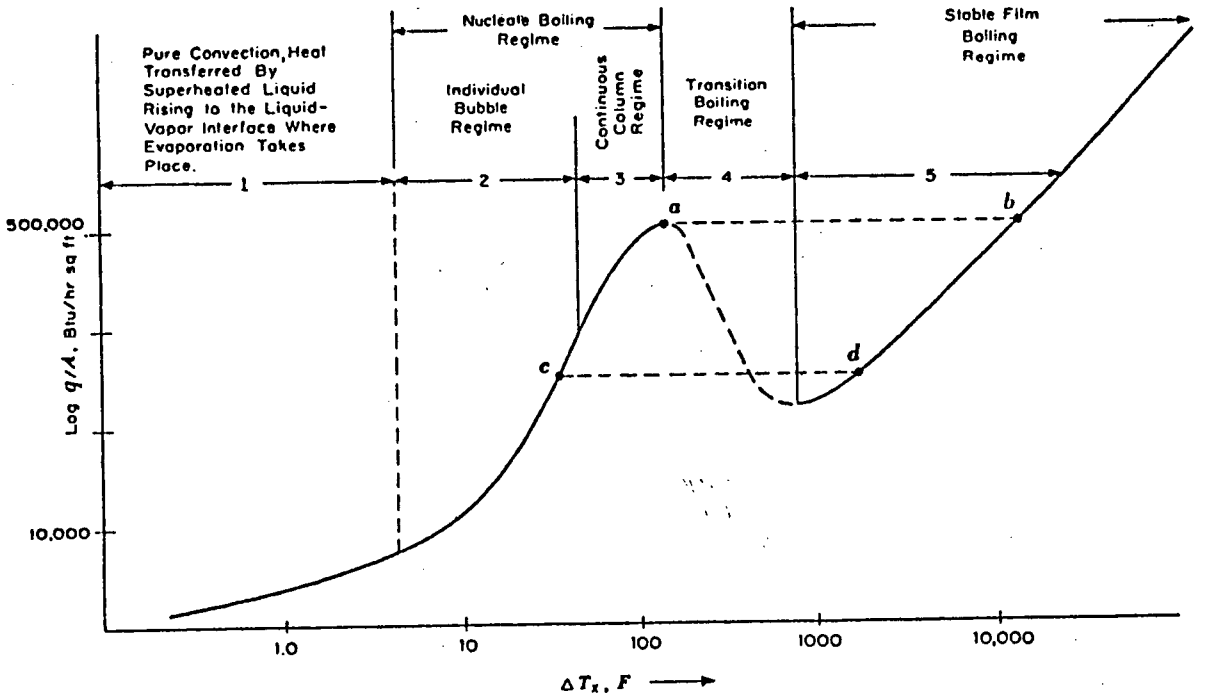

Figure 4 Typical boiling curves for a wire, tube, or horizontal surface in a pool of water at atmospheric pressure. From Kreith.[27]

heat flux then is approached because the space between rising bubble columns is too small to accommodate the streams of liquid which must move towards the hot surface to replace the evaporated liquid.

A further increase in surface temperature beyond this point leads ultimately to the formation of a continuous vapour film between the hot surface and liquid. Because the rate of heat removal is limited then by conduction through the vapour film, the surface heat flux decreases rapidly. In the case of an element to which a constant energy is supplied, a rapid increase of temperature results, which can lead to "burnout," or melting of the element. If temperature is controlled, a transition region is entered in which nucleate and stable film boiling can occur alternately at a given location on the heater surface. The temperature above which stable film boiling occurs is known as the "Leidenfrost point," and is also referred to as the "critical point" in the heat-transfer literature. The heat flux at higher temperatures increases due to the increased importance of radiation heat transfer.

The above discussion, though useful in gaining a physical understanding of heat-transfer mechanisms, is limited in its range of applicability, particularly to situations involving impingement of water droplets such as in continuous casting.

In the next section it shall be seen that the Leidenfrost temperature is much higher for the case of water droplets impinging on a plate than for the case illustrated in Figure 4. Of critical importance is the answer to the question: "Under what conditions is the Leidenfrost phenomenon stable?" Bell[28] has noted that this question quickly reduces to a discussion of how the Leidenfrost point was determined. Though most workers agree that film boiling becomes increasingly stable relative to nucleate and mixed modes at increasing surface temperatures, very little agreement exists between various workers on the true value of the Leidenfrost point for any given set of conditions. The existence of a thermal resistance, for example, such as an oxide film on the metal surface, has been shown to be capable of causing stable film boiling to break down to the transition regime.[29] The peak heat fluxes attainable in the transition regime have also been shown to be markedly affected by surface conditions such as can be caused by oxidation. For example, it has been found that the peak heat flux attainable in nucleate boiling can be altered by 100 per cent, depending on the surface structure of the heater.[30] Despite the lack of real understanding of how these effects are influencing a particular experiment, the Leidenfrost temperature must be kept in mind in analyzing a given set of results.

2.2 Heat Transfer to Water Droplets Impinging on Hot Surfaces

In order to gain a physical understanding of spray cooling, early work was undertaken to observe the behaviour of individual drops both impinging and resting on hot surfaces.

The objectives of the studies of sessile droplets were to model the rates of evaporation and heat transfer to droplets resting on a hot surface.[31,32,33] The results of Wachters et al.[31] showed that the bottom of the droplets assumed a flat shape parallel to the surface. Moriyama[33] was able to predict heat-transfer rates to single sessile droplets, and attempted to extrapolate the model to the case of impinging sprays. However the assumptions which were necessary in such an extrapolation were not an accurate representation of real physical behaviour in impinging-spray systems in which droplets interact.

Wachters and his coworkers[34,35] extended their work to the case of impinging droplets, but found that their models based on rates of heat transfer to sessile droplets[31] could not predict the rate of cooling obtained for the impinging case. This was attributed to two factors:

i) The drop stays in the vicinity of the hot surface for a relatively short time before rebounding.

ii) The models of the previous work assumed that the droplets were of a spheroidal shape. For the

case of impinging droplets at the temperatures studied (up to 400°C) the spheroidal state was not obtained.

The heat transfer due to the impact of a single drop has also been studied by several other workers. McGinnis and Holman[36] found that the efficiency of cooling is affected by the angle of impingement of the drop, but pointed out that the effects of droplet interaction, and the mechanism of droplet disintegration upon impacting the surface were not understood. Photographic studies by Pederson[37] in the second regard pointed to the existence of three heat-transfer regimes during impact, which were labelled as "wetting," "transition," and "non-wetting." These regimes are thought to correspond to the nucleate boiling, transition, and film boiling regions, respectively, which were discussed previously. In the regime termed "wetting," the drops spread out and contact the hot surface, and evaporation takes place mainly by nucleate boiling within the drop. In the "nonwetting" state, the droplets spread out and vaporize suddenly upon striking the surface, and then break up into smaller droplets which rebound. Lower rates of heat transfer were found in this regime, and the rate increased when the speed of impact of the drops increased. Toda[38] has attempted to model the heat transfer which occurs during impingement and vaporization of an impinging drop in the non-wetting regime. The schematic process sequence is illustrated in Figure 5.[39]

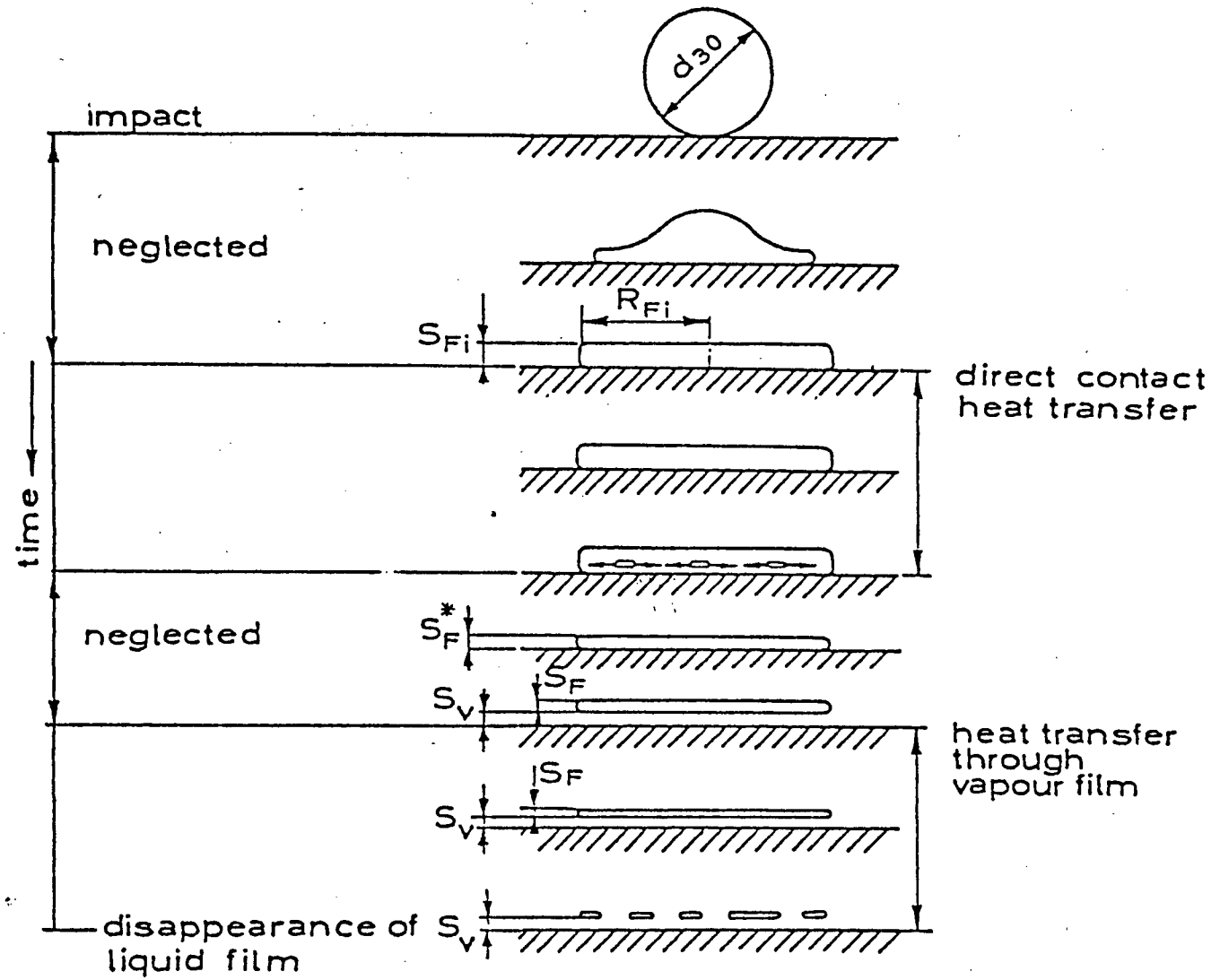

Figure 5 Schematic representation of droplet behaviour upon impinging a hot metal surface in the non-wetting regime.[38,39]

The complexity of the heat-transfer process involved in spray cooling is now apparent. The process of heat transfer to even single droplets impacting a hot surface involves boiling heat transfer coupled with the dynamics of the droplets. Boiling heat transfer under simpler conditions is still not completely understood, and when the additional complication of droplet dynamics is added the problem becomes intractable. In this light, attempts to characterize the behaviour of real spray systems based on the idealized models presented thus far would seem unrealistic. Accordingly, the majority of work reported has been empirical.

2.3 Laboratory Studies of Spray Cooling

There has been a large number of investigations carried out on the spray cooling of hot surfaces,[40-59] and a wide range of results has been obtained. Often the results of different investigations are conflicting, and a lack of information regarding the experimental conditions makes meaningful comparisons impossible. There are many experimental factors that can influence the results of a particular series of experiments, which may be enumerated as follows:

i) The general type of spray cooling experiment, i.e. transient or steady-state.

ii) The means of determining surface temperature, i.e. pyrometer measurements or calculated from results of an imbedded thermocouple.

iii) The initial temperature of the sprayed surface.

iv) The type of material and surface condition of the sprayed surface.

v) The orientation of the sprayed surface with respect to the spraying nozzle, and to the horizontal plane.

vi) The surface area of the sprayed surface, and whether heat-transfer results are correlated to water fluxes averaged over the sprayed area, or to peak values of water flux.

vii) The type of spray nozzle and its distance from the surface which influence the characteristics of the water spray, i.e. spray pressure, water flux, impact velocity and size of droplets.

viii) Spray water temperature.

The studies which have been performed are summarized in Tables IIa and IIb, for the case of transient and unsteady-state measurements, respectively. The results of the experimental investigations, in which relationships are given between heat-transfer coefficients and water flux, are plotted in Figure 6.

Transient measurements are carried out by allowing the surface temperature of the plate to fall as the surface is sprayed. The temperature-time profile obtained from measurements by pyrometer or imbedded thermocouple are used to determine the rate of heat extraction at the plate surface by

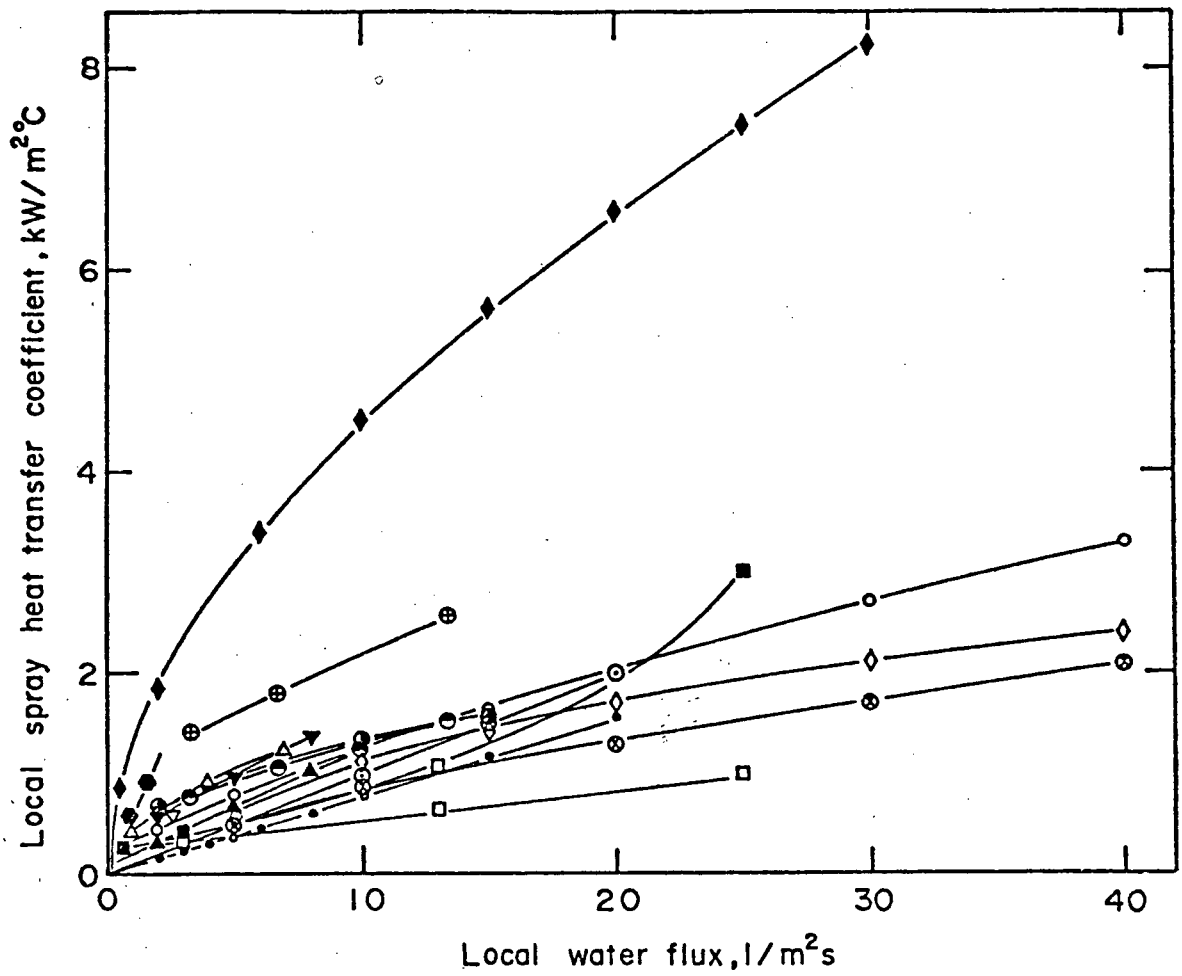

Line	Ref.	Comments
♦	45	T_w 25 C
•	49	276 kPa
⊙	49	620 kPa
▲	53	v 11 m/s
▼	53	v 32 m/s
○	61	
■	44	900 C
□	44	700 C

Line	Ref.	Comments
○	50	900 C
△	55	down
▽	55	up
◊	48	cone, 900 C
⊗	48	flat, 900C
⊖	59	900 C
⊕	59	700 C
◐	57	

Figure 6 Variation of the spray heat-transfer coefficient with water flux as reported in various laboratory studies of spray heat extraction.

TABLE IIa Summary of Studies of Heat Extraction in Sprays - Transient Measurements

Investigator & Reference No.	Nature of the Heated Surface	Direction of Spraying	Initial Temperature °C	Spray Nozzle Type	Spray Fluxes ℓ/m^2s	Comments
Gaugler[40]	Horizontal upper face of chrome plated copper cylinder heated in a furnace. Surface area 1.2 sq. cm.	Downwards	400	Full cone 1/8 GG 1 1/8 GG 3001.4	.716 to 3.7	$h = 3.695\ \dot{W}^{0.33} \pm 10\%$ Increasing droplet momentum increases h. Heat transfer to each drop decreases as $\dot{W}$ increases. Film boiling for T_s>250°C.
Corman[41]	Same as Gaugler	Downwards	900	Full cone 1/8 GGS	Up to 57	Increasing $\dot{W}$ increases h and moves critical point to higher temperatures.
Auman et al.[42]	Moving horizontal AISI stainless steel slab, furnace heated. Area 300 sq. cm.	Downwards	1100	Full cone and fan jet.	Up to 217	Increasing $\dot{W}$ increases h. Critical temp 650°C. Nucleate boiling increases h fourfold.
Lambert and Economopoulos[43]	Cylindrical nickel probes. Area 3.1 sq.cm.	Horizontal	800			Only spray pressure of 0.098 MPa reported. Results similar to that of Gaugler.
Hoogendoorn and Den Hond[44]	Horizontal AISI 321 stainless steel plate, furnace heated. Area 269 sq. cm.	Downwards	350 to 1000	Full cone	0.6 to 25	Increasing $\dot{W}$ and drop velocity increases critical temperature, to as much as 900°C Scatter ± 20%. Critical temperature unaffected when spraying horizontally, but h is slightly less.
Shimada and Mitsutsuka[45]	Horizontal low carbon steel plate, heated in a resistance furnace. Area 484 sq. cm.	Upwards and downwards simultaneously	930	Full cone	1 to 50	$h = a\dot{W}^n(1-bT_w)$ $0.65<n<0.75$ for $\dot{W}>.08\ \ell/m^2s$ n is dependent on surface temperature $0.005<b<0.008$ for $\dot{W} = 10.3\ \ell/m^2s$ h decreases as T_w increases. Critical temperature 500 - 600°C for $\dot{W} = 0.98\ \ell/m^2s$.
Mitsutsuka[46]	See Ref. 45					$h = 1.57\ \dot{W}^{0.55}(1 - 0.0075\ T_w)$
Sugitani et al.[47]	Vertical stainless steel plate heated in a resistance furnace. Surface area 500 sq. cm.	Horizontal	1000 to 1200	Full cone and flat jet	Up to 60	h is a strong function of T_s even above 700°C. Critical point about 1000°C for $\dot{W} = 6.7\ \ell/m^2s$, much above 1000°C for $\dot{W} > 20\ \ell/m^2s$.

TABLE IIa Summary of Studies of Heat Extraction in Sprays - Transient Measurements (continued)

Investigator & Reference No.	Nature of the Heated Surface	Direction of Spraying	Initial Temperature °C	Spray Nozzle Type	Spray Fluxes ℓ/m^2s	Comments
Etienne et al.[48]	Polished surface of a platinum rod, heated by a resistance wire wound around it. Surface area 0.79 sq. cm.	Downward	700 to 900	Full cone	1.5 to 50	h is a function of T_s even above 700°C. h increases as T_s decreases. Scatter increases as T_s decreases T_s has little effect below 5 ℓ/m^2s. T_s has large effect above 10 ℓ/m^2s. $Q = -87.7 + 313.5\ \dot{W}^{0.54} \pm 12\%$(900°C) $Q = -356.0 + 492.4\ \dot{W}^{0.18} \pm 17\%$(800°C) $Q = -793.4 + 492.4\ \dot{W}^{0.4} \pm 25\%$(700°C) No effect of nozzle type or distance (except when very close).
				Flat jets	1 to 15	T_s has little effect on h below 4 ℓ/m^2s. At 900°C, for $d_n = 8$ cm $Q = 182.4 + 77.2\dot{W}^{0.93} \pm 12\%$ $d_s = 11$ cm for $d_n = 20$ cm $Q = 80.0 + 218.8\dot{W}^{0.81} \pm 12\%$ $d_s = 35$ cm
Mizikar[49]	Vertical AISI 304 stainless steel plate, heated in a resistance furnace. Area 161 sq. cm.	Horizontal	1000	Full cone 1/4 GG 10 1/4 GG 6.5 3/8 GG 15	0 to 20	Critical point 560°C. Radiation included in h. Increasing spray pressure increases h for the same $\dot{W}$. No effect of impingement angle. h increases with increasing droplet momentum. $h = 0.0776\dot{W} + 0.22$ (0.276 MPa) $h = 0.1\dot{W} + 0.22$ (0.620 MPa)
Sasaki et al.[50]	18-8 stainless steel plate heated in resistance furnace.	Horizontal sprayed on both sides.	700 to 1200	Full cone and fan jet	1.67 to 41.8	Temperature measured with pyrometer. h decreases with increasing T_s. No effect of nozzle type, pressure, or distance. h decreases slightly with increasing T_w. $h = 708\ \dot{W}^{0.75}\ T_s^{-1.2} + 0.116$

TABLE IIa Summary of Studies of Heat Extraction in Sprays - Transient Measurements (continued)

Investigator & Reference No.	Nature of the Heated Surface	Direction of Spraying	Initial Temperature °C	Spray Nozzle Type	Spray Fluxes ℓ/m^2s	Comments
Bamberger et al.[51]	Nonferrous materials Ni, Ar, Cu.		Various, depending on material.		10 to 100	$h = 0.1\,\dot{W}^{0.55}\,0.07\sqrt{K\rho C_p}\,\exp\left(\frac{0.0049\,T_s}{+\,28}\right) + h_{radiation}$ Large scatter in results at low temperatures.
Prabhakar[56]	Vertical AISI 304 stainless steel, heated in gas or induction furnace. Area 5.1 sq. cm.	Horizontal	1100	Full cone and flat jet	4 to 36	Correlations of form $h = a\dot{W}^n \pm 25\%$ n = 0.23 to 0.65 depending on temperature h is surface temperature dependent for temperatures greater than 800°C, up to 1000°C. No effect of spray pressure or nozzle type. Scatter increased as temperature decreased. Unstable film boiling in all experiments. h increased by water flowing down surface

TABLE IIb Summary of Studies of Heat Extraction in Sprays - Steady-State Measurements

Investigator & Reference No.	Nature of the Heated Surface	Direction of Spraying	Initial Temperature °C	Spray Nozzle Type	Spray Fluxes ℓ/m^2s	Comments
Junk[52]	Resistance heated flattened steel pipes. Area 83 to 207 sq.cm.	Horizontal		Oval		Correlations not given. Heat flux increases with pressure of spray. Stable film boiling.
Mueller and Jeschar[53]	Resistance heated steel plates. Area 25 to 65 sq. cm.	Horizontal	700 to 1200	Full cone and flat jet	0.3 to 9	Droplet velocities 10 to 35 m/s. Scatter ± 13%. h is a function of drop velocity. $h = 0.01\ v + (0.107 + 6.8 \times 10^{-4} v)\dot{W}$ h is independent of T_s. Film boiling in studied range, unstable below 700°C. No difference between nozzle types.
Bolle and Moreau[54,55]	Resistance heated flat AISI 300 stainless steel plate. Area 128 sq. cm.	Downwards	500 to 1000	Fan	1 to 7	$h = 0.423\ \dot{W}^{0.556}$ ± 17% $627 < T_s < 927$°C
		Upwards	As above		0.8 to 2.5	$h = 0.360\ \dot{W}^{0.556}$ $727 < T_s < 1027$°C 15% less than spraying downward.
Urbanovich[58]	Specimen heated in moist air in furnace.	Plate at 45% to horizontal, spraying at 90° to plate	Up to 1200	Flat jet		12% error in h. h dependent on spray distribution in impact area. h increases as spray angle decreases. h decreases with increasing distance from specimen.

solution of the applicable heat-conduction equation. Steady-state measurements are carried out by supplying a hot metal sample with an energy input equivalent to that extracted from the sample by the impinging spray. The measured value for the energy input and the sample temperature allow the calculation of surface heat fluxes and the heat-transfer coefficients.

Because details of experiments are not always given, it is difficult to evaluate directly the effect of each factor on the results reported. All workers agree that increasing the droplet momentum in the spray, either by increasing the droplet size or velocity, increases the heat-transfer coefficient. They are also in agreement that at constant droplet size and velocity, increasing the water flux to the surface increases the heat-transfer coefficient. The heat-transfer coefficient depends on the water flux raised to a power n where n has been found to be between 0.2 and 1.0. Other factors that have been reported to influence the spray heat-transfer coefficient are the spray water temperature and the temperature of the sprayed surface.

Mitsutsuka et al.[45,46] and Sasaki[50] are the only workers to have found an effect of water temperature on the spray heat-transfer coefficients. Their results are given in Figure 7, which shows that Mitsutsuka reports a strong dependence on the water temperature while the dependence reported by Sasaki is

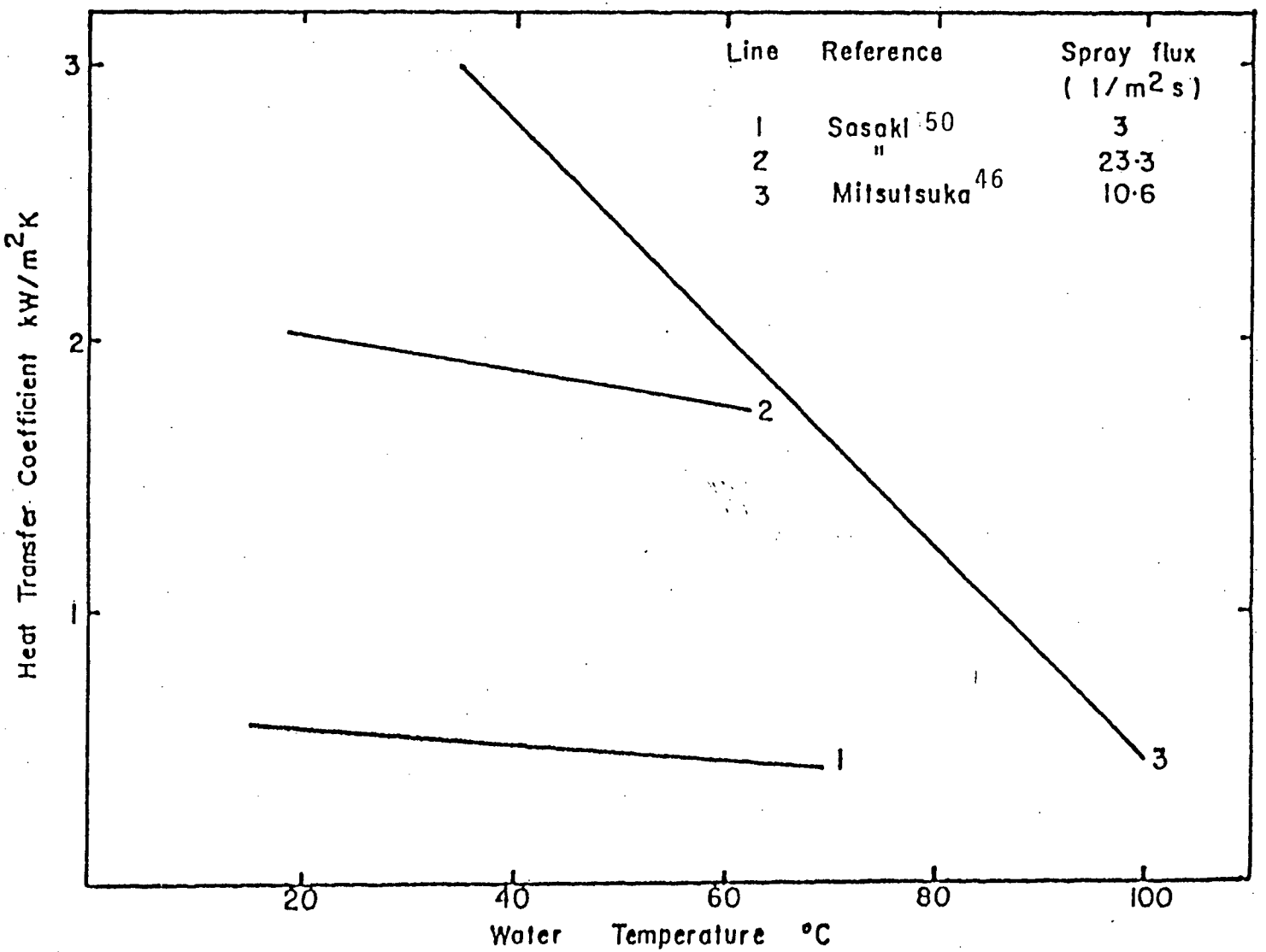

Figure 7 Effect of spray water temperature on the heat-transfer coefficient, as reported by various workers. From Prabhakar.[56]

marginal. Other workers do not report having studied the effect of water temperature. Thus the extent to which the spray water temperature affects the heat-transfer coefficient is not clear.

Perhaps the most important, and interesting variable, is the temperature of the sprayed surface. As has been discussed previously, different boiling regimes and heat-flow rates exist in different ranges of solid temperature. Of particular interest is the Leidenfrost temperature, below which heat-transfer coefficients are found to be strongly temperature dependent. The important fact that emerges from the literature is that the Leidenfrost temperature itself is dependent on the magnitude of the local spray water flux.[41,44,47,50] This dependence, as reported by several workers, is shown in Figure 8. The critical temperature is shown to increase with spray water flux, and may be as high as 800 to 900°C for water fluxes of 20 ℓ/m^2s. Other workers[49,53,54,55] have found stable film boiling to be the operating regime for all water fluxes at temperatures much lower than these (i.e. 500-600°C). In contrast, Prabhakar[56] found transition boiling to be the operating regime at all water fluxes greater than 2 ℓ/m^2s, for temperatures as high as 1000°C. In general, it is apparent that the film boiling mode prevails in steady state measurements, whereas unstable film boiling occurs in the transient measurements at high values of water flux even for temperatures

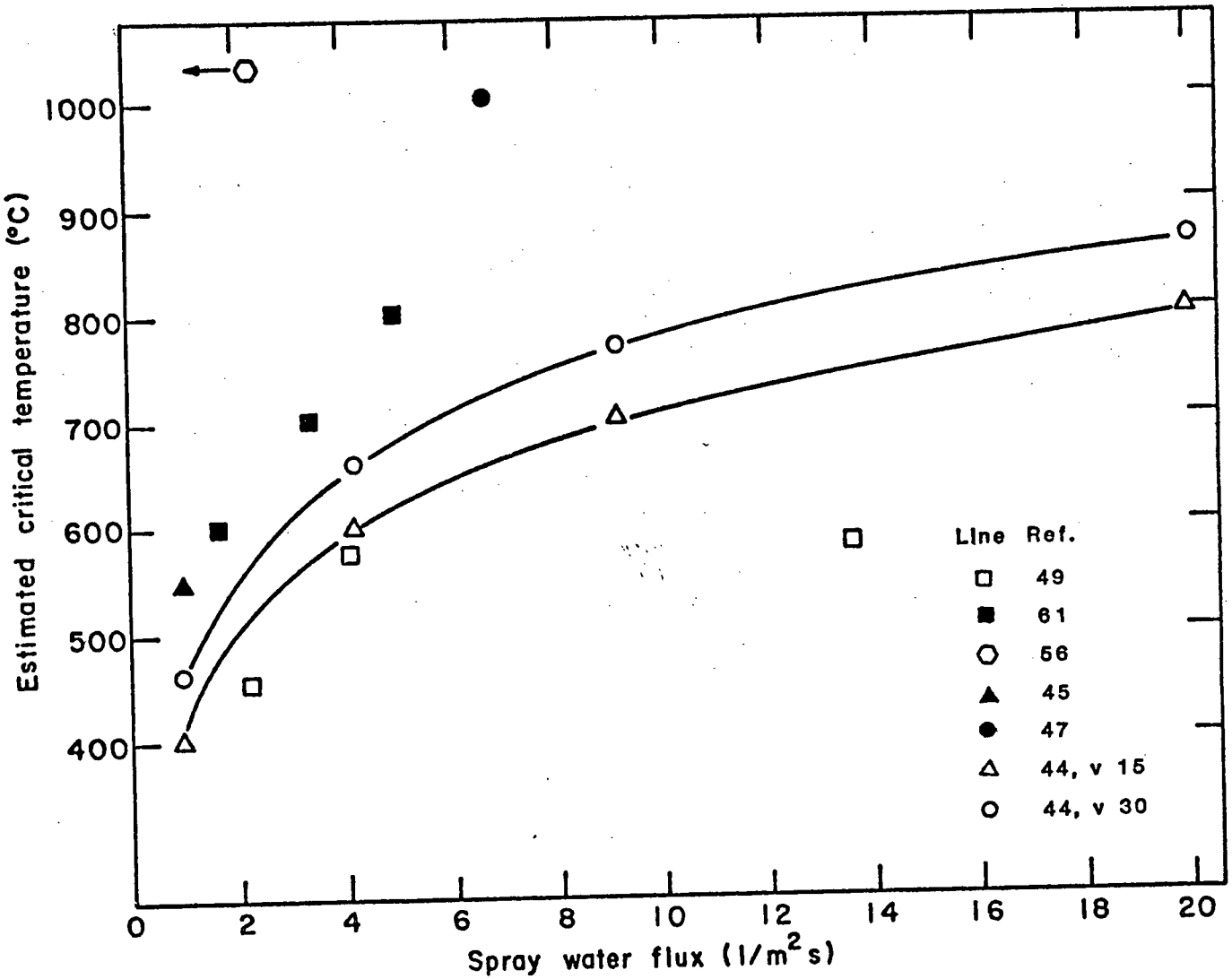

Figure 8 Variation of the critical (Leidenfrost) temperature with water flux.

exceeding 700 - 800°C,[47,48,50,51] except in the case of Mizikar.[49]

The surface temperature dependence of the heat-transfer coefficient has been summarized in Figure 9, from various studies of spray heat extraction. In this figure, the variability of reported values of critical temperature is again seen. The strong dependence of the heat-transfer coefficient on surface temperature in the transition boiling regime is also apparent. Hoogendoorn[44] for example, has found values for the heat-transfer coefficient of 0.250 to 1.500 kW/m^2K at high temperatures, whereas below the Leidenfrost temperatures the values reached 4.000 to 6.000 kW/m^2K and were less affected by the water flux.

Prabhakar[56] has pointed out that it is necessary to have a consistent approach to the calculation of spray water fluxes in order to make meaningful comparisons. This is because the water flow distribution over the area sprayed by a particular nozzle is not uniform. As illustrated in Figure 10,[56] the spray flux distribution from a ¼U8020 nozzle exhibits a plateau in the centre of the sprayed area. Obviously the peak water flux of such a spray distribution can be much greater, depending on the nozzle characteristics, than the average water flux over the sprayed area. Values of heat-transfer coefficient at a particular point would be correlated to average values which are somewhat less than the peak values. This has the effect

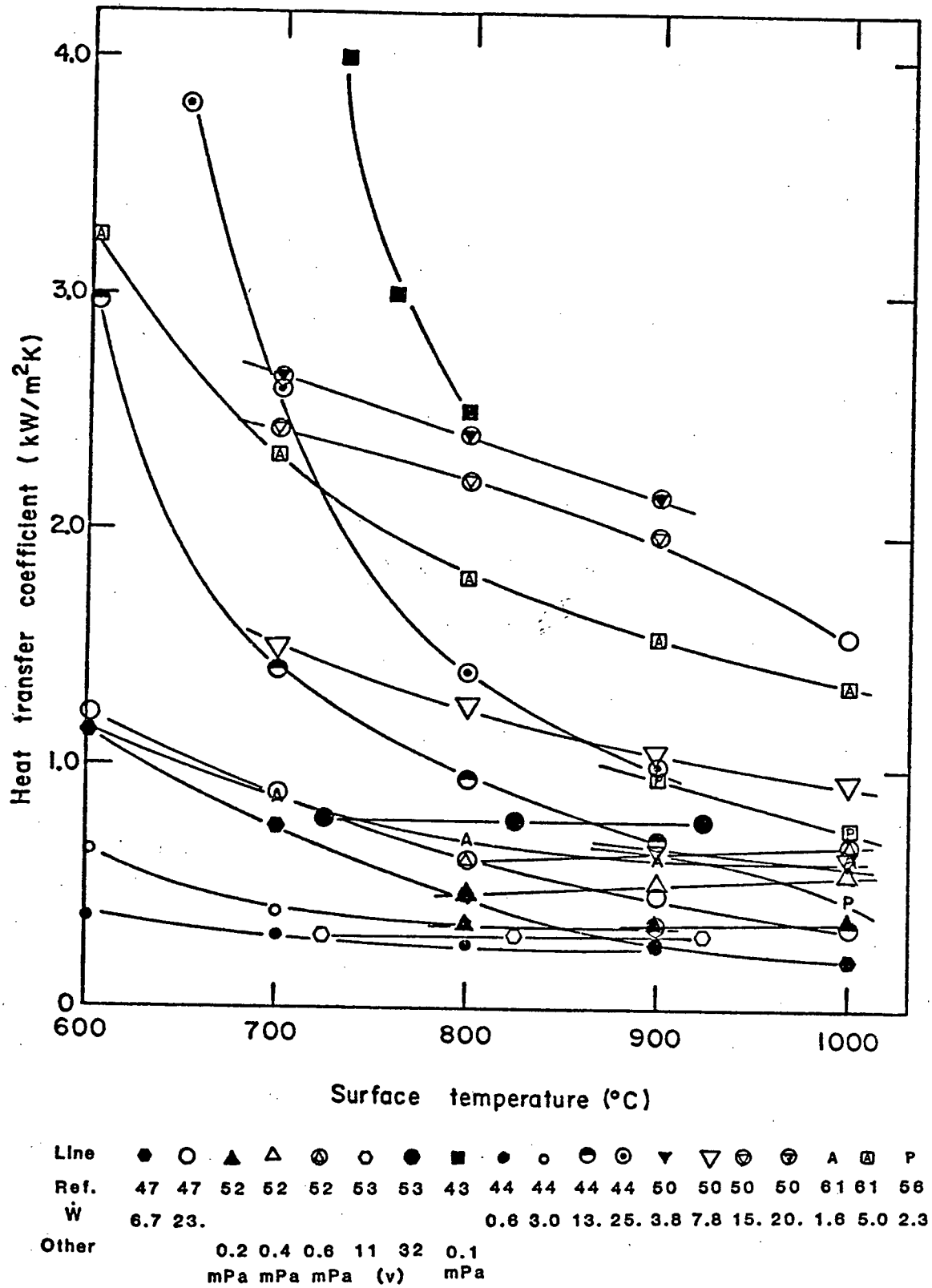

Line	●	○	▲	△	◈	○	●	■	●	o	◓	⊙	▼	▽	⊽	⊽	A	A	P	P
Ref.	47	47	52	52	52	53	53	43	44	44	44	44	50	50	50	50	61	61	56	56
$\dot{W}$	6.7	23.							0.6	3.0	13.	25.	3.8	7.8	15.	20.	1.6	5.0	2.3	9.0
Other			0.2 mPa	0.4 mPa	0.6 mPa	11 (v)	32	0.1 mPa												

Figure 9 Variation of spray heat-transfer coefficients with surface temperature, from various studies of spray heat extraction.

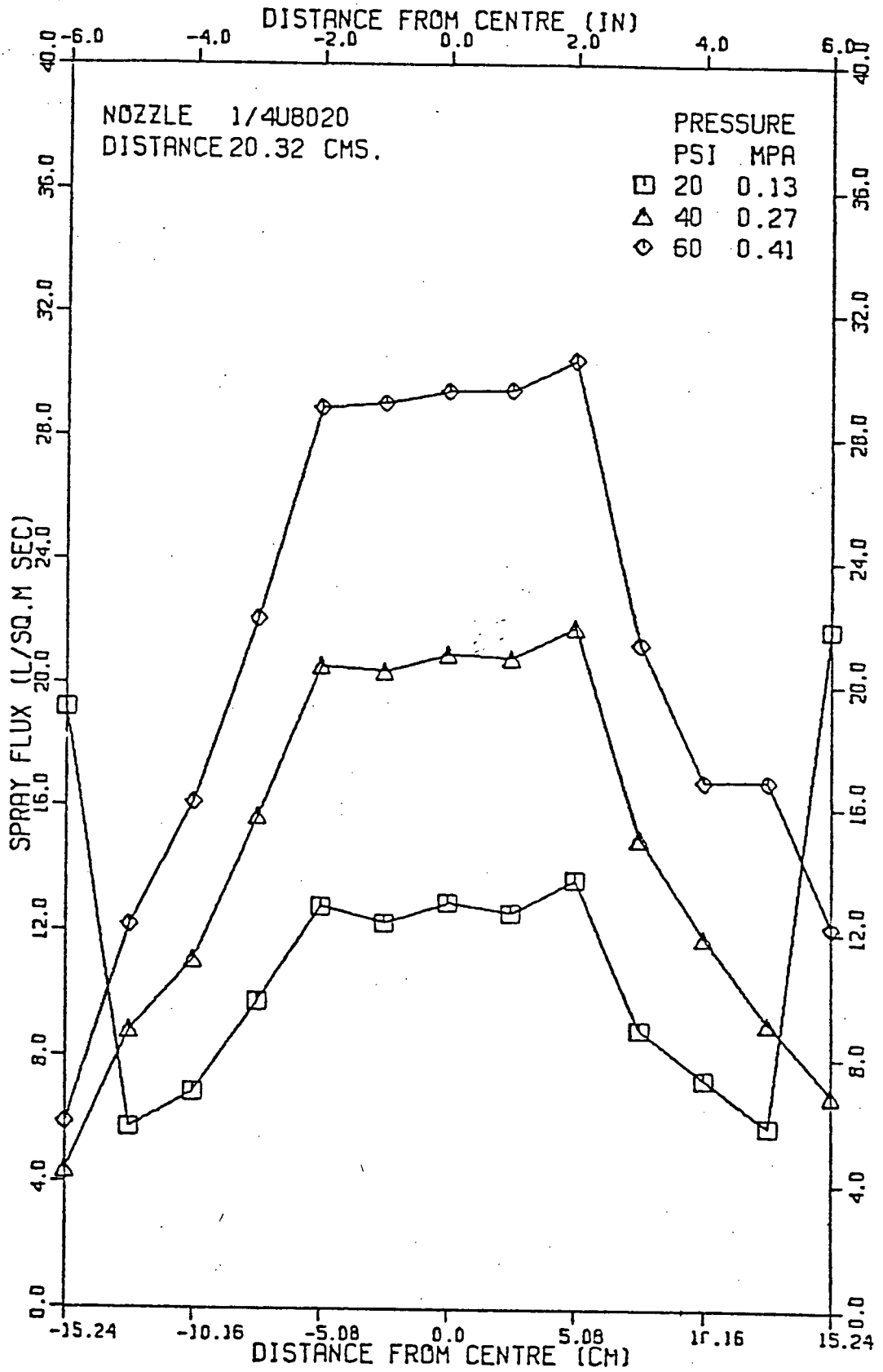

Figure 10 An example of spray water flux distribution for a 1/4 U8020 nozzle. From Prabhakar.[56]

of shifting any plotted relationships upward. Figure 11, which is taken from the fitted curves of Prabhakar at 800°C, indicates an upward shift of as much as 40 per cent when the same data is fitted to averaged, rather than to peak water fluxes. A summary of the method used by various investigators for determination of water fluxes is given in Table III. However comparison of the method used with the results plotted in Figure 6 does not produce a clear correlation.

The only other factors which have been reported to have a possible effect on measured values of the spray heat-transfer coefficient are the direction of spraying and the presence of a water film. Bolle and Moreau[55] reported that the heat-transfer coefficient, when spraying upwards, is 15 per cent less than that when spraying downwards. Prabhakar[56] noted that the presence of water flowing down a vertical measuring plate can also increase the heat-transfer coefficient. Since the data of Sasaki,[50] lies in the middle of the results reported by other workers (Figure 6), it is not evident that his measurements, utilizing optical pyrometers, were affected by the measurement technique. The only works that appear to grossly deviate from those reported by others, are Kojima,[59] and Shimada and Mitsutsuka.[45] The high values of Kojima are for a surface temperature of 700°C. His reported values at 900°C lie in the range of the other works plotted; thus the high values at lower temperature are likely due to unstable film boiling.

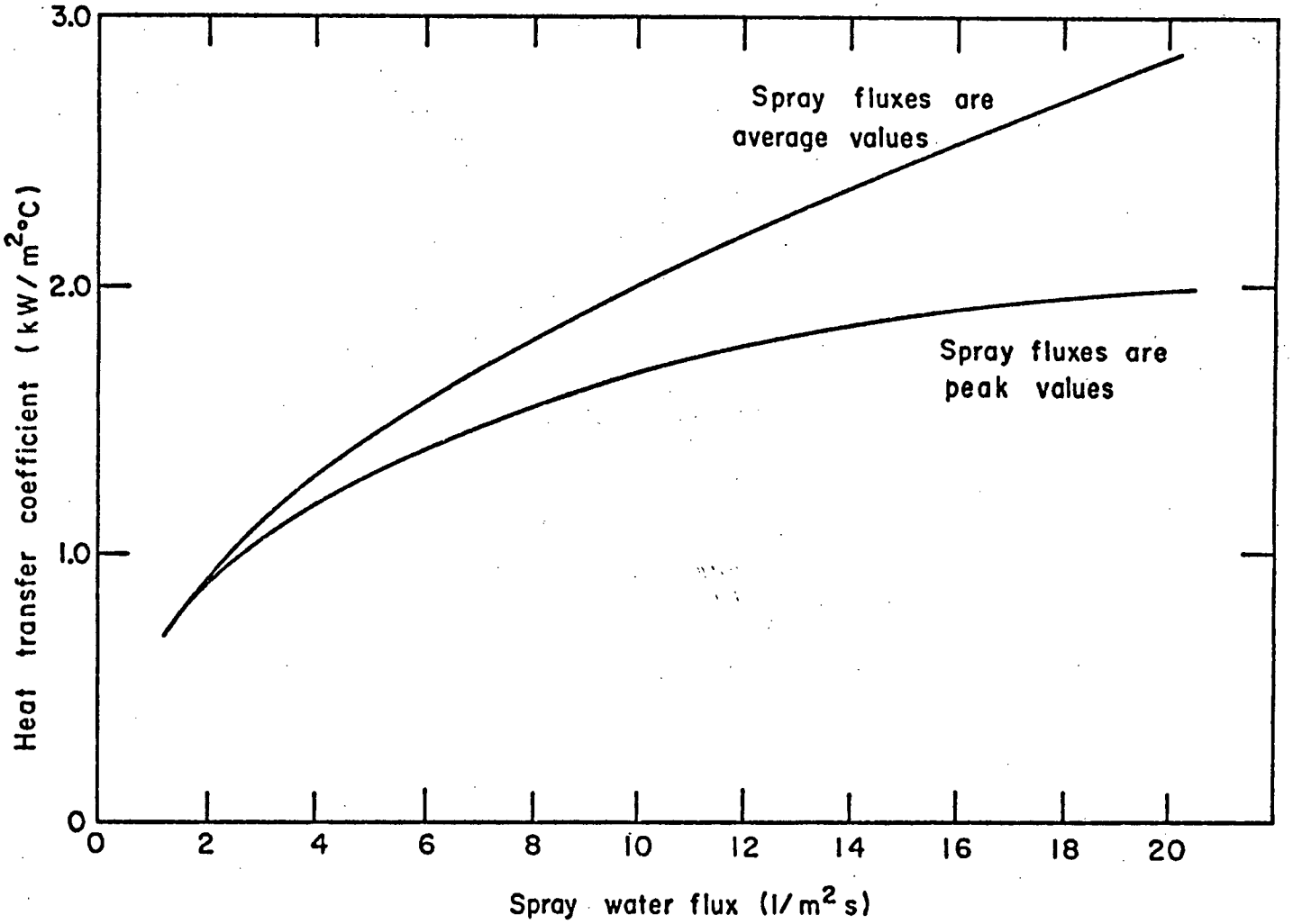

Figure 11 The effect on the regression curve of relating the heat-transfer coefficient to average and peak values of spray water flux. From Prabhakar.[56]

TABLE III Basis for the Determination of Water Fluxes by Various Investigtors of Spray Heat Extraction (from Prabhakar[56])

Investigator	Basis for the Calculation of Water Fluxes
Mitsutsuka[45,46]	Average, over the sprayed area
Etienne et al.[48]	Average, depending on nozzle position, for veejet nozzles
Auman[42]	Average, over the sprayed area
Hoogendoorn et al.[48]	Peak water fluxes, unknown collector area
Mizikar[49]	Peak water fluxes, 6 mm dia. collectors
Sugitani et al.[47]	Peak water fluxes, 6 mm dia. collectors
Junk[52]	Peak water fluxes, unknown collector area
Muller and Jeschar[53]	Peak water fluxes, 120 mm^2 to 600 mm^2 collector area
Bolle and Moreau[54,55]	Peak water fluxes, 40 mm x 20 mm collectors

Other details of the experiments in which these values were determined are not given. The gross deviations reported by Shimada and Mitsutsuka may be due to a number of effects. In particular, plain carbon steels were used in the experiments, and these steels tend to scale easily. Table IIa also indicates that the plate was sprayed from top and bottom simultaneously, and the reported results are for specific temperature differences. Thus results reported for cooling from 930 to 500°C may result in erroneously large values of heat-transfer coefficients at 930°C, due to the sensitivity of the spray heat-transfer coefficient to surface temperature in the unstable film boiling region.

The reported scatter of the results in the literature ranges from 13 to 25 per cent for a particular investigation. The scatter is generally found to increase as temperature decreases, as might be expected with the onset of unstable film boiling at lower temperatures.

The complexity of the heat-transfer process during spray cooling of hot surfaces is evident. Though the data which has been reported is useful in the general design of continuous casting machines, its limitations with respect to slab caster secondary cooling systems must be recognized. To begin with, the spray chamber does not have water uniformly distributed over the entire surface of the slab in a particular zone. The

water is sprayed at high local fluxes in narrow transverse strips throughout the length of the secondary cooling system. For this reason, factors such as the effect of water flux on Leidenfrost temperature must be kept in mind. Furthermore, the majority of laboratory measurements have been made under idealized conditions frequently using oxidation-resistant metals such as stainless steel to minimize uncontrollable effects of surface oxides. However the real surface of a continuously-cast slab at high temperature is heavily oxidized, often to the extent that areas of semidetached scale exist on the slab surface. The true effect is not known, but conceivably the surface condition may influence the mechanism and magnitude of heat transfer. The particular configurations of the secondary cooling systems of continuous casting machines also vary. These concerns have provided the incentive to characterize the heat transfer in operating machines through in-plant measurements.

2.4 Industrial Investigations of Secondary Cooling

The heat-transfer mechanisms in the secondary cooling system of a slab casting machine are indicated in Figure 12.[61] There are well defined regions where the water spray directly impinges on the slab surface, and where the containment rolls are in direct contact with the slab. Between these regions, the behaviour is less clear. Alberny[61] has suggested that

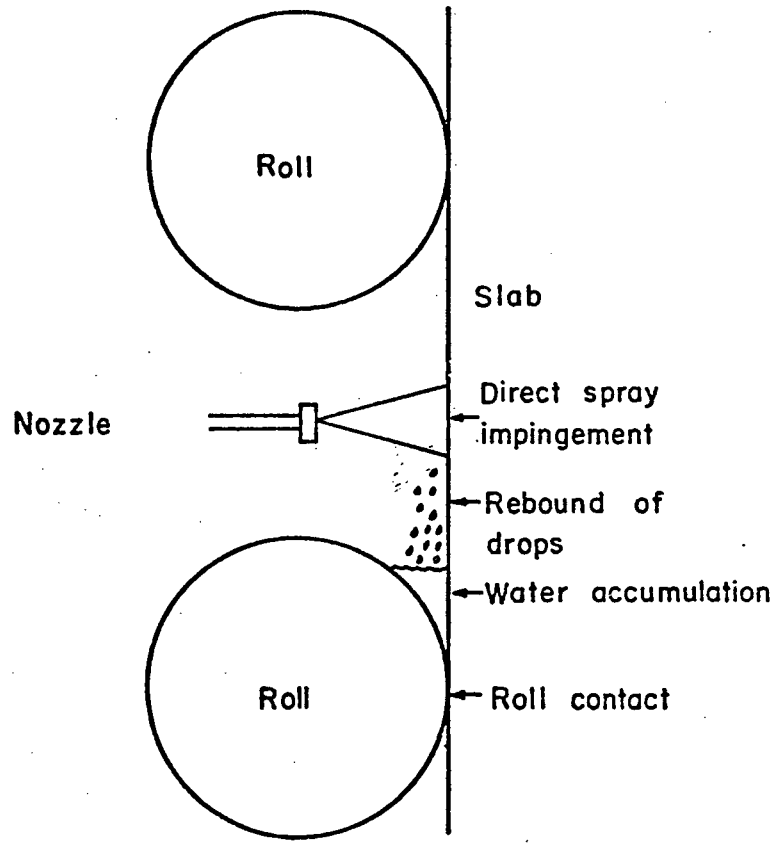

Figure 12 Heat transfer mechanisms in the secondary cooling system. From Alberny.[61]

the impinging spray drops rebound after impact and then accumulate in a pool above the roll. The amount of water which accumulates, if any, is questionable, however, as improper alignment or irregularities on the slab surface will allow it to drain. These conditions will also influence the thermal contact resistance between roll and slab and thus influcence the amount of heat transferred to the roll. Radiation heat transfer, of course, occurs throughout the secondary cooling system.

The number of industrial investigations of secondary cooling is not large. The situations which have been studied vary, in that various combinations of machine type and measurement technique are possible. A summary of these measurements is presented in Table IV. Numerical results of average heat-transfer coefficients obtained for secondary cooling systems are shown in Figure 13. In general, there have been two approaches: to obtain average results based on in-plant measurements of strand surface temperatures, or to combine measurements of heat transfer to rolls with laboratory measurements of spray cooling in order to obtain an overall characterization of heat flow.

The in-plant measurements of surface temperature have been carried out using either pyrometric devices[6,19,48,57,60-63] or thermocouples.[59,64,65] Although thermocouple measurements provide a useful indication of the real temperature excursion of a particular slab surface element as it passes through the

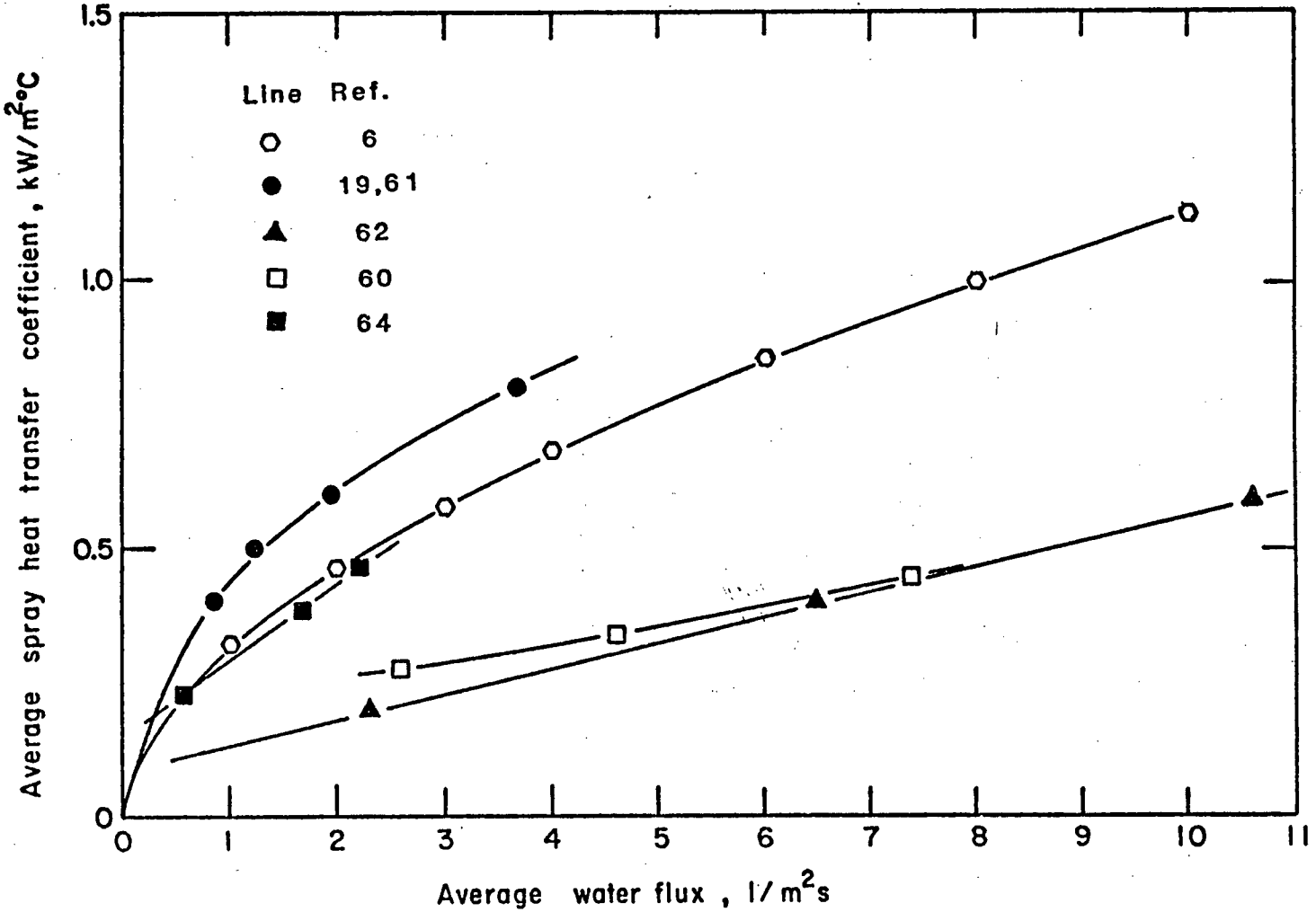

Figure 13 Variation of average heat-transfer coefficient with average spray water flux, as reported in industrial studies of secondary cooling.

TABLE IV Summary of Industrial Measurements of Heat Extraction in Secondary Cooling

Investigator & Reference No.	Type of Machine	Type of Measurement	Location of Measurements	Spray/Roll Configuration	Average Spray Fluxes ℓ/m^2s	Comments
Alberny et al.[60,61]	centrifugal, 120 mm rounds	2 colour pyrometers	9 measurement points throughout machine at entrance and exit of each cooling zone 0.5 to 7.8 m below meniscus	4 zones separated by guide rolls. Full cone nozzles.	Up to 56	h increases with increasing $\dot{W}$ to a certain value of $\dot{W}$ and then stays constant beyond this value.
Benoit et al.[62]	centrifugal 90-160 mm rounds	2 colour pyrometers	5 measurement points	4 zones 2 sets of guide rolls 1/4 and 1/8 HHSQ nozzles, 60 mm set back.	0 - 17	h increases linearly with $\dot{W}$. Achieved large increase in average h through air-water atomisation. > 200°C variation in measured temperatures at same locations.
Nozaki[6]	slab	pyrometer	At unbending point only	Spray/roll combinations. Fan sprays.		Altered form of Mitsutsuka's equation $h = 1.57\ \dot{W}^{0.55}(1-0.0075T_w)/\alpha$ $\alpha = 4$, based on in-plant measurement.
Akimenko et al.[57]	slab	pyrometer	At exit from secondary cooling zone.	Spray/roll combinations. Skid cooling.	1.5 to 6	h increases linearly with $\dot{W}$. Average h determined for entire secondary cooling system. h is greater for skid cooling than roll.
Samoilovich et al.[64]	slab	W-Rh. thermocouples imbedded in interior and surface of strand.	Thermocouple block added to mould travelled through machine with slab.	Fan sprays	0 to 2.5	h determined by solution of inverse boundary problem h increases linearly with $\dot{W}$.
Alberny et al.[63] Birat et al.[19]	slab	2 colour pyrometers and infrared pyrometers	6 measurement points 3.3 to 29 m below meniscus.	Fan spray/roll combinations. Single and multiple spray nozzles.	0 to 4.4	Linear temperature profile assumed between measurement points. h increases as $\dot{W}^n$, where $n < 1$. h is higher at lower temperatures. h increased by using multiple nozzles at same flow rate. h decreases with increasing use of a nozzle Contributions to heat removal: 28% radiation 17% conduction to rolls 16% direct spray impact 39% water flowing down surface.

TABLE IV Summary of Industrial Measurements of Heat Extraction in Secondary Cooling (continued)

Investigator & Reference No.	Type of Machine	Type of Measurement	Location of Measurements	Spray/Roll Configuration	Average Spray Fluxes ℓ/m^2s	Comments
Kojima et al.[59]	slab	Thermocouple welded to slab surface	Welding gun at first roller apron.	Fan and oval sprays.		Cooling/reheating cycles of 100 to 200°C between and under spray nozzles. Industrial measurements agreed with laboratory work of Mitsutsuka and Sasaki.
Weisinger et al.[65]	slab	NiCr/Ni thermocouple pressed into slab surface	Inserted low in machine, exact location not given	Segmented support rolls, cooled by external sprays.		Heat transfer to rolls is larger lower in in machine. In sprayed areas, contribution is 29% radiation 26% roll contact 29% direct spray impact 16% convection
Etienne et al.[48]	slab	optical pyrometer Used thermocouples to determine heat loss to support rolls by internally circulating water	10.2 m and 15.6 m below meniscus Rolls 5.3, 7.5 and 17 m below miniscus	Internally water cooled rolls		Applied laboratory measurements in sprayed region and average heat flux outside sprayed areas to obtain verification of temperatures with heat flow model. Evaluated combined heat loss due to convection to running water and contact with the rolls. Results: $Q = 125\ kW/m^2$, $\dot{W} > 5\ \ell/m^2s$ $Q = 110\ kW/m^2$, $1 < \dot{W} < 5$ $Q = 90\ kW/m^2$, $\dot{W} < 1$ Heat removed by rolls increases deeper in machine.
Diener et al.[66]	slab	Rolls instrumented with thermocouples	Rolls 6.3, 7.8 and 10.7 m below meniscus	Rolls not internally water cooled. Various spray configurations.		Flow of heat to rolls is small high in the machine. Flow is greater low in machine where ferrostatic pressure is larger. See Figure 14.

secondary cooling system, pyrometer measurements would seem more appropriate in obtaining an accurate temperature measurement at a particular location. Thermocouples imbedded in the strand surface may be inaccurate in providing a "real" temperature because the thermocouple could be measuring the temperature of a point a small distance below the surface in addition to the temperature of the spray water or rolls which may contact it. Proper compensations for surface emissivity and absorption of energy by water and steam make surface temperature measurements by pyrometer more viable.

The most extensive pyrometric measurements of surface temperatures have been carried out by Alberny[60,61] and Birat[62] on centrifugal casting machines producing round sections. These studies employed 2-colour pyrometers located at several locations throughout the secondary cooling system. It should be noted, however, that the casting machines studied by these workers have only a few containment rolls. These are located between spray zones so that the results reported would not refer to combined spray/roll heat transfer. In addition, the operating temperatures in these machines are expected to be higher than in a slab machine where bulging can be a problem. Figure 13 shows that heat-transfer coefficients obtained are lower than those reported for other machine types.

Of the reported measurements carried out on slab casters,

only those of Alberny[63] are rigorous. The studies of Nozaki[6] and Akimenko[57] indicate that measurements were performed at the unbending point just outside the spray chamber. Nozaki's equation modifies the form of Mitsutsuka's equation[46] through the use of an accomodation coefficient based on the in-plant measurement at the straightener. Because, as noted, Mitsutsuka's laboratory results are much higher than those reported by other workers, the use of the value $\alpha = 4$ (see Table IV) to obtain agreement with the measured temperatures seems arbitrary. The measurements of Akimenko[57] enabled calculation of an average heat-transfer coefficient for the entire secondary cooling system and were related to an overall average water flux. This approach does not provide an understanding of the real behaviour of the slab as it passes through the various spray zones. The work of Alberny[63] attempts a more detailed characterization, but measurements were not carried out above 3.3 m below the meniscus or for average water fluxes greater than 4.4 ℓ/m^2s.

The results of the measurements reported above again reveal that h increases with $\dot{W}^n$, where n varies from 0.55 to 1.0. In these industrial systems it is difficult to characterize specific effects due to nozzle type, spray pressure, etc., and it has generally been considered that water flux is the main influencing variable in the correlation. Alberny[63] does report that the heat-transfer coefficient is higher at lower surface temperatures, but does not quantify this observation

through correlations. Alberny also found that the heat-transfer coefficient increased when multiple spray nozzles were used to provide the same water flow rates, and that h decreased with increased time of use of a particular nozzle. The latter observation is presumably due to nozzle plugging. Unfortunately the reported correlations do not provide the data obtained from individual experiments, and thus the amount of scatter in the results is not known.

Etienne et al.[48] and Diener et al.[66] have studied the heat transfer to rolls in the secondary cooling systems of slab casters. The rolls in Etienne's study [48] were internally water cooled, so that water temperatures entering and exiting the roll were measured to obtain an indication of the total heat removed. These measurements were combined with laboratory measurements of spray heat extraction and surface temperature measurements using pyrometers to obtain values for the "average" heat flux in the non-sprayed strips in the secondary cooling system. This value was found to be primarily a function of the water flux, as indicated in Table IV. Measurements at roll locations 5.3, 7.5, and 17 m below the meniscus indicated that heat transfer to rolls is greater lower in the machine. Diener[66] obtained direct temperature measurements, using thermocouples, in rolls which were not internally water cooled. The heat transferred to the rolls was found to be very low high in the machine, but in agreement with the

findings of Etiene et al.,[48] measurements at 6.3, 7.8 and 10.7 m indicated that the heat transfer to the rolls increased with distance below the meniscus. This is attributed to the increased ferrostatic pressure deep in the machine. The peak values of heat transfer were also influenced by the roll/spray configuration. The average flow of heat between successive roll centres is shown as a function of distance below the meniscus in Figure 14, as reported by Diener et al.

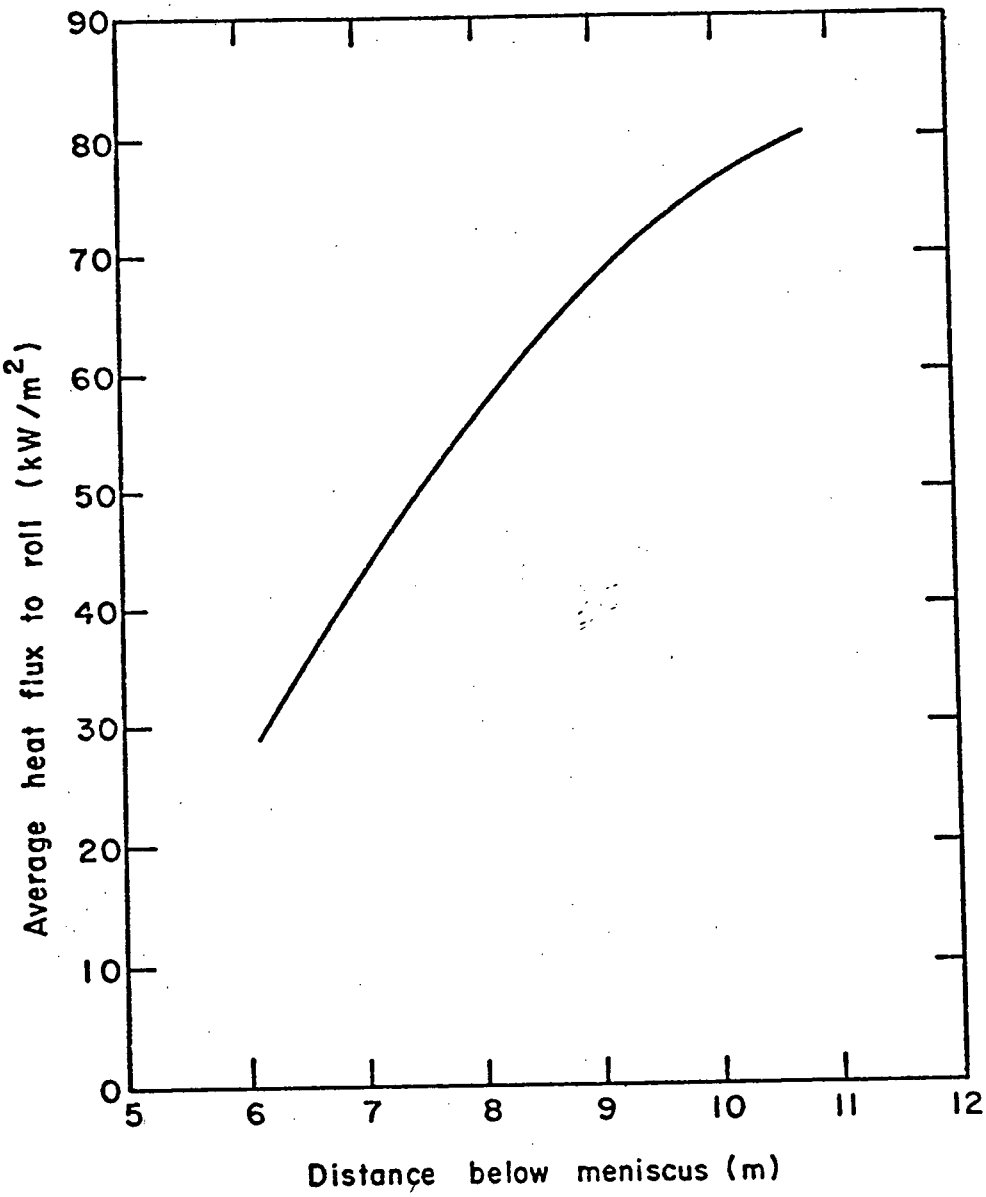

Figure 14 Average heat flux to the containment rolls of a continuous slab caster. From Diener et. al.[66]

Chapter 3

EXPERIMENTAL

In order to characterize heat transfer in the secondary cooling system, measurements of slab surface temperatures were required. These measurements were carried out on the No. 1 Slab Caster of Inland Steel Co. An infrared pyrometer system manufactured by Vanzetti, Inc. was procured by Inland Steel for the purpose of making the measurements. This chapter describes the measurement system, the conditions under which the measurements were made and the procedures followed.

3.1 Theory

The measurement of surface temperatures by pyrometric techniques depends on the fact that the radiant emissions from a hot surface vary in a predictable way with temperature, wavelength, and surface emissivity. The emissive power of a theoretically perfect emitting surface is described by Planck's Radiation Law:

$$E_\lambda = c_1 \lambda^{-5} [\exp(c_2/\lambda T) - 1]^{-1} \qquad (1)$$

where T is the absolute temperature in degrees K. For surface temperatures up to several thousand degrees and for wavelengths less than several micrometers, this equation may be written as:

$$E_\lambda = c_1 \lambda^{-5} / \exp(c_2/\lambda T) \qquad (2)$$

For a non-blackbody surface, an emissivity value, ε, is introduced which reduces the emission by a given amount at each wavelength:

$$E_\lambda = \varepsilon c_1 \lambda^{-5} / \exp(c_2/\lambda T) \qquad (3)$$

From this formula, curves may be drawn which relate the emissive power to wavelength and temperature. These are shown in Figure 15 for blackbody surfaces.[67] For "greybody" surfaces, which have wavelength-independent emissivities less than unity, the curves would be shifted downward by a factor equal to the emissivity. The curves have other shapes in the case of wavelength-dependent emissivities.

The maximum emission occurs at a wavelength, λ_{max}, given by Wien's displacement law:

$$\lambda_{max} T = 0.2898 \text{ cm-K} \qquad (4)$$

The total amount of radiation from a blackbody surface varies over broad spectra with the fourth power of absolute temperature, according to the Stefan-Boltzmann law:

$$E = \sigma T^4 \qquad (5)$$

where σ is the Stefan-Boltzmann constant. In narrow wavelength bands the general form of this equation for a non-blackbody is

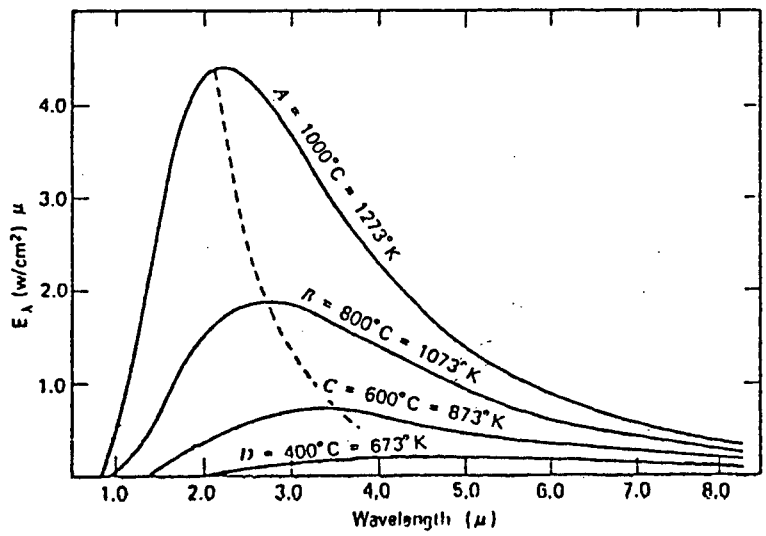

Figure 15 Spectral distribution of blackbody radiation. From Vanzetti.[67]

$$E = \varepsilon\sigma T^n \tag{6}$$

Taking the differential of Equation 6 and dividing by E leads to:

$$\frac{1}{n}\frac{dE}{E} = \frac{1}{n}\frac{d\varepsilon}{\varepsilon} + \frac{dT}{T} \tag{7}$$

Thus as n becomes higher the sensitivity of temperature resolution to errors in the assumed value of emissivity is decreased. Also the amount of radiant emission is more sensitive to values of the temperature of the emitter. If radiant emission is measured in wavelength bands at or shorter than the peak wavelength, n can have values of 16 or greater.[68] Thus an instrument measuring at wavelengths near the visible portion of the spectrum will have high accuracy and low sensitivity to emissivity fluctuations. The most common radiometric methods which have evolved for measurement of surface temperatures are the total radiance, the spectral radiance, the peak wavelength, and the spectral radiance ratio methods. The Vanzetti measurement system employs the spectral radiance method in which the measurement is restricted to a defined wavelength interval.

3.2 Vanzetti Measuring System

The Vanzetti Thermal Monitor System used in this study is an infrared radiation pyrometer, which utilizes fiber optics to transmit the radiation emitted from the target to a

radiation detector and electronic console. The fiber-optic assembly consists of a fiber-optic bundle and a long quartz rod, encased in a protective stainless steel tube. The entire assembly is air-purged in order to provide cooling for the fiber-optic bundle, and to maintain an air curtain to keep the quartz tip (which sights on the target) clean. A schematic diagram of the fiber-optic assembly is presented in Figure 16.

The fiber-optic bundle is connected to the infrared radiation detector which converts the incoming radiation to an electrical signal. The system utilizes a silicon detector which responds to radiation in the 0.7 to 0.97 μm wavelength band. This results, as discussed previously, in high temperature resolution with low sensitivity to errors in surface emissivity setting. This range is also outside of the absorption bands of water vapour.

The electronic console consists of filters, gain adjustments, and switching circuitry to allow the use of up to six radiation detectors and fiber-optic assemblies with one Thermal Monitor. The control panel of the unit contains a power supply, a peak detector with automatic reset, a current amplifier, an emissivity control and a digital temperature readout.

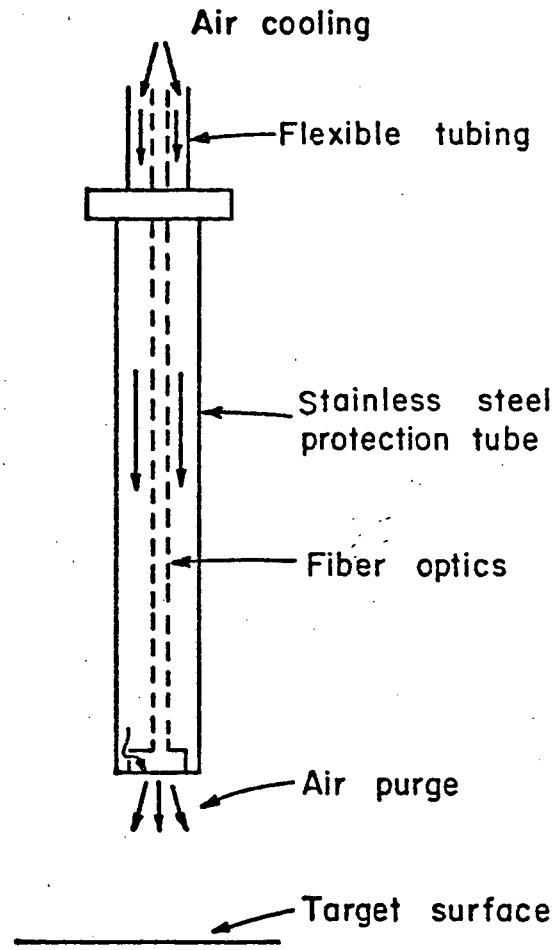

Figure 16 Schematic diagram of the Vanzetti fibre-optic assembly.

The specifications of the system are listed in Table V.[69] In operation, the radiation emitted from the target is collected by the quartz tip, whose field of view is approximately 60°, and transmitted through the fiber optics. The radiation is filtered to the desired wavelength band before reaching the infrared sensing unit, which contains the silicon detector and a 400 Hz tuning-fork oscillator located between the detector and the incoming radiation. The detector converts the modulated infrared signal into a 400 Hz electrical signal which is passed through an A.C. preamplifier. The amplified electrical signal is then transmitted to an A.C. to D.C. converter which generates a D.C. signal proportional to temperature. The measured temperature is then displayed on the control panel of the Thermal Monitor.

The Thermal Monitor unit used in these experiments was provided with a linearized temperature range of 650 to 1400°C. The system was calibrated by the manufacturer prior to shipment, and calibration checks were performed prior to its use. This aspect will be detailed in a subsequent section. In order to test the capability of the system to provide accurate temperature measurements, evaluations of system accuracy, drift and sensitivity to emissivity error, were performed[70] prior to undertaking this study. System accuracy and drift were found to be within $\pm$ 1.5 per cent of the actual temperature, and at operating temperatures expected in normal

TABLE V System Specifications of the Vanzetti Thermal Monitor

Feature	Details	Specification
Size	Electronic Console	13.5 x 48.3 x 39.4 cm. 5.4 kg
	Detector Head	6.9 x 10.2 x 14.5 cm. 0.8 kg
Thermal Environment	Electronic Console	20°C ± 10°C ambient
	Detector Head	30°C ± 20°C ambient
	Fiber optics and lens cell	150°C max. ambient
Target Temperature	Resolution for Blackbody	1% of reading or better
	Response Time	100 mSec
	Power Consumption	50 watts (max)
Options	Display	Digital Panel Meter
	Linearization	Linearized Module, °C Linear 1 mV/°C output
	Output	4 to 20 mA DC
	Signal Processing Capability	0 to 10 sec Peak Sense and Hold
	Emissivity Adjustment	Range .05 to 1.0
	Multichannel Capability	6 channels
	Fiber Optic Detector Head Assembly	Environmentally Sealed Responds to radiant energy from 0.7 to 0.97 micrometers
	Control Capability	None

operation a change of 0.2 in surface emissivity gave an error in temperature measurement of only 20°C.

3.3 Inland Steel No. 1 Slab Caster

The No. 1 Slab Caster of Inland Steel Co. is a two-strand, curved-mould machine of DEMAG design, and has a radius of curvature of 12.2 m. A schematic diagram of the secondary cooling system of the machine is shown in Figure 17. The secondary cooling system comprises 9 independent cooling zones - Zones 1, 2, 3-top, 3-bottom, 4-top, 4-bottom, 5-top, 5-bottom, and "Narrows." The broad faces of Zones 1 and 2A employ square spray nozzles whereas the remaining zones employ fan-type spray nozzles. In addition Zone 2 has cone-type sprays distributed down the narrow face. The nozzles in Zone 2 differ in such a way that 44 per cent of the water goes to region 2A, 25 per cent to region 2B, and 31 per cent to region 2C. The lengths of the cooling zones and type of nozzles employed in each are given in Table VI.

The range of steel grades cast during the experimental period of this study is presented in Table VII. These are nearly all low-carbon grades for deep-drawing, automotive applications. One grade of 0.14 per cent carbon was cast in addition to a microalloyed steel containing Cb, but the 527-XX class made up a large majority of the steel cast.

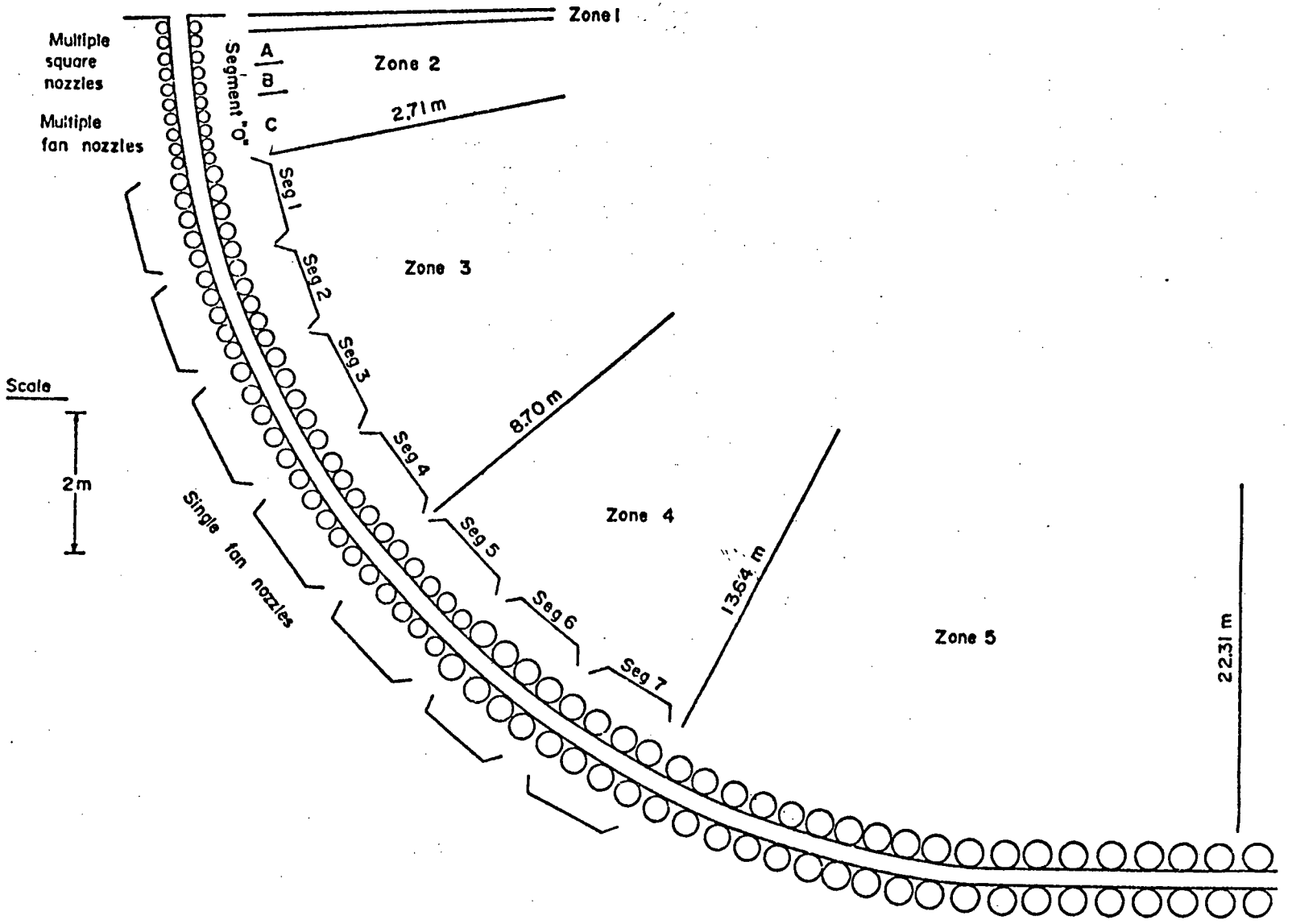

Figure 17 Schematic diagram of the secondary cooling system of the Inland Steel No. 1 Slab Caster.

TABLE VI Secondary Cooling System Configuration at Inland Steel No. 1 Slab Caster

Zone	Length, m	Nozzles				
		Number	No. Per Row	Type	Set Back, cm	Spacing, cm
1	0.34	70	16	Square	11.4	8.9
1 - Narrows	1.77	16	8	Cone	18.4	10.2 (down length)
2 - A (2 rows)	0.41	74	17	1/4 HHSQ (Square)	8.9	8.9
- B (2 rows)	0.41	12	3	302125 (Fan)	17.8	53.3
- C (4 rows)	0.95	24	3	302125 (Fan)	17.8	53.3
3 - Top	5.99	20	1	302125 (Fan)	58.4	-
- Bottom		20	1	302125 (Fan)	58.4	-
4 - Top	4.94	13	1	302125 (Fan)	58.4	-
- Bottom		13	1	302125 (Fan)	58.4	-
5 - Top	8.67*	27	1	302125 8U5060 (Fan)	58.4	-
- Bottom		18	1	302125 (Fan)	58.4	
- Top	14.43**	38	1	302125 8U5060 (Fan)	58.4	-
- Bottom		29	1	302125 (Fan)	58.4	-

*Prior to April 5, 1981
**After April 5, 1981

TABLE VII Steel Grades - Inland Slab Caster

GRADE	Composition (%)											
	C	Mn	P	S	Si	Cu	Ni	Sn	Cr	Mo	Al	Cb
527-08	.06 max	.28/ .34	.015 max	.023 max	.01 max	.12 max	.10 max	.02 max	.06 max	.05 max	.040/ .060	-
521-08	.06 max	.28/ .34	.015 max	.020 max	.01 max	.12 max	.10 max	.02 max	.06 max	.05 max	.040/ .060	-
528-01	.08/ .09	.34/ .40	.015 max	.023 max	.01 max	.12 max	.10 max	.02 max	.06 max	.05 max	.040/ .050	-
516-07	.05 max	.35/ .45	.05/ .08	.020 max	.15 .25	.12 max	.10 max	.02 max	.06 max	.05 max	.080/ .100	-
580-01	.14/ .14	.40/ .50	.010 max	.023 max	.20/ .25	.12 max	.10 max	.02 max	.06 max	.05 max	.040/ .060	-
823-01	.06 max	.35/ .45	.05/ .07	.020 max	.01 max	.12 max	.10 max	.02 max	.06 max	.05 max	.045/ .055	.018/ .023

Normal secondary-cooling practice at the No. 1 Slab Caster stipulates a minimum and maximum overall volumetric flow rate for each zone, between which the water flow rate varies as a function of casting speed for a given "set-point" which is set by the operator according to standard practice. Table VIII indicates the general secondary-cooling practices used for the various steel grades cast at the No. 1 Slab Caster.

It should also be noted that the containment rolls in Zones 1 to 4 are internally water cooled. Zone 5 lies outside the "spray chamber," and rolls are not internally water cooled. The machine regularly casts 235 mm thick slabs of width 762 to 1168 mm (Strand 1) and 1219 to 1753 mm (Strand 2).

3.4 Installation of Equipment for In-Plant Measurements

Due to the hostile and dangerous environment in the secondary cooling system during continuous-casting operation, access to the spray chamber and nearby areas is restricted. This precludes the use of electronic or recording equipment in the vicinity of the spray chamber. In addition, as Table V indicates, the ambient environment for safe operation of the infrared pyrometer system must be protected. With these considerations in mind, the experimental configuration indicated in Figure 18 was implemented.

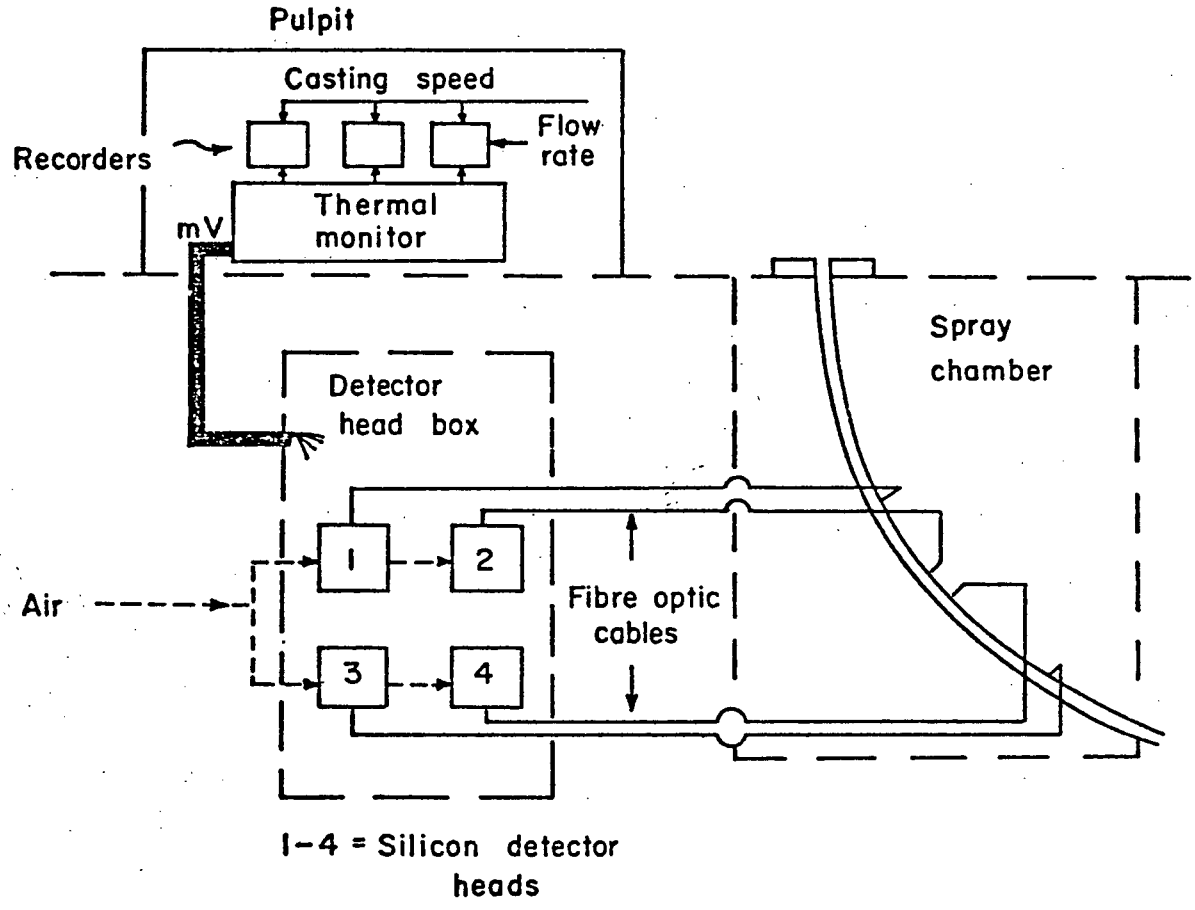

Figure 18 Schematic diagram of the Thermal Monitor System installation.

TABLE VIII Secondary Cooling Practices at the Inland Slab Caster

Zone		Flow Rate, ℓ/min (Pressure at Flow Rate, MPa)			
		Standard Practice Grades 527-xx, 521-xx		Cb Practice Grades 826-03, 528-01	Modified Cb Practice Grades 823-01, 523-01 516-07, 580-01
		762-1168 mm wide	1219-1676 mm wide		
1 -	Set.	568	568	568	568
	Min.	454	454	568	568
	Max	795	795	568	568
2 -	Set.	1325 (.345)	1325 (.345)	1325 (.345)	1325 (.345)
Wide	Min.	947	947	947	947
Face	Max.	-	-	-	-
3 -	Set.	833 (.448)	1136 (.965)	833 (.448)	833 (.448)
Top	Min.	454	454	454	454
& Bottom	Max.	1181	1181	1181	1181
4 -	Set.	416 (.345)	757 (1.068)	416 (.345)	416 (.345)
Top	Min.	284	284	284	284
& Bottom	Max.	769	769	769	769
5 -	Set.	492	947 (.690)	492	341
Top	Min.	492	492	492	341
& Bottom	Max.	1075	1075	492	341

Note: Standard practice, Mould powders are C994, P327 (high heat flux)
Modified practice, Mould powders are P389 (low heat flux)

The Vanzetti system was well suited to these requirements. The fiber-optic cables could be run from the probe tips located inside the spray chamber to a box which was mounted just outside the chamber. Here the detector heads and air pressure regulators were mounted. The detector heads and fiber-optic cables were supplied with the air purge connected to a nearby valve. This configuration also allowed gain adjustment of the detector head during in-situ calibration checks. The electrical signals from the detector heads were run through conduit to the electronic console located in the protected, air-conditioned pulpit on the main floor of the shop. The linearized signal from the electronic console could be tapped to provide continuous temperature recordings on chart recorders. Casting speed and water flow-rate signals similarly were input to the recorders. This location also allowed continuous observation of the casting operation so that observations could be noted on the recorders and in the log book.

A detailed representation of the probe installation is presented in Figures 19 and 20. Figure 19, which shows the case of Zone 3, is representative of the Zone 3 and 4 measurements. A mounting bracket with a pivoting head was designed, and could be clamped to the top or bottom of the desired segment. The probe could be secured in a sleeve which could be rotated to sight at the desired location. Measurements in

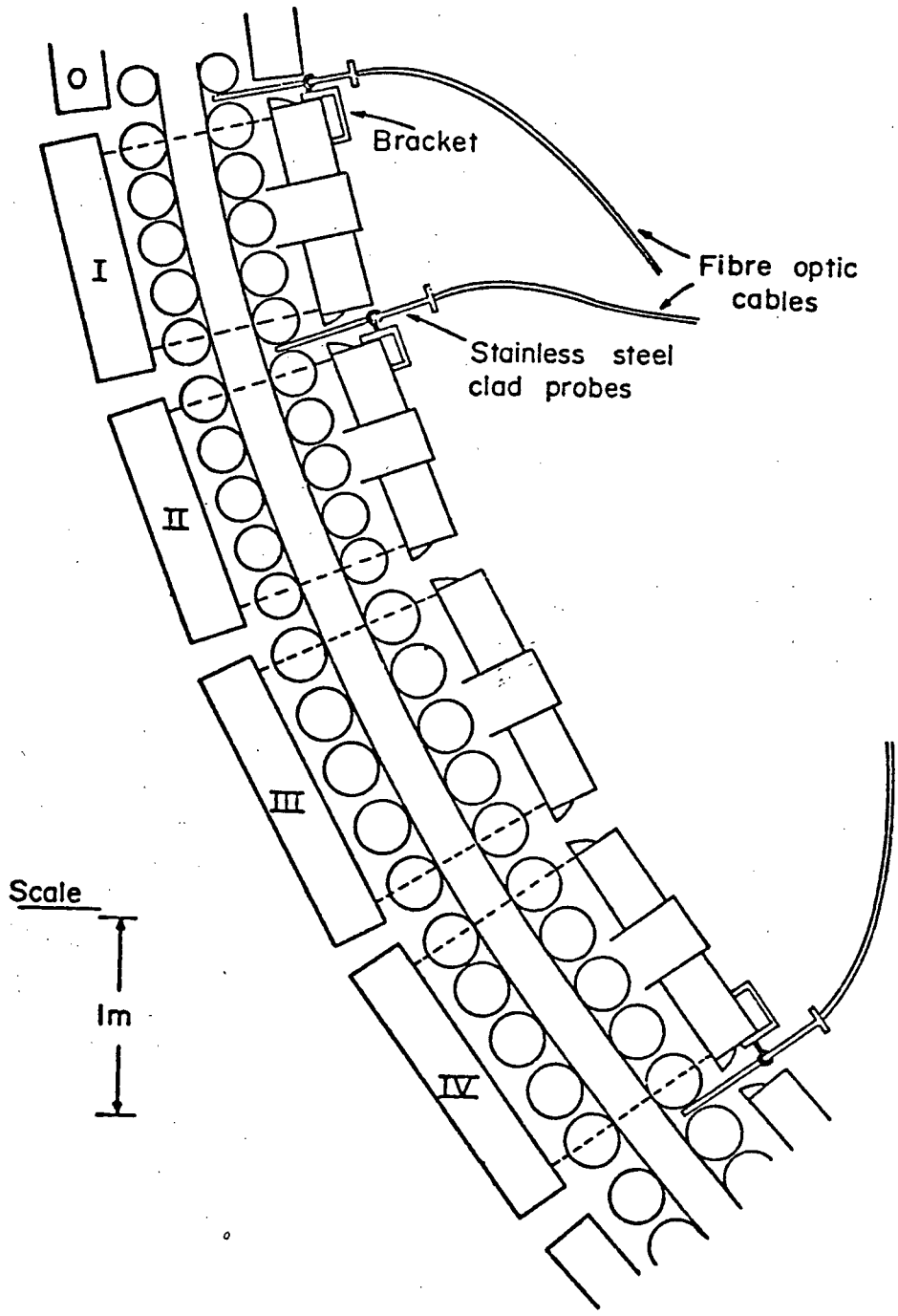

Figure 19 Schematic diagram of the Vanzetti probe installation in Zone 3 of the No. 1 Slab Caster.

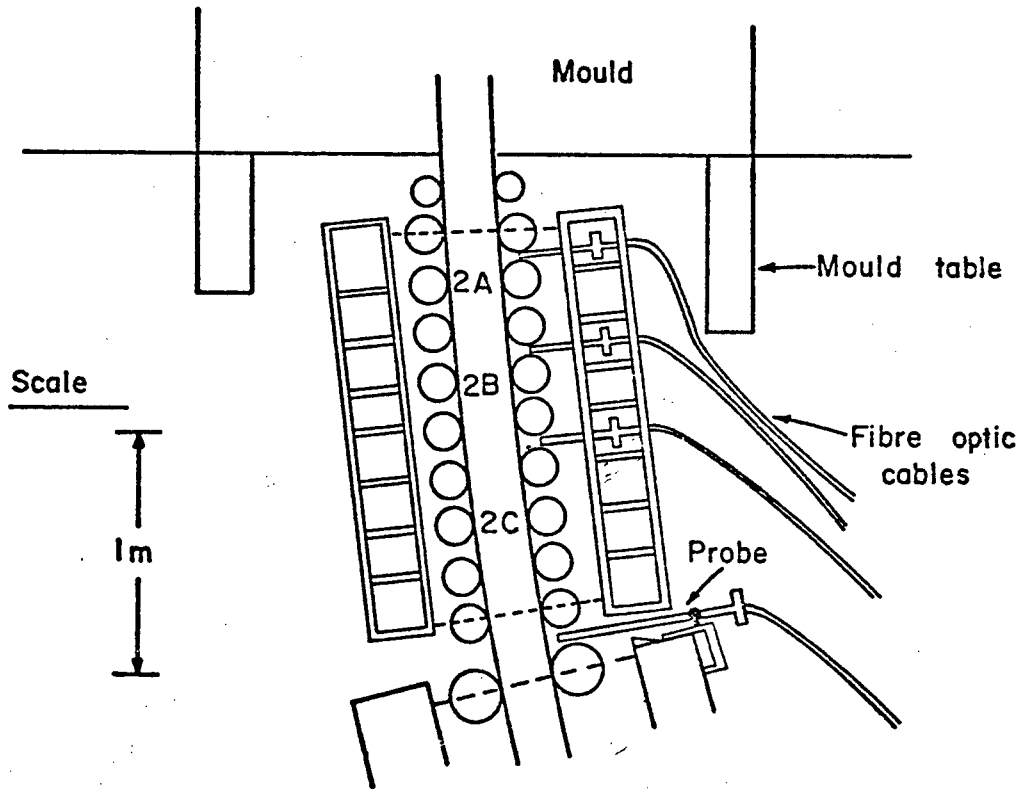

Figure 20 Schematic diagram of the Vanzetti probe installation in Zone 2 of the No. 1 Slab Caster.

Zones 3 and 4 were made at a location 10 to 15 cm from the centreline of the broad face. The configuration of the adjacent spray nozzle did not allow the probe to be sighted at the centreline. An attempt was made to ensure that the probe tip was as close to the slab surface as possible. This normally meant that the tip was less than approximately 6 cm from the slab surface. Measurements in Zones 3, 4 and 5 were carried out with the spray nozzle adjacent to the measurement point capped, in order that the sighting location of the probe with respect to the impingement point of the spray did not cause variability in the measured temperatures.

Figure 20 shows the configuration employed in the Zone 2 measurements. Because Zones 2A and 2B consist of only 2 rows of nozzles, it was thought that capping these nozzles would have a significant effect on the spray heat transfer. Accordingly, the nozzles in Zone 2 were not capped and the surface temperatures were measured in the spray-impingement area. The bracket design employed in the Zone 2 measurements allowed the probe to be attached directly to the nozzles, and so it was assumed that the measurement point was constant with respect to the spray-impingement area. All Zone 2 measurements were carried out at the centreline of the broad face.

3.5 Data Collection Procedures

In order to ensure maximum utilization of man hours and

equipment during the varying schedules of a high-productivity operation, collection of data was performed on a 24-hour continuous basis. This required standardized procedures in terms of equipment maintenance and experimental method.

3.5.1 Pyrometer Calibration and Maintenance

Before the Thermal Monitor was received by Inland Steel, the Vanzetti system was calibrated by the manufacturer so that a linearized output could be obtained in the expected range of temperatures. Gain adjustments on the Thermal Monitor unit then allowed user calibration of the system with a blackbody radiation source. However because of the hostile and dirty conditions in plant, and the need for rapid calibration checks during normal operation, a blackbody source is not suitable for routine work. Accordingly, the manufacturer provides a portable reference light source with which in-situ calibration checks may be performed. The procedure in maintaining pyrometer calibration was thus to perform initial calibration of all measurement probes using a standard blackbody calibration source at a temperature near the middle of the linearized range. The calibrated pyrometers were then used to determine the "reference temperature" of the portable light source. The radiant energy from this source is provided by a 12-volt tungsten filament lamp. Lamp brightness from this source is regulated in order to eliminate voltage variations

from the rechargeable nickel-cadmium batteries.

Initial operation of the Thermal Monitor system in the spray chamber showed a gradual drop in measured temperatures over a period of several casts. This was attributed to fouling of the probe tips and in subsequent measurements the tips were cleaned between each cast with "Q-tips" and a grease-free solvent. This resulted in short-term reproducibility of temperature measurements without the need to perform continuous calibration checks. Calibration checks were performed when down-time allowed, approximately every 2 to 3 days. Calibration drift during these time intervals was less than 15°C when the probe tips were regularly cleaned. The drift that did occur is presumably due to the introduction of defects in the fiber-optic cable during normal operation.

3.5.2 Water Flow Measurement and Control

During these experiments the objective was to study effect of the spray-water variables on the amount of heat transferred in the secondary cooling zones. Because little control was possible over nozzle type and orientation during the experimental period, the approach was to vary the water flow-rate to each secondary-cooling zone in turn, when the measurements were being carried out on that zone. For example, when probes were located in Zone 3 the water flow-rate set-point of Zone 3 would be set at 3 different values

for a duration of 2 to 3 heats per set-point during a normal 6 to 8 heat cast. The chosen values of set-points were such that the maximum range of flow rates could be obtained for the particular zone, under constraints imposed by the valving systems in operation and the co-operation of the foreman. The normal "speed-tie" practice was in operation during the experiments, which did provide minor fluctuations in the actual water flow rates obtained, except for the cases in which a throttling, slide-gate metering nozzle was being tested on the tundish. It should be noted at this point that, except in cases where drastic speed fluctuations were occurring due to events such as nozzle-plugging and rodding of the tundish, the temperature recordings obtained during normal operation were not different in character than those obtained during throttling slide-gate use. In the cases where drastic speed fluctuations did occur, the data was not used.

Three indications of the actual water flow rate obtained were used. The most reliable were the continuous recording obtained on a multi-pen recorder and that stored in the on-line computer. Unfortunately these two data sources were not available during all casts and the observations of the metallurgical observer on the Slab Caster "heat sheets" had to be used in some cases. Since the latter cannot be regarded as a reliable indication of the true water flow rate for a particular set-point and casting speed, composite plots were drawn

from the three data sources to provide relationships between casting speed and water flow rate at the various set-points during the experiments. The accuracy of the flow rates thus obtained is discussed in Chapter 5.

3.6 The Scale Problem

Prior to undertaking this project, it was recognized that some error could be introduced to the measurement of slab surface temperatures due to the presence of scale on the slab surface.[71,74] Recent publications by Mairy and Ramelot[72,73] have claimed that descaling of the slab surface is necessary before the measurement point. Initial visual observations and pyrometer measurements at the Inland slab caster indicated that the extent of scale present on the slab surface was much greater on Strand 1 than Strand 2.[74] The reason for this behaviour was not clear. Nevertheless, some work was conducted by Inland Research in attempting to develop a descaling device.[75] The results of the test work performed with this device were inconclusive, and further experimentation was abandoned due to the extreme difficulty encountered with its operation. However, surface-temperature profiles measured on Strand 2 under normal operating conditions did not indicate the large temperature fluctuations which Mairy and Ramelot claim are due to the presence of semi-detached scale on the slab surface. Accordingly, it was decided that accurate

temperature measurements could be obtained on Strand 2 with the current pyrometer system and its "peak-picking" capability. The work reported in this thesis proceeded under those circumstances, on the inside radius of Strand 2.

After the experimental portion of this thesis was completed, the DESCATHERM (Trademark of C.R.M.) system was obtained by Inland Research and tested on the inner radius of Strand 2.[76] The results, which are presented in Appendix B, indicated that under the test conditions the descaling device did not have a significant effect on the temperatures measured.

Chapter 4

MATHEMATICAL MODEL

In order to relate the surface-temperature measurements performed in the experimental part of this thesis to heat fluxes and heat-transfer coefficients, it was necessary to develop a mathematical heat-transfer model of the continuous casting process. A one-dimensional model was chosen for this purpose since the measurements had been carried out in the vicinity of the centreline of the broad face, where corner effects would be negligible.

4.1 Mathematical Model Formulation

Heat transfer in a continuously-cast slab may be described by the one-dimensional unsteady-state heat-conduction equation:

$$\left(\frac{\partial}{\partial x}\right) K\left(\frac{\partial T}{\partial x}\right) = \rho C_p\left(\frac{\partial T}{\partial t}\right) \tag{8}$$

If K is assumed constant over small time intervals, this equation becomes

$$K\left(\frac{\partial^2 T}{\partial x^2}\right) = \rho C_p\left(\frac{\partial T}{\partial t}\right) \tag{9}$$

Solution of this second-order partial-differential equation requires knowledge of one initial condition and two boundary conditions. For the case of continuous casting, the initial condition is:

$$t = 0, \quad T = T_{pour} \quad \text{for all } x \tag{10}$$

The two boundary conditions may be determined by considering continuity of heat transfer at convenient interfaces. Thus at the surface of the slab:

$$-K \frac{\partial T}{\partial x} = Q \quad \text{for all } t \tag{11}$$

When convective heat transfer is being considered, the surface heat flux, Q may be expressed as the product of a heat-transfer coefficient and a temperature difference between the slab surface and surrounding medium:

$$Q = h (T_s - T_a) \tag{12}$$

If radiation is also present the surface heat flux becomes:

$$Q = h (T_s - T_a) + \varepsilon\sigma (T_s^4 - T_a^4) \tag{13}$$

The second boundary condition may be determined by consideration of heat transfer across the midplane of the slab thickness. If symmetry of heat transfer to each broad face is assumed, the net rate of heat transfer across the midplane is 0, so that:

$$\frac{\partial T}{\partial x} = 0 \qquad \text{for all } t \qquad (14)$$

Solution of the differential equations for heat conduction has in the past been accomplished by analytical and numerical methods. The numerical methods have proved themselves to be the most versatile in the solution of solidification problems because they permit use of varying boundary conditions, release of latent heat over a broad freezing range and temperature-dependent thermophysical properties. Of the various numerical methods, the explicit and implicit finite-difference techniques have been employed widely in casting applications. The implicit method has an advantage in that it is free of a stability criterion that restricts the independent choice of time and distance intervals in the explicit technique.[77] For the purposes of the present work, which involved a large number of computer runs of the mathematical model, this was justification for use of the implicit finite-difference method.

4.2 Derivation of the Finite-Difference Equations

The most elegant solution of the unsteady-state, heat-conduction equation involves the approximation of the partial differentials of Equation 9 by the use of Taylor series.[77] Though the derivation of the finite-difference equations in this way is more rigorous in that the order of the errors in the approximation is known, identical equations can be derived by performing a simple heat balance for each node.

If a one-dimensional section through the slab thickness is divided into elements or nodes containing a nodal point at the centre of each (Figure 21), heat balances on the interior nodes may be derived. Similarly heat balances may be derived for half nodes at the surface and midplane as shown. In the absence of heat generation or consumption, the law of conservation states:

Rate of heat input - Rate of heat output

= Rate of heat accumulation (15)

or

$$\dot{q}_{in} - \dot{q}_{out} = \frac{\Delta q}{\Delta t} \tag{16}$$

The finite-difference approximation incorporating Fourier's Law of heat conduction leads to, for the general case of an interior node i:

$$K_1 A\left(\frac{T_{i-1}^1 - T_i^1}{\Delta x}\right) - K_2 A\left(\frac{T_i^1 - T_{i+1}^1}{\Delta x}\right) = (A \cdot \Delta x)\rho C_p\left(\frac{T_i^1 - T_i}{\Delta t}\right) \tag{17}$$

Here T^1 refers to unknown nodal temperatues at the end of a particular time step and T_i refers to the known temperature of node i at the beginning of the time step. The thermal conductivities have been calculated as the average values between adjacent nodes, where

$$\text{a) } K_1 = \frac{K_i + K_{i-1}}{2} \qquad \text{b) } K_2 = \frac{K_i + K_{i+1}}{2} \tag{18}$$

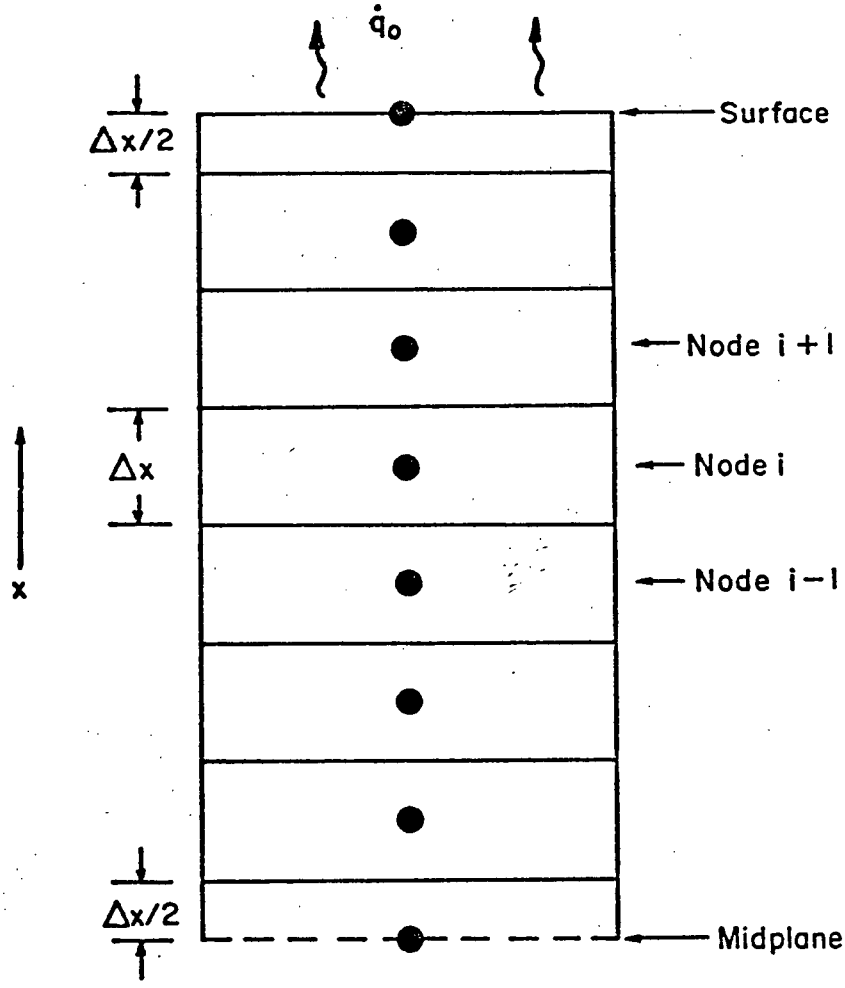

Figure 21 Mathematical model node convention.

Equation (17) may be arranged to give:

$$-\left(\frac{K_1}{\rho C_p}\right)\left(\frac{\Delta t}{(\Delta x)^2}\right)T_{i-1}^1 + \left(\frac{K_1+K_2}{\rho C_p}\right)\left(\frac{\Delta t}{(\Delta x)^2}\right)T_i^1 - \left(\frac{K_2}{\rho C_p}\right)\left(\frac{\Delta t}{(\Delta x)^2}\right)T_{i+1}^1 = T_i \quad (19)$$

The heat balance for the surface half node is

$$K_1 A\left(\frac{T_{s-1}^1 - T_s^1}{\Delta x}\right) - \dot{q}_o = \rho C_p \cdot A\left(\frac{\Delta x}{2}\right)\left(\frac{T_s^1 - T_s}{\Delta t}\right) \quad (20)$$

Rearranging,

$$-\left(\frac{K_1}{\rho C_p}\right)\left(\frac{2\Delta t}{(\Delta x)^2}\right)T_{s-1}^1 + \left(\frac{K_1}{\rho C_p}\right)\left(\frac{2\Delta t}{(\Delta x)^2} + 1\right)T_s^1 = T_s - \frac{2}{\rho C_p}\left(\frac{\Delta t}{\Delta x}\right) \quad (21)$$

In this derivation the surface heat flux is approximated by its value at the beginning of the time step. For the case of the midplane half node, the heat balance is:

$$0 = K_2 A\left(\frac{T_o^1 - T_1^1}{\Delta x}\right) = \rho C_p\left(A\cdot\frac{\Delta x}{2}\right)\left(\frac{T_o^1 - T_o}{\Delta t}\right) \quad (22)$$

Rearranging

$$\frac{K_2}{\rho C_p}\left(\frac{2\Delta t}{(\Delta x)^2} + 1\right)T_o^1 - \left(\frac{K_2}{\rho C_p}\right)\left(\frac{2\Delta t}{(\Delta x)^2}\right)T_1^1 = T_o \quad (23)$$

Because each of the equations which have been derived contain at least two unknown temperatures, none can be solved independently. However, when all the equations are written down a simple system of n linear equations in n unknowns results. If we define

$$A = \frac{K_1}{\rho C_p} \frac{\Delta t}{(\Delta x)^2} \tag{24a}$$

$$B = \frac{K_1}{\rho C_p} \frac{\Delta t}{(\Delta x)^2} \tag{24b}$$

$$C = 1 + A + B \tag{24c}$$

$$D = 1 + 2 \times A \tag{24d}$$

$$E = 1 + 2 \times B \tag{24e}$$

the following tridiagonal system of equations is obtained:

$$\begin{array}{rl}
ET_o^1 - 2BT_1^1 = & f_o \\
-AT_o^1 + CT_1^1 - BT_2^1 = & f_1 \\
\hline
-AT_{i-2}^1 + CT_{i-1}^1 - BT_i^1 = & f_{i-1} \\
- AT_{i-1}^1 + CT_i^1 - BT_{i+1}^1 = & f_i \\
- AT_i^1 + CT_{i+1}^1 - BT_{i+2}^1 = & f_{i+1} \\
\hline
- AT_{s-2}^1 + CT_{s-1}^1 - BT_s^1 = & f_{s-1} \\
- 2AT_{s-1}^1 + DT_s^1 = & f_s
\end{array} \tag{25a}$$

where

$$f_s = T_s - 2A\left(\frac{\Delta x}{K_1}\right) Q \tag{25b}$$

$$f_i = T_i, \quad i=o,\cdots,s-1 \tag{25c}$$

This system of equations is easily solved by Gaussian elimination. Comparison of model-predicted temperatures with an

analytical solution to Equation 8 showed very good agreement for the case of a slab of initial uniform temperature with constant surface boundary condition and thermophysical properties.

4.3 Characterization of Input Conditions

An important aspect of mathematical model formulation is the manner in which thermophysical properties and boundary conditions are handled. In particular characterization of the thermal conductivity of the liquid and the release of latent heat must be considered. Turbulent mixing in the liquid pool makes it difficult to assign proper values to the thermal conductivity. The release of latent heat is generally accomplished by utilizing an artifically large value of heat capacity in the region between the liquidus and solidus temperatures. Fortunately it has been shown that the exact form of the latent heat release[78] and the exact value of the thermal conductivity[20] employed in the liquid pool do not affect the calculated temperature field significantly. Thus the effective thermal conductivity in the liquid pool has been estimated from the literature to be seven times the actual thermal conductivity of the liquid metal at the particular temperature. The latent heat has been evolved as a linear function of temperature between the liquidus and solidus temperatures. The values of thermophysical properties used in this study are given in Table IX.

TABLE IX Thermophysical Properties Used in the Heat-Transfer Calculations

Property	Range, °C	Value
Liquidus Temperature, °C	—	1516
Solidus Temperature, °C	—	1477
Thermal Conductivity, kW/m°C	>1516	.260
	879 to 1516	.017 + .000012 T
	<879	.064 - .000043 T
Heat Capacity, J/g°C	>1516	.690
	1477 to 1516	8.540
	879 to 1477	.540 - .0000941 T
	727 to 879	7.200 - .007531 T
	<727	-1.900 + .00586 T
Density, kg/m^3	—	7530.

The surface boundary conditions in the present work are evaluated as heat fluxes. The heat flux in the mould is calculated from the results of Samarasekera[79] in which slab moulds were instrumented with thermocouples. The relationships between surface heat flux and time in the mould are shown in Figure 22 for both low and high heat flux mould powders. This data is regarded as more accurate for locations not far from the meniscus than data which has been reported previously, based on mould water temperature increase. Below the mould, the total heat flux is given by Equation 13 .

4.4 Application of the Model to the Present Work

The usual application of mathematical models of the continuous casting process has been to predict the steady-state temperature distribution of the strand for a prescribed set of operating and boundary conditions. In the secondary cooling zones, the normal procedure has been to calculate an average heat-transfer coefficient for a particular zone based on the water flux in the zone. Mathematical models are also capable of calculating the desired heat-transfer coefficient profile through the secondary cooling system based on an input temperature profile which may prevent the formation of a particular defect.[11]

In the present work, a different approach has been taken. The calculations were performed by a trial-and-error method

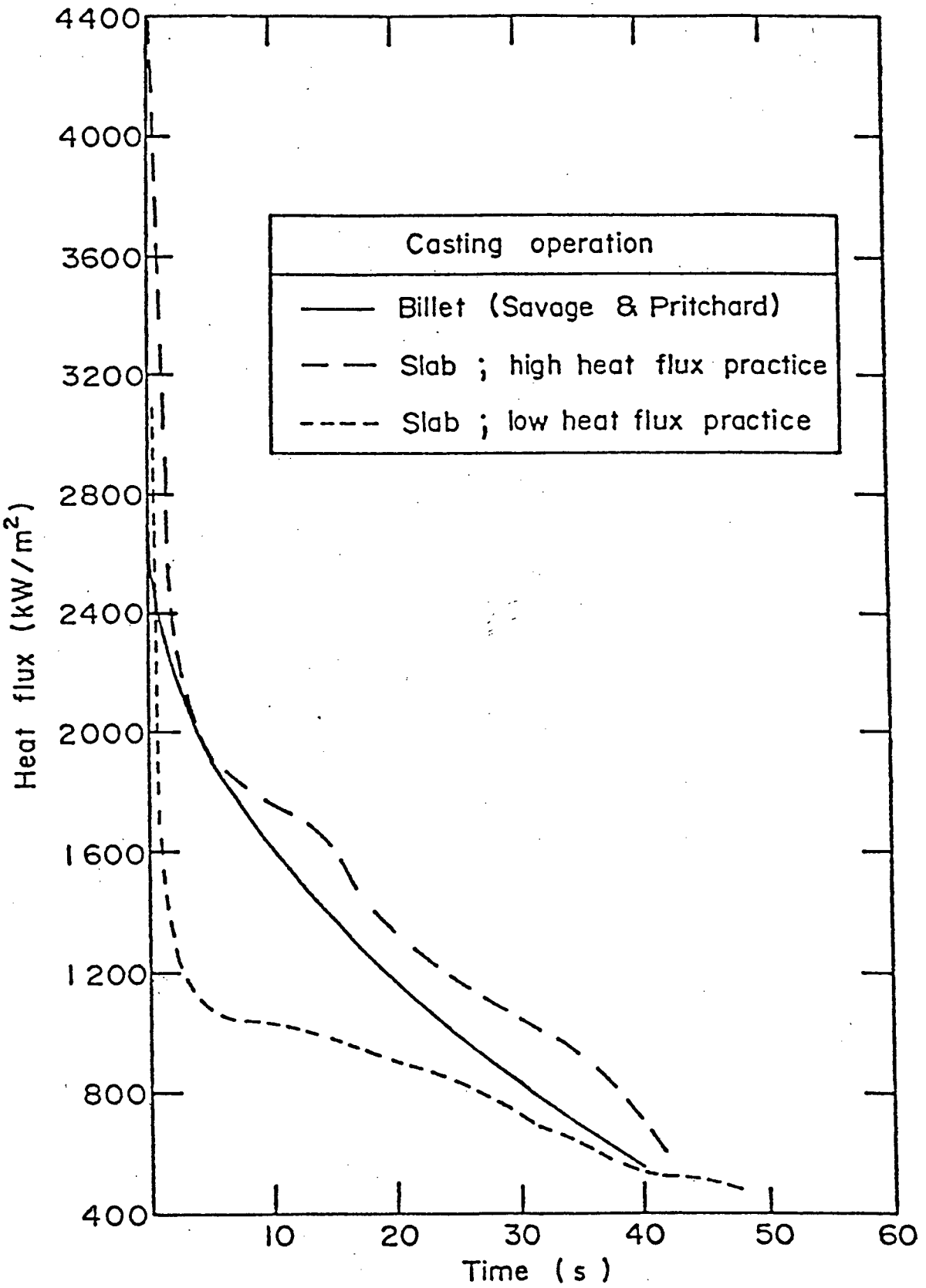

Figure 22 Relationship between surface heat flux and time-in-the-mould. From Samarasekera.[79]

in which a constant heat-transfer coefficient was applied over the entire secondary cooling zone under investigation. The heat-transfer coefficient was determined for particular experiments by obtaining agreement between predicted and measured surface temperatures at the top and bottom of the zone. This approach was deemed necessary in order to calculate average heat-transfer coefficients that would actually predict the measured temperatures. If the heat-transfer coefficient is assumed constant over the entire zone, the surface temperatures at the top and bottom of the zone will uniquely determine the temperature profile together with the value of the heat-transfer coefficient. An iterative technique would be necessary in order to simultaneously calculate the surface temperature profile and a constant heat-transfer coefficient that would result in the measured temperature at the bottom of the zone.

In order to reduce the number of computer runs in the present study, theoretical composite diagrams were drawn which relate heat-transfer coefficients to measured values of casting speed and temperature for each zone.

Chapter 5

RESULTS OF IN-PLANT MEASUREMENT

The experimental work has resulted in the acquisition of a large amount of data. The characteristics of the data (e.g., homogeneity of temperature traces, reliability of the measured flow rates) from each zone varies. Therefore in order to ensure uniformity of data analysis, and in order to attach significance to the variability of the data collected, standard techniques were developed. The purpose of this chapter is to discuss these techniques and to document the results of the in-plant measurements.

5.1 Treatment of Casting Speed and Temperature Data

In order to minimize fluctuations in the surface-temperature recordings that could be caused by the hostile measuring environment or intermittent surface scale, the 10-second peak-sense-and-hold feature of the Thermal Monitor System was utilized. This is an option provided with the Vanzetti system which maintains a maximum measured temperature reading for 10 seconds (or less, if desired), or until a higher temperature is measured (see Table V). The 10-second peak-sense-and-hold feature was used during all measurements except when it was desired to observe the local fluctuations caused by process

transients and the possible presence of scale. The peaks of the temperature traces, as discussed in Chapter 3, were considered to provide an accurate measurement of the true slab-surface temperature. Consequently, a statistical analysis was performed of the peaks of the temperature traces. This enabled the reporting of a mean value, and standard deviation, of peak temperature for the measurement period.

During normal casting operation, the metal level in the mould was maintained by operator adjustment of the casting speed. This results in a step-type characteristic of the casting-speed traces. The magnitude of the step changes is not large during usual operation, and thus periods in which small casting speed variations occurred were regarded as "steady-state." A statistical analysis of the plateaux in the casting speed traces during steady-state operation was performed. Means and standard deviations were determined for each period from which temperature measurements were used.

The values of temperature and casting speed are presented in the Table of Appendix A. Means and standard deviations of both variables are reported for each experiment. The steady-state period during which the reported measurements were made was usually 5 to 10 minutes.

5.2 Flow Rate Determination

In order to relate the temperature data to specific water fluxes, water flow rates were monitored. Values were read from magnetic and differential flowmeters provided for normal shop operation. As discussed previously, it was necessary to draw composite plots of water flow rate versus casting speed for each set point used in each zone. This was because chart recordings and on-line computer monitoring were not available for all casts. The relationships are presented in the figures of Appendix A. Because the readings of the metallurgical observer were not regarded as reliable, the chart-recorded and computer-stored data were used to determine the relationships shown. The scatter obtained from these sources was within 38 to 58 ℓ/min of the results given. Nearly all the readings of the metallurgical observer were found to be within the same range. This gave rise to a maximum expected error of approximately 13 per cent in the case of the lowest flow rates in Zone 5, and 5, 6 and 7 per cent respectively for Zones 2, 3 and 4.

The water flow rates theoretically obtained are given by the "speed-tie" equation:

$$F = F_c(-0.50 + 0.030(CSP)) \qquad (26)$$

It should be noted that the relationships given in Appendix A differ from the theoretical values of water flow rate determined

by the above equation. The average water fluxes which are reported were determined by dividing the overall flow rate to the zone by the surface area of the entire zone.

Chapter 6

CALCULATED RESULTS AND DISCUSSION

6.1 Sensitivity of the Calculations to Previous Thermal History

The calculation of heat-transfer coefficients from the measured surface temperatures required use of the mathematical heat-transfer model which has been described in Chapter 4. In order to calculate the heat-transfer coefficient corresponding to a particular set of measurements, the boundary conditions for the secondary cooling system were varied to obtain the desired slab surface temperature at the entrance and exit of each spray zone. Thus prediction of the correct temperatures at the top and bottom of Zone 4, for example, required choosing the appropriate boundary conditions in Zones 3 and 4. However, the boundary conditions for all zones prior to the one under study also must be given to the model. It was therefore of concern that inaccurate knowledge of the thermal history of the strand would cause inaccuracies in determining the "true" heat-transfer coefficient of a given spray zone. This possibility was studied systematically.

The effect of the pouring temperature of the steel on the model predictions was first considered. During the experimental period reported tundish temperatures ranged from 1535 to

1568°C. A statistical analysis of tundish temperatures measured during the experimental period resulted in a mean temperature of 1550 ± 12°C to a 95 per cent confidence level. The range of reported temperatures resulted in model-predicted temperatures with maximum errors of ±10, ±5, and ±3°C for Zones 2, 3, and 4, respectively. Because these deviations are approximately constant over the length of each zone, and because calculated heat-transfer coefficients are determined by temperatures measured at both the entrance and exit of the zones, these deviations are not considered significant. In particular, Zone 2, which is most affected by an error in tundish temperature input, is also more sensitive to the temperature measured at the top of the zone, as discussed in the next section. Thus the calculated values of heat-transfer coefficients are less sensitive to tundish temperature than are the predicted temperatures. A pouring temperature of 1550°C was used in all simulations.

The procedure for evaluating the effect on the heat-transfer coefficient of a given spray zone of thermal history in preceding cooling zones is illustrated by considering the particular case of Zone 3. In order to evaluate the effect of thermal history on the temperature profile in Zone 3, three different temperatures at the entrance to Zone 3 were selected, and the model was run for each for a wide range of temperatures at the top of Zone 2. It was found that when temperatures at the entrance to Zone 2C were varied by ±100°C

the temperatures at the exit of Zone 3 varied by a maximum of ±6°C for a given temperature at the top of Zone 3. The sensitivity became less as entrance temperatures in Zone 3 dropped below 1000°C. Therefore it was concluded that predicted temperature profiles and calculated heat-transfer coefficients are not significantly affected by the thermal history of the slab prior to its entering Zone 3.

Similar checks showed that the predicted temperature profiles in Zones 4 and 5 are less sensitive to thermal history than the profile in Zone 3. The sensitivities of exit temperatures in Zones 2B and 2C to entrance temperatures in Zones 2A and 2B was similar to the case of Zone 3. Though the next section will indicate that heat-transfer coefficients calculated in Zone 2 are more sensitive to temperature than those of the other zones, the fact that temperatures were measured simultaneously over the entirety of Zone 2 means that the thermal history is known. Thus heat-transfer coefficients calculated simultaneously for Zones 2A, 2B, and 2C will be uniquely determined. Thus it may be concluded that results reported in the remainder of the present work are not significantly affected by the "unknown" thermal history of the slab.

6.2 Theoretical Relationships Between Heat-Transfer Coefficients and Temperatures

The trial-and-error method for the calculation of

heat-transfer coefficients necessitated a means of obtaining a good initial approximation of a particular value for particular experimental conditions and measurements. The approach taken to solve this problem was to determine the relationships between the average heat-transfer coefficient and the exit temperature of the slab for each secondary cooling zone. These relationships are shown graphically for different casting speeds in Figures 23 to 28. Thus for given measured values of casting-speed and slab-surface temperatures at the entrance and exit of a particular zone, it is possible to estimate the appropriate heat-transfer coefficient from these figures. Also, Figures 23 to 28 may be used to evaluate the sensitivity of the heat-transfer coefficient to the measured values of temperature. A worthy point of note is that the heat-transfer coefficient is much more sensitive to surface temperature at the end of a zone than to either the casting speed or the temperature at the top of the zone. The sensitivity is dependent on both the position of the zone (i.e., distance below the meniscus) and the zone length. Thus heat-transfer coefficients for Zone 2 are more sensitive to the measured values of temperature than those of Zones 3 or 4.

6.3 Approach to Calculation of Average Heat-Transfer Coefficients for Zone 2

Slab-surface temperatures in Zone 2, as has been mentioned,

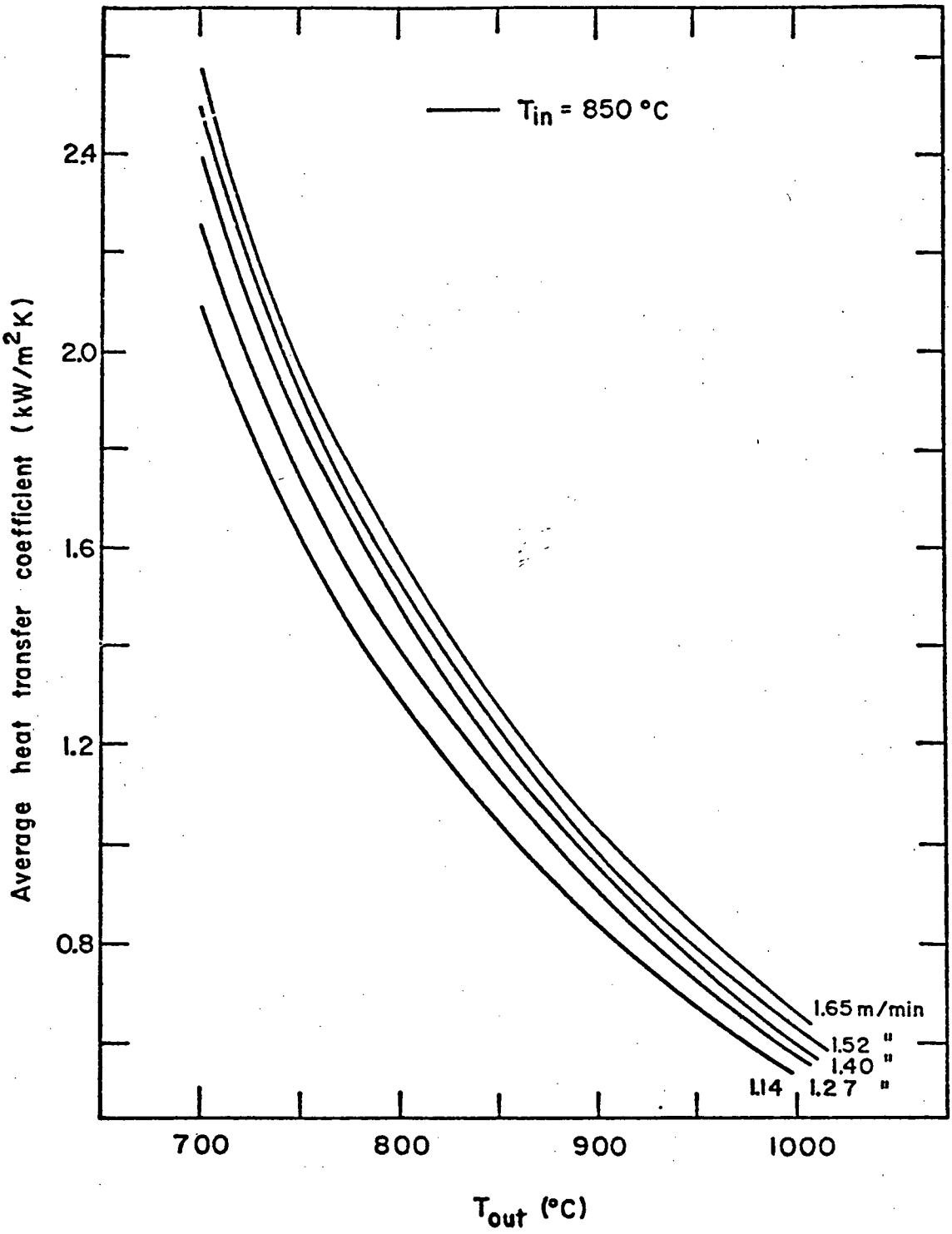

Figure 23 Model-predicted relationships between heat-transfer coefficient and temperature, Zone 2A.

a) Effect of casting speed.

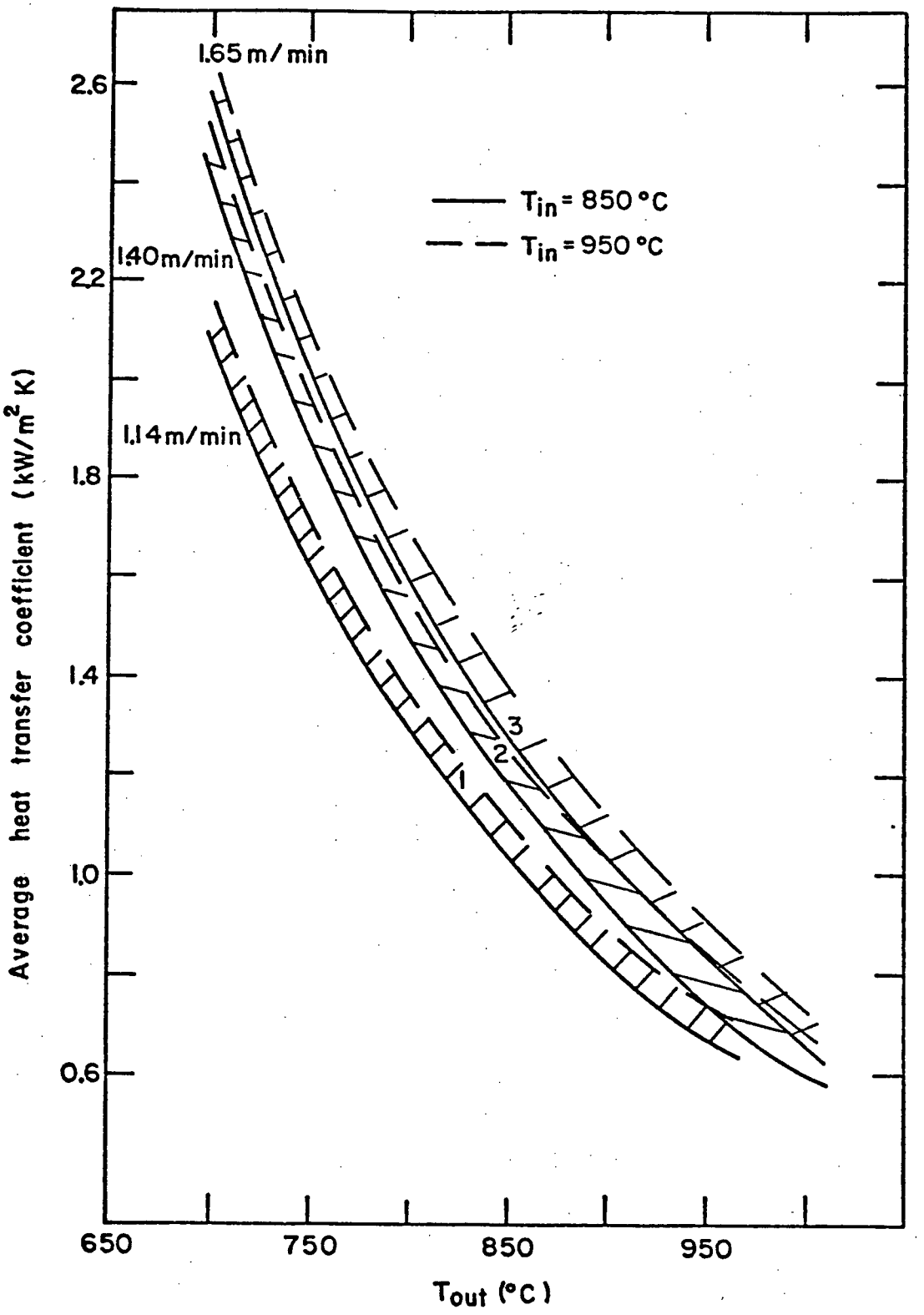

Figure 23 b) Effect of temperature entering the zone.

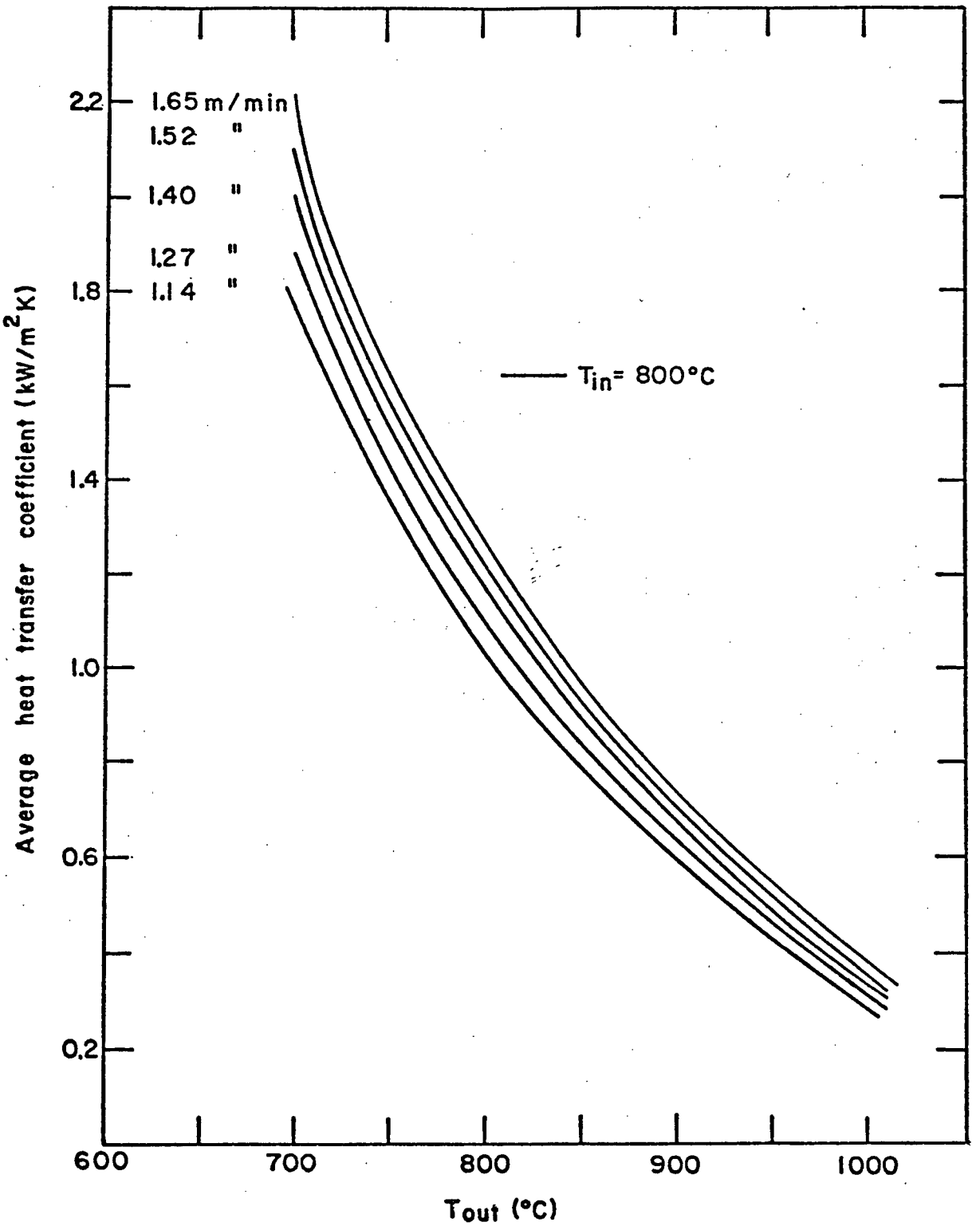

Figure 24 Model-predicted relationships between heat-transfer coefficient and temperature, Zone 2B.

a) Effect of casting speed.

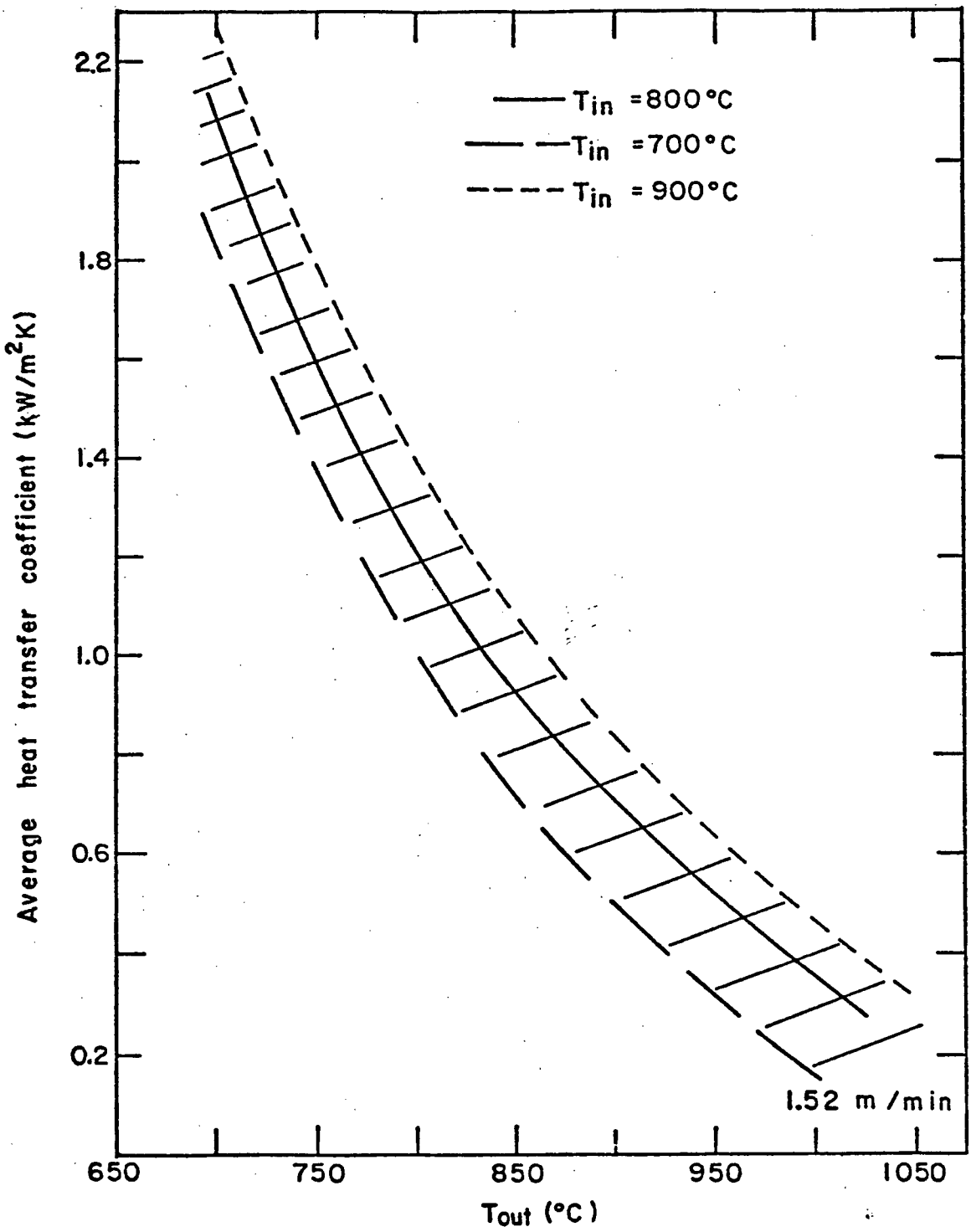

Figure 24 b) Effect of temperature entering the zone.

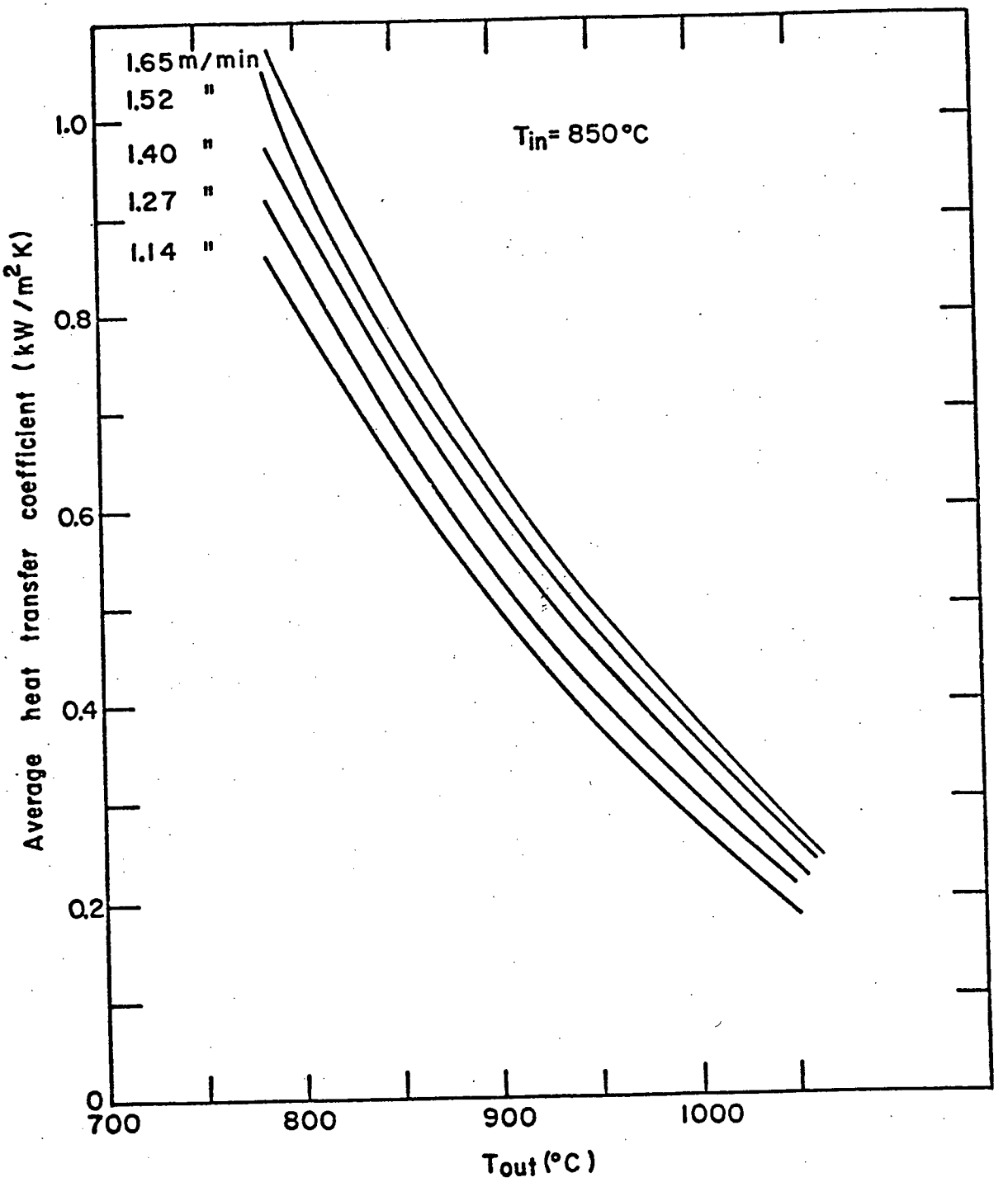

Figure 25 Model-predicted relationships between heat-transfer coefficient and temperature, Zone 2C.

a) Effect of casting speed.

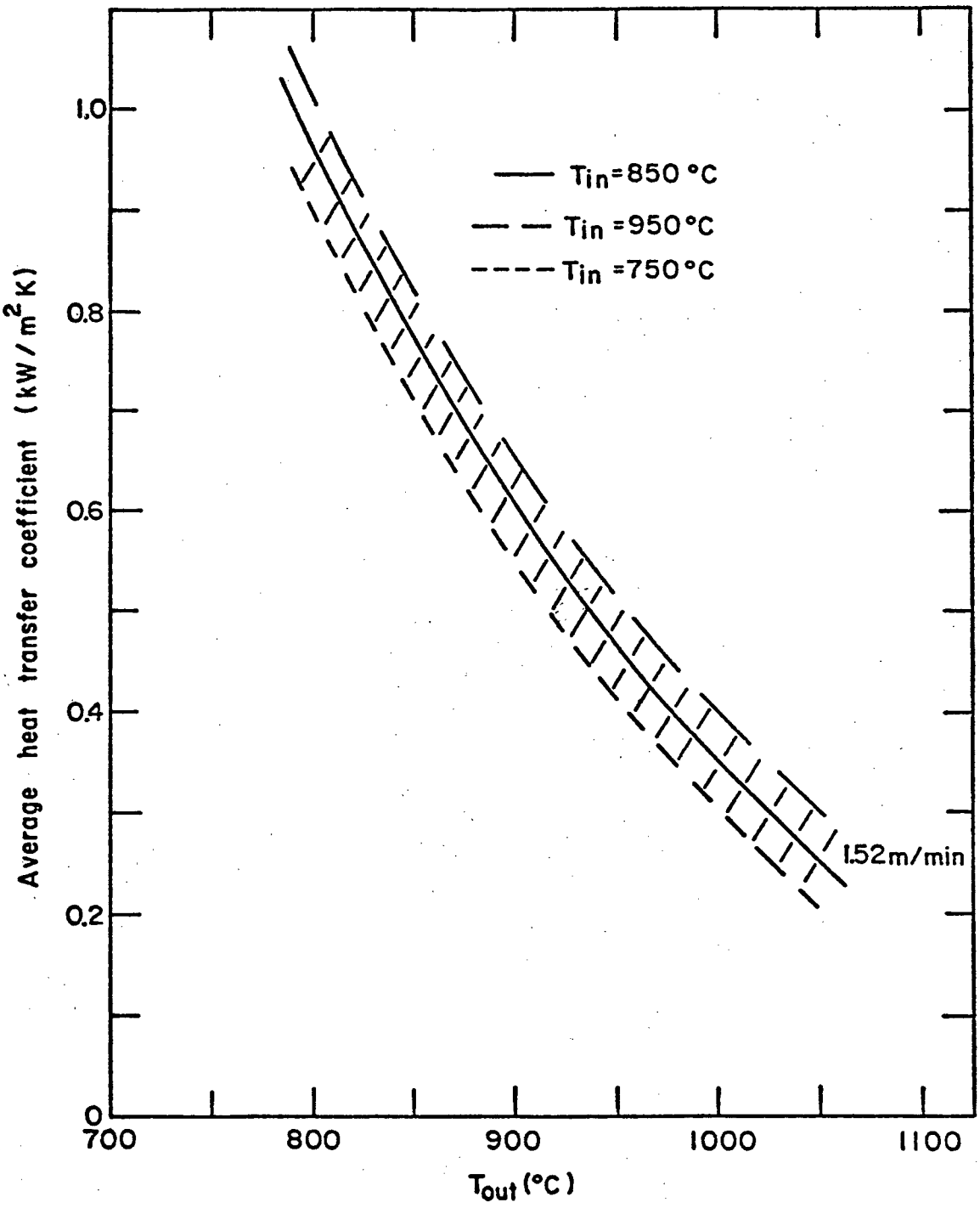

Figure 25 b) Effect of temperature entering the zone.

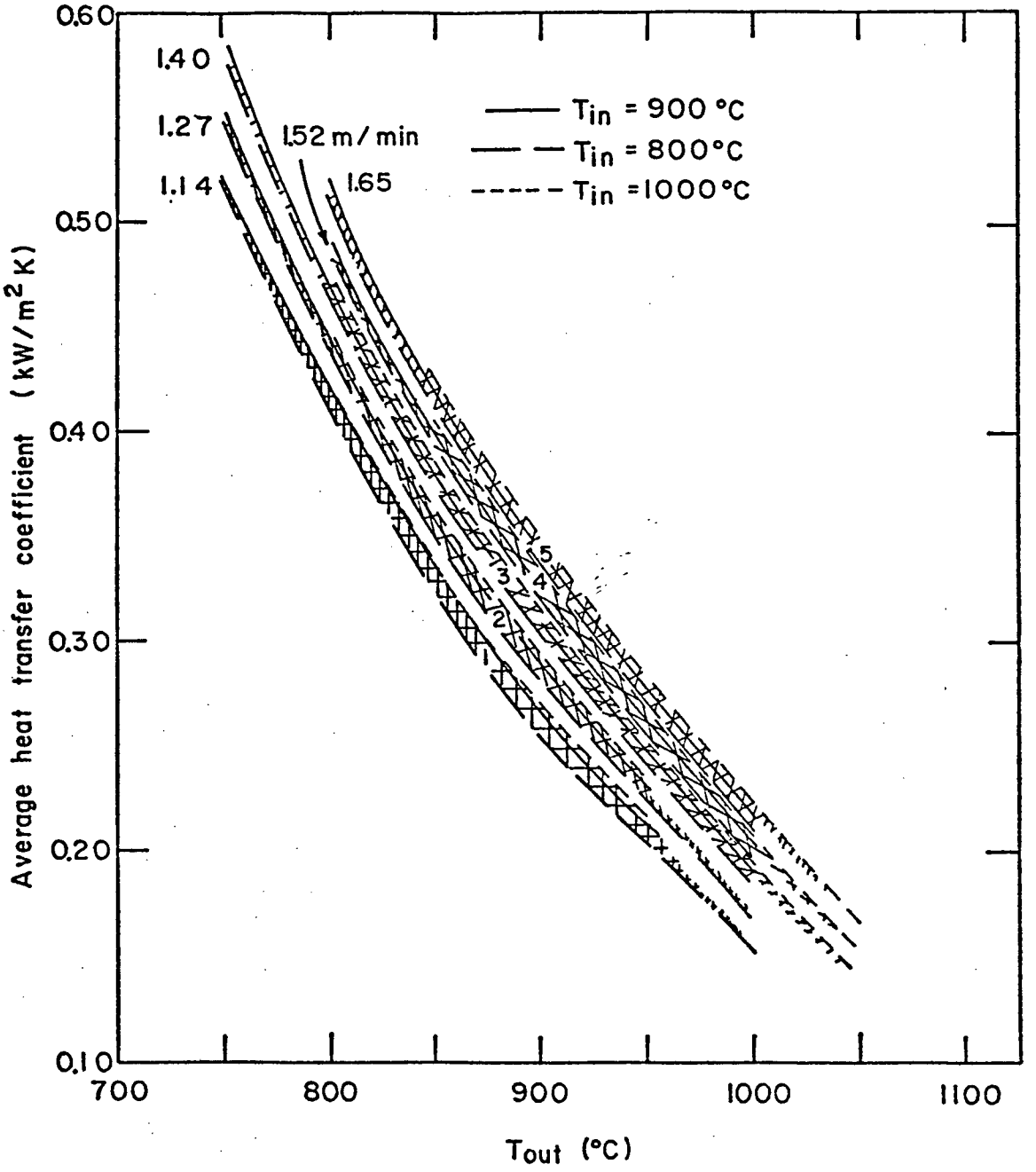

Figure 26 Model-predicted relationships between heat-transfer coefficient and temperature, Zone 3.

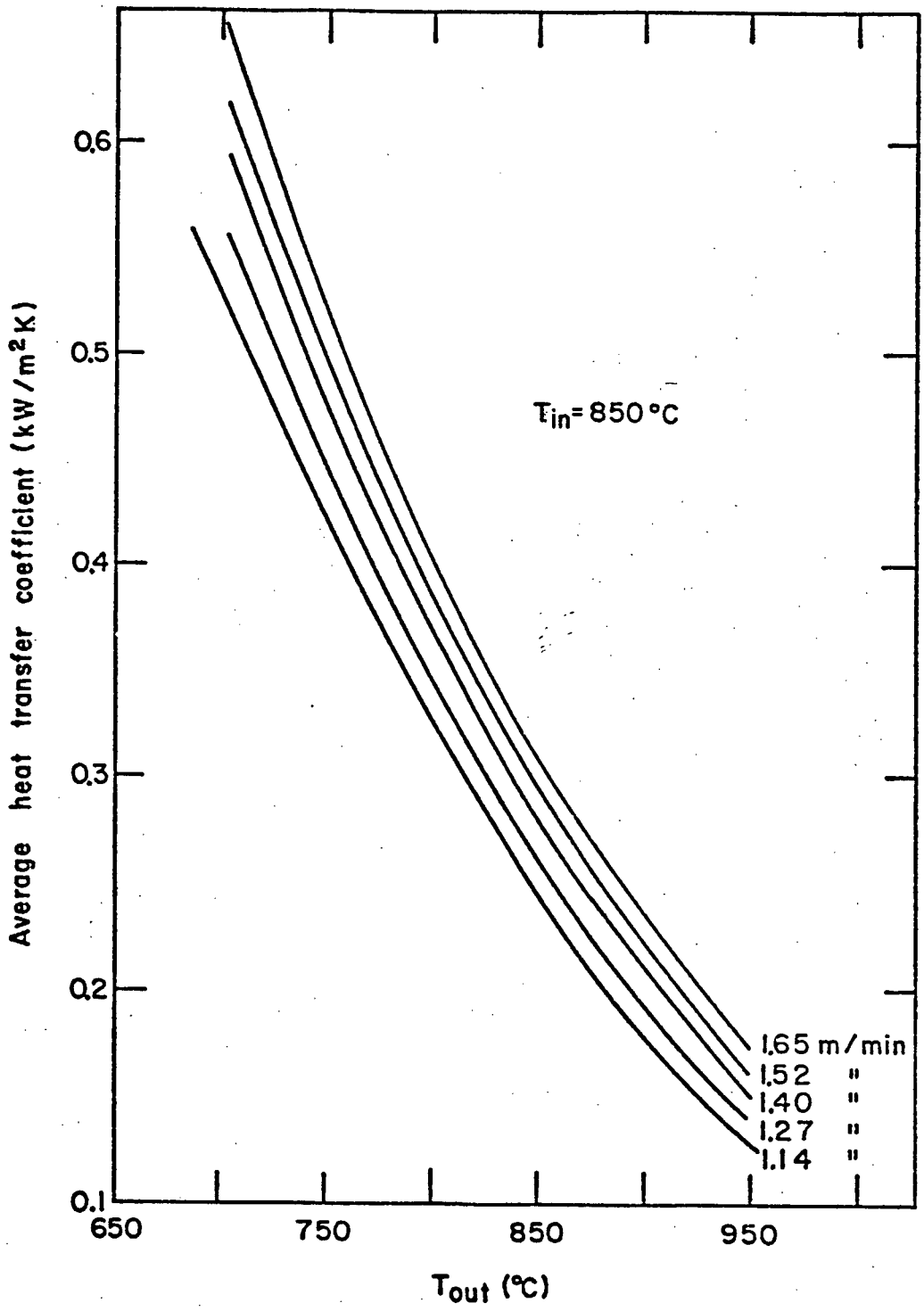

Figure 27 Model-predicted relationships between heat-transfer coefficient and temperature, Zone 4.

a) Effect of casting speed.

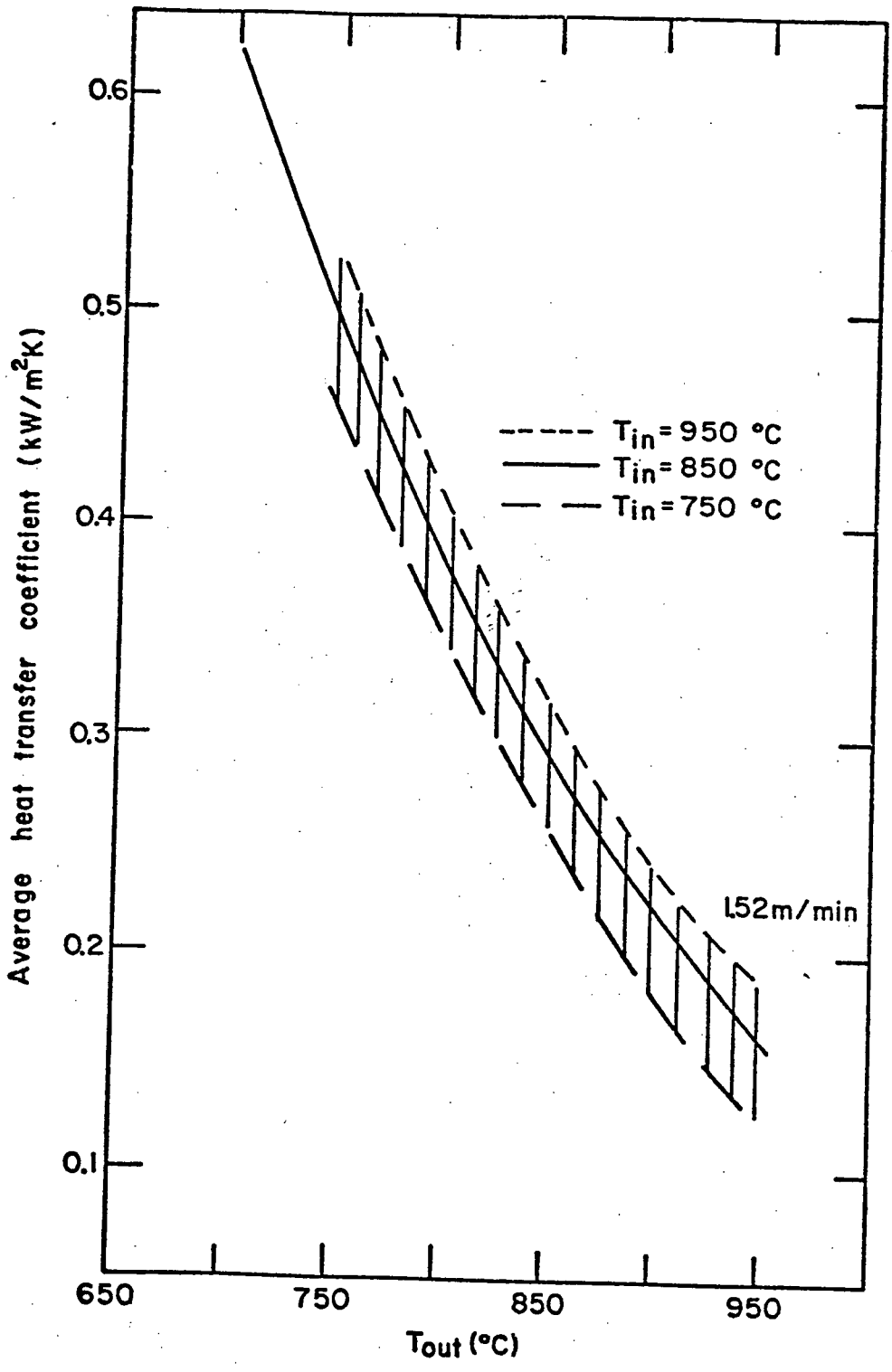

Figure 27 b) Effect of temperature entering the zone.

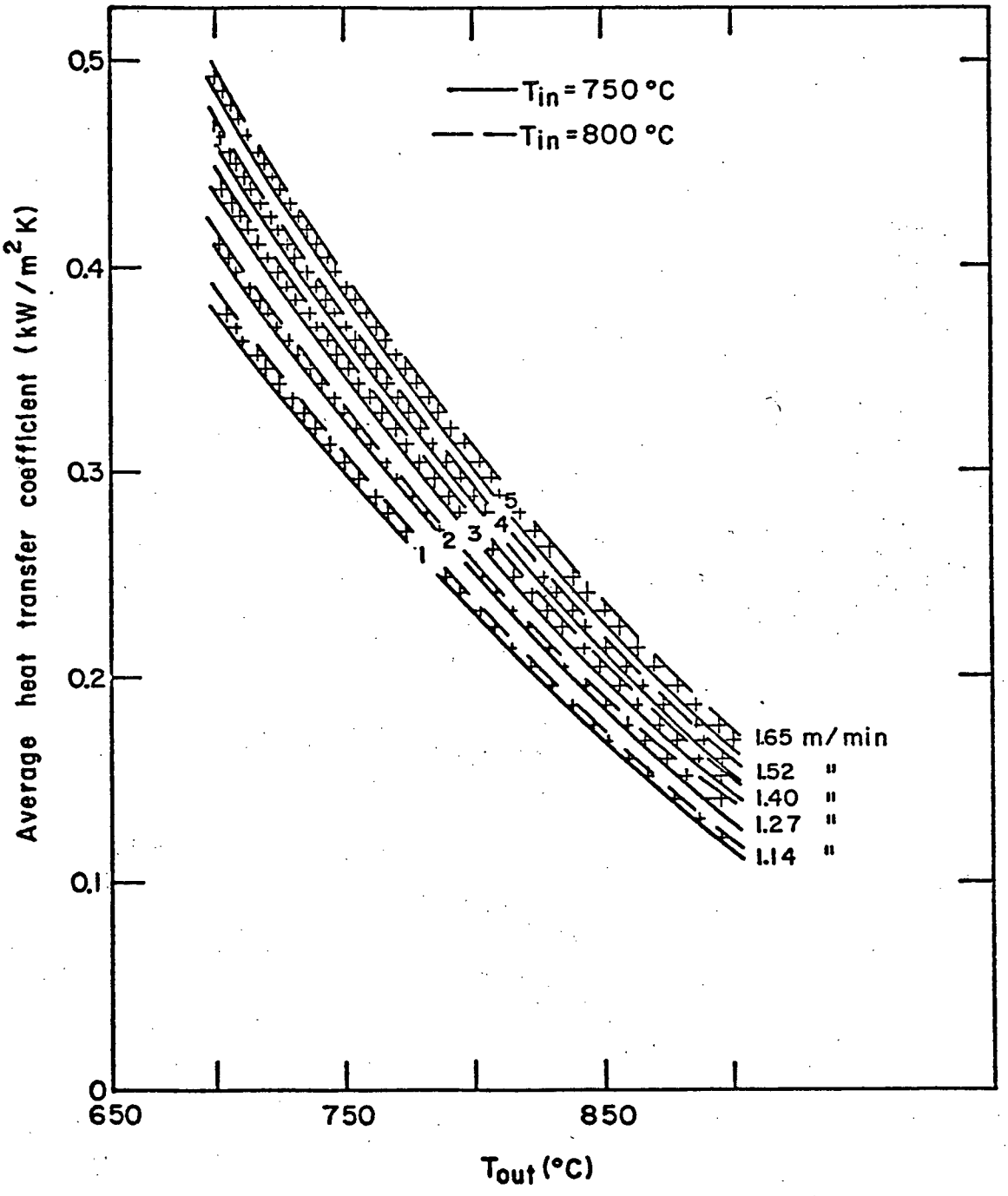

Figure 28 Model-predicted relationships between between heat-transfer coefficient and temperature, Zone 5.

were measured in the spray-impingement area. Because it was expected that there would be large differences between the amount of heat extracted in the sprayed and the non-sprayed areas, these measurements were not considered suitable for direct determination of average heat-transfer coefficients. This was further complicated by the fact that the measurement points were not at the "boundaries" between Zones 2A, 2B or 2C. The boundaries in Zone 2 are considered in the present modelling work to be at the point of roll contact between nozzles of the different zones.

The approach to calculating heat-transfer coefficients in Zone 2 was thus to initially determine local heat-transfer coefficients in the spray-impingement area. This was accomplished by forming many "subzones" in each of which the heat flux could be independently evaluated. The local heat-transfer coefficient in the spray-impingement area was determined by varying the boundary condition to achieve the desired temperature at the centre of the pyrometer sighting area. In the non-sprayed areas, the temperature rises due to the much smaller heat fluxes obtained in the presence of only radiation, roll contact, and convection to water running down the surface. The works of Etienne et al.[48] and Diener et al.[66] indicate that the amount of heat removed by convection and roll contact in the non-sprayed areas is very small this high in the machine.

In fact, preliminary calculations based on these works indicate that heat fluxes in the non-sprayed areas would be about 5 per cent of those in the sprayed areas. Approximately one-half of this 5 per cent would be due to radiation. Thus the exact characterization of heat transfer in the non-sprayed areas is not significant in determining the overall temperature profile, or the value of the local heat-transfer coefficient. On this basis, the predicted profile determined from the local heat-transfer coefficient in the sprayed area and radiation heat transfer in the non-sprayed area was used to estimate the temperatures at the entrance and exit of each zone. These calculated temperatures were then used, assuming a smoothed profile as in the calculations of the other zones, to determine the "average" heat-transfer coefficient of Zones 2A, 2B and 2C. This approach has allowed an overall correlation between average heat-transfer coefficient and average water flux for each zone to be obtained. It has also allowed comparison of values of local heat-transfer coefficient determined from these industrial measurements to those obtained in laboratory studies. Furthermore, the existence and significance of the local temperature profile as the slab passes through regions of varying cooling intensity has been brought out. These points will be discussed in detail later.

6.4 Correlations Between Heat-Transfer Coefficients and Spray Water Fluxes

Heat-transfer coefficients were calculated for each experiment and related to the pertinent operating parameters by use of the procedures discussed in the previous sections. The numerical results of these calculations are presented in Tables X to XV. Tables X, XI and XII give the casting conditions, measured-surface temperatures of the slab at the start and end of the zones, and calculated average heat-transfer coefficients for Zones 3, 4 and 5, respectively. Tables XIII, XIV and XV give similar data for Zones 2A, 2B and 2C. In the latter tables the local heat-transfer coefficients, calculated temperatures at the top and bottom of the zone, and corresponding average heat-transfer coefficients are given, in addition to the relevant operating data.

The experimental limitations of this work did not allow independent study of spray variables such as spray pressure, nozzle type or nozzle setback for a particular zone. Any effect that may have been due to differences in these variables between the different secondary cooling zones was not discernable. The observable spray-related differences in heat-transfer coefficients that were determined could be attributed entirely to the spray water flux obtained in the different zones. The effect of variables such as spray pressure, nozzle setback and

TABLE X Zone 3 Measured and Calculated Results

Cast	Casting Speed (m/min)	Average Water Flux (ℓ/m^2s)	Temperature, °C		Average Heat Transfer Coefficient (kW/m^2K)	Average Heat Flux (MW/m^2)
			Entering Zone	Exiting Zone		
9732	1.34	0.94	917	964	.225	.332
	1.27	1.05	891	945	.235	.331
	1.33	1.57	947	915	.283	.367
	1.48	2.00	916	866	.364	.416
9737	1.42	1.65	1041	926	.288	.385
9738	1.52	1.19	1050	950	.273	.383
9757	1.40	1.62	994	854	.374	.423
	1.40	1.97	1000	800	.480	.477
9757	1.44	1.17	1003	1024	.172	.314
9760	1.25	1.03	920	949	.229	.329
	1.35	1.57	946	934	.263	.357
	1.36	1.96	970	892	.320	.391
9763	1.57	1.26	1043	1045	.165	.319
	1.36	1.58	1038	953	.246	.357
	1.56	2.03	1047	903	.340	.423
9974	1.49	1.21	819	993	.200	.314
	1.44	1.66	832	926	.279	.359
9777	1.51	1.22	825	981	.217	.326
	1.55	1.79	803	934	.281	.362
	1.51	2.01	814	911	.306	.375
9781	1.39	1.13	857	962	.228	.331
	1.47	1.70	881	918	.296	.376
	1.40	1.97	821	862	.351	.393
9786	1.38	1.12	839	827	.409	.423
9787	1.49	1.21	824	906	.309	.377
9788	1.37	1.11	839	993	.190	.337

TABLE XI Zone 4 Measured and Calculated Results

Cast	Casting Speed (m/min)	Average Water Flux (ℓ/m^2s)	Temperature, °C		Average Heat Transfer Coefficient (kW/m^2K)	Average Heat Flux (MW/m^2)
			Entering Zone	Exiting Zone		
9810	1.52	1.52	785	778	.414	.376
	1.73	1.52	812	795	.415	.389
	1.52	1.33	882	905	.227	.291
9851	1.33	1.52	903	748	.481	.426
	1.46	1.52	868	866	.263	.307
	1.42	1.27	857	898	.217	.253
9856	1.52	1.00	942	942	.195	.284
9857	1.56	1.52	923	877	.277	.330
	1,60	1.38	898	951	.180	.276
9858	1.54	1.52	912	873	.276	.324
	1.52	1.33	896	896	.241	.302
9859	1.49	1.52	842	751	.488	.426
	1.42	1.27	860	835	.306	.326
9860	1.45	0.96	945	937	.194	.282
9861	1.40	0.93	958	955	.169	.267
9862	1.57	1.52	928	894	.259	.321
	1.35	1.23	922	900	.221	.289
	1.48	0.98	897	907	.223	.291
9863	1.38	0.91	927	957	.158	.252
9901	1.44	0.95	814	914	.184	.248
9902	1.73	1.52	861	788	.450	.419
	1.48	1.30	872	796	.397	.383
	1.60	1.05	849	851	.298	.325
9903	1.63	1.52	872	763	.497	.444
	1.22	1.15	844	900	.187	.249
	1.47	1.52	864	712	.589	.482
9906	1.60	1.52	905	805	.404	.397
	1.59	1.52	877	783	.446	.415
	1.56	1.35	888	811	.380	.379
9907	1.65	1.52	890	819	.378	.381
	1.30	1.46	831	786	.374	.354
	1.49	1.52	811	767	.441	.395
	1.38	1.24	850	862	.250	.291
9910	1.49	1.52	1016	819	.389	.408
	1.43	1.27	1022	858	.310	.363
	1.46	0.97	1018	895	.266	.340
9911	1.47	1.52	912	736	.544	.468
	1.52	1.33	846	734	.534	.453
	1.52	1.00	755	802	.536	.336

TABLE XII Zone 5 Measured and Calculated Results

Cast	Casting Speed (m/min)	Average Water Flux (ℓ/m^2s)	Temperature, °C		Average Heat Transfer Coefficient (kW/m^2K)	Average Heat Flux (MW/m^2)
			Entering Zone	Exiting Zone		
0288	1.45	0.87	862	844	.215	.255
	1.44	0.95	807	835	.219	.250
0299	1.55	0.95	811	771	.338	.320
	1.52	0.95	764	762	.338	.311
0314	1.53	0.95	696	761	.320	.287
	1.57	0.95	687	760	.322	.287
0317	1.30	0.45	779	787	.268	.269
	1.45	0.57	779	807	.262	.271
0401	1.30	0.27	843	865	.168	.223
0402	1.47	0.27	922	873	.192	.254
0403	1.60	0.58	807	836	.238	.266
	1.46	0.58	797	818	.250	.267
0404	1.51	0.57	789	857	.194	.236
	1.34	0.56	783	825	.218	.243
0406	1.57	0.47	754	841	.216	.245
	1.37	0.48	765	838	.200	.232
	1.61	0.58	775	836	.233	.259
0417	1.45	0.53	768	815	.247	.261
	1.49	0.58	768	798	.279	.280
0449	1.61	0.58	853	819	.273	.292
	1.45	0.58	808	796	.284	.287
0451	1.61	0.58	870	810	.295	.303
	1.60	0.58	813	812	.277	.289
0452	1.40	0.27	950	807	.280	.300
0453	1.44	0.53	769	797	.273	.276
	1.42	0.58	726	787	.272	.266

TABLE XIII Zone 2A Measured and Calculated Results

Cast	Casting Speed (m/min)	Local Water Flux (ℓ/m^2s)	Measured Temp. (°C)	Local Heat Transfer Coefficient (kW/m^2K)	Calculated Temperature (°C)		Average Water Flux (ℓ/m^2s)	Average Heat Transfer Coefficient (kW/m^2K)	Average Heat Flux (MW/m^2)
					Entering Zone	Exiting Zone			
9950	1.32	15.00	746	3.170	841	772	7.85	1.600	1.304
9951	1.33	15.09	741	4.850	933	704	7.90	2.580	1.972
	1.57	16.79	844	2.450	932	877	8.79	1.170	1.119
9954	1.55	16.64	821	3.400	934	820	8.71	1.630	1.453
9966	1.46	16.02	710	4.450	754	697	8.39	2.280	1.642
	1.40	13.45	737	4.080	846	725	7.04	2.094	1.607
	1.53	18.47	758	3.660	850	755	9.67	1.905	1.519
9967	1.66	11.88	848	1.980	859	907	6.22	1.027	0.990
	1.47	13.76	793	2.790	855	815	7.20	1.410	1.209
	1.53	16.52	761	3.480	833	762	8.65	1.820	1.457
9968	1.40	15.56	786	3.000	873	796	8.14	1.498	1.268
	1.46	17.88	761	3.500	838	757	9.67	1.830	1.456
9970	1.34	13.20	798	2.250	828	847	6.9o	1.100	0.983
	1.47	16.06	787	3.070	874	796	8.41	1.550	1.307
	1.48	18.03	731	4.600	842	713	9.44	2.280	1.719
9971	1.51	13.95	780	3.150	840	790	7.30	1.590	1.317
	1.43	15.79	788	3.024	867	800	8.27	1.500	1.270
	1.46	17.88	737	4.570	838	697	9.36	2.450	1.810
9972	1.47	11.14	782	3.080	854	793	5.85	1.550	1.292
	1.49	13.81	772	3.350	841	778	7.23	1.663	1.362
	1.50	16.31	744	3.540	820	752	8.54	1.875	1.473
9973	1.33	13.16	768	3.180	834	769	6.89	1.637	1.324
	1.53	16.52	765	3.450	835	766	8.65	1.790	1.439
	1.52	18.34	788	3.080	854	798	9.60	1.550	1.301
9974	1.45	11.11	865	1.550	841	950	5.81	0.775	0.794
	1.40	13.45	854	1.610	847	948	7.04	0.767	0.787
	1.48	16.16	766	3.420	830	770	8.46	1.710	1.379
9976	1.52	16.45	790	3.000	882	811	8.61	1.480	1.271
	1.57	18.81	835	1.990	847	908	9.85	0.974	0.939
9977	1.60	14.30	787	3.050	850	794	7.49	1.618	1.351
	1.60	17.00	793	3.170	863	802	8.90	1.570	1.327
	1.53	18.47	756	3.740	855	752	9.67	1.935	1.540
9978	1.45	11.11	776	3.120	843	783	5.81	1.610	1.327
	1.54	16.58	767	3.470	834	767	8.68	1.780	1.430
	1.51	13.95	755	3.800	841	749	7.30	1.925	1.519
9980	1.44	13.64	849	1.670	841	928	7.14	0.843	0.837
	1.49	16.24	789	3.060	859	807	8.50	1.483	1.261
	1.48	18.03	763	3.560	842	765	9.44	1.770	1.424
9982	1.47	11.14	827	2.140	854	879	5.85	1.050	0.978
	1.57	14.20	750	4.000	847	743	7.44	2.033	1.595
	1.54	16.58	770	3.390	841	771	8.68	1.765	1.426

TABLE XIV Zone 2B Measured and Calculated Results

Cast	Casting Speed (m/min)	Local Water Flux (ℓ/m^2)	Measured Temperature (°C)	Local Heat Transfer Coefficient (kW/m^2K)	Calculated Temperature (°C)		Average Water Flux (ℓ/m^2)	Average Heat Transfer Coefficient (kW/m^2K)	Average Heat Flux (MW/m^2)
					Entering Zone	Exiting Zone			
9950	1.32	16.00	723	4.870	772	758	4.46	1.380	1.077
9951	1.33	16.09	725	4.400	704	777	4.49	1.230	0.951
	1.57	17.91	731	7.800	877	712	4.99	2.165	1.646
9954	1.55	17.75	742	6.000	820	766	4.95	1.680	1.344
9966	1.40	14.35	763	2.720	725	853	4.00	0.725	0.630
	1.46	17.09	739	2.330	697	850	4.77	0.648	0.555
	1.53	19.70	752	4.380	755	790	5.49	1.210	0.975
9967	1.66	12.67	877	2.950	907	933	3.53	0.762	0.786
	1.47	14.68	804	2.960	815	873	4.10	0.788	0.733
	1.53	17.62	761	4.050	762	804	4.91	1.120	0.923
9968	1.40	17.70	768	4.340	796	797	4.63	1.175	0.977
	1.46	19.07	720	5.750	757	731	5.32	1.645	1.233
9970	1.34	14.08	807	3.180	847	868	3.93	0.820	0.765
	1.47	17.13	773	3.770	796	817	4.78	1.080	1.080
	1.48	19.23	702	5.300	713	738	5.36	1.480	1.094
9971	1.51	14.88	806	2.530	790	908	4.15	0.650	0.626
	1.43	16.84	795	3.030	800	867	4.70	0.793	0.772
	1.46	19.07	710	4.820	697	745	5.32	1.360	1.006
9972	1.47	11.88	873	0.920	793	1019	3.32	0.275	0.350
	1.49	14.73	842	1.290	778	994	3.91	0.370	0.418
	1.50	17.39	788	2.350	752	887	4.85	0.643	0.592
9973	1.33	14.04	770	3.380	769	826	3.91	0.930	0.793
	1.53	17.62	765	3.900	766	812	4.9o	1.080	0.900
	1.52	19.56	715	7.300	798	712	5.45	1.965	1.462
9974	1.45	11.85	894	2.540	950	963	3.30	0.635	0.701
	1.40	14.35	877	3.000	948	918	4.00	0.775	0.798
	1.48	17.23	718	5.580	770	748	4.81	1.535	1.180
99.76	1.52	17.54	762	5.090	811	778	4.89	1.395	1.134
	1.57	20.06	742	7.800	908	713	5.60	2.165	1.657
9977	1.60	15.25	865	1.290	794	999	4.26	0.358	0.418
	1.60	18.13	839	2.100	802	944	5.06	0.565	0.579
	1.53	19.70	768	3.440	752	832	5.49	0.940	0.800
9978	1.45	11.85	860	1.000	783	1018	3.30	0.265	0.339
	1.51	14.88	817	1.340	749	971	4.15	0.360	0.393
	1.54	17.68	818	1.800	767	944	4.93	0.485	0.496
9980	1.44	14.55	990	0.670	928	1093	4.06	0.202	0.362
	1.49	17.32	886	1.000	807	1020	4.83	0.298	0.377
	1.48	19.23	809	1.870	765	940	5.36	0.459	0.501
9982	1.47	11.88	957	0.725	879	1071	3.32	0.220	0.341
	1.57	15.15	838	0.650	743	1017	4.23	0.198	0.266
	1.54	17.68	849	1.000	771	1008	4.93	0.275	0.340

TABLE XV Zone 2C Measured and Calculated Results

Cast	Casting Speed (m/min)	Local Water Flux (ℓ/m^2s)	Measured Temperature (°C)	Local Heat Transfer Coefficient (kW/m^2K)	Calculated Temperature (°C)		Average Water Flux (ℓ/m^2s)	Average Heat Transfer Coefficient (kW/m^2K)	Average Heat Flux (MW/m^2)
					Entering Zone	Exiting Zone			
9950	1.32	9.92	821	0.850	758	1060	2.39	.150	.254
9951	1.33	9.98	790	2.400	777	971	2.40	.390	.444
	1.57	11.11	747	2.500	712	961	2.67	.397	.429
9967	1.66	7.86	922	1.800	933	1062	1.66	.300	.436
	1.47	9.10	792	4.200	873	868	2.19	.690	.674
	1.53	10.93	775	3.500	804	903	2.63	.575	.574
9968	1.40	10.29	847	1.230	797	1046	2.48	.225	.329
9970	1.34	8.72	791	3.800	868	884	2.10	.625	.626
	1.47	10.63	849	1.320	849	1047	2.56	.240	.348
	1.48	11.93	731	3.700	738	863	2.87	.608	.561
9971	1.51	9.22	798	4.120	908	884	2.22	.675	.676
	1.43	10.45	807	3.150	867	936	2.52	.510	.556
	1.46	11.83	743	3.300	745	896	2.84	.520	.506
9972	1.47	7.37	845	4.200	1019	893	1.78	.685	.714
	1.49	9.13	780	5.620	984	809	2.20	.965	.872
	1.50	10.79	768	5.030	887	809	2.60	.915	.808
9973	1.33	8.70	789	2.980	826	927	2.09	.485	.516
	1.53	10.93	773	3.600	812	897	2.63	.595	.590
	1.52	12.13	750	1.920	712	978	2.92	.328	.374
9974	1.45	7.35	858	3.440	963	943	1.77	.562	.630
	1.40	8.89	869	2.700	918	974	2.14	.461	.545
	1.48	10.69	754	2.980	748	919	2.57	.485	.492
9976	1.52	10.88	750	3.850	778	875	2.62	.625	.598
	1.57	12.45	749	2.500	713	953	3.00	.410	.437
9977	1.60	9.46	798	4.680	999	872	2.28	.760	.766
	1.60	11.25	776	5.150	944	838	2.71	.865	.810
	1.53	12.22	753	5.000	832	818	2.94	.870	.768
9978	1.45	7.35	847	4.070	1018	1016	1.77	.380	.503
	1.51	9.22	809	4.410	971	872	2.22	.710	.712
	1.54	10.97	780	5.280	944	820	2.64	.910	.827
9980	1.44	9.02	938	3.200	1093	984	2.17	.505	.628
	1.49	10.74	853	3.940	1020	916	2.58	.635	.688
	1.48	11.93	857	2.750	940	977	2.87	.440	.525
9982	1.47	7.37	906	3.410	1071	966	1.78	.540	.645
	1.57	9.39	826	4.700	1017	861	2.26	.775	.771
	1.54	10.97	789	5.960	1008	802	2.64	1.020	.916

nozzle type was thus considered to be incorporated in the spray water flux.

The variables other than water flux, that the literature indicates may affect the heat-transfer coefficient, are spray water temperature and slab surface temperature. It was also thought possible that slab width might cause an effect because wider slabs tend to bulge more and would perhaps lose more heat to the rolls. The influence of spray water temperature could not be assessed because under steady-state conditions the temperature was nearly constant at 27°C. It was found that the steel grade, slab width and slab surface temperature did not affect the heat-transfer coefficient. It should be noted that in the latter case the surface temperature referred to is that at the entrance to the zone under study. Although the surface temperature at the top of the zones did not influence the heat-transfer coefficient, this does not mean that there is no effect of surface temperature anywhere in the secondary cooling system. It is conceivable that if the local temperature fluctuations the slab experiences as it passes through regions of direct spray-impingement, roll contact and convection cause the temperature to drop below the Leidenfrost temperature intermittently, there will be a surface temperature effect. However under the conditions of this study it is not possible to quantify this effect in terms of measured values of temperature at the entrance of the zones. This is

an important point and will be discussed in detail later.

Attempts to correlate the heat-transfer coefficients to spray water flux were carried out using linear and logarithmic regressions. It was found that the best fit was obtained when the data from all zones was correlated by linear regression. The regression line and data are plotted in Figure 29. The regression equation for the entire data set was found to be

$$h = 0.084 + 0.187\,\dot{W} \quad \pm 50\%,\ r^2 = 0.75 \qquad (27)$$

Figure 29 also shows the range of water flow rates that were attained in each zone.

Correlations were also obtained from the data sets for individual zones. The data and regression lines of Zones 3, 4, 5 and 2 are shown in Figures 30, 31, 32 and 33 respectively. In these zones, the best correlations obtained between average heat-transfer coefficient and average water flux were as follows:

Zone 3	$h = 0.213\dot{W}^{0.665}$	$\pm 25\%$, $r^2 = 0.60$	(28)
Zone 4	$h = 0.212\dot{W}^{1.424}$	$\pm 40\%$, $r^2 = 0.31$	(29)
Zone 5	$h = 0.182 + 0.122\,\dot{W}$	$\pm 25\%$, $r^2 = 0.31$	(30)
Zone 2A	$h = 0.274\dot{W}^{0.834}$	$\pm 40\%$, $r^2 = 0.21$	(31)
Zone 2B	$h = -1.279 + 0.474\dot{W}$	$\pm 50\%$, $r^2 = 0.35$	(32)
Zone 2C	- No correlation found		
Zone 2 (overall)	$h = 0.080 + 0.188\dot{W}$	$\pm 60\%$, $r^2 = 0.60$	(33)

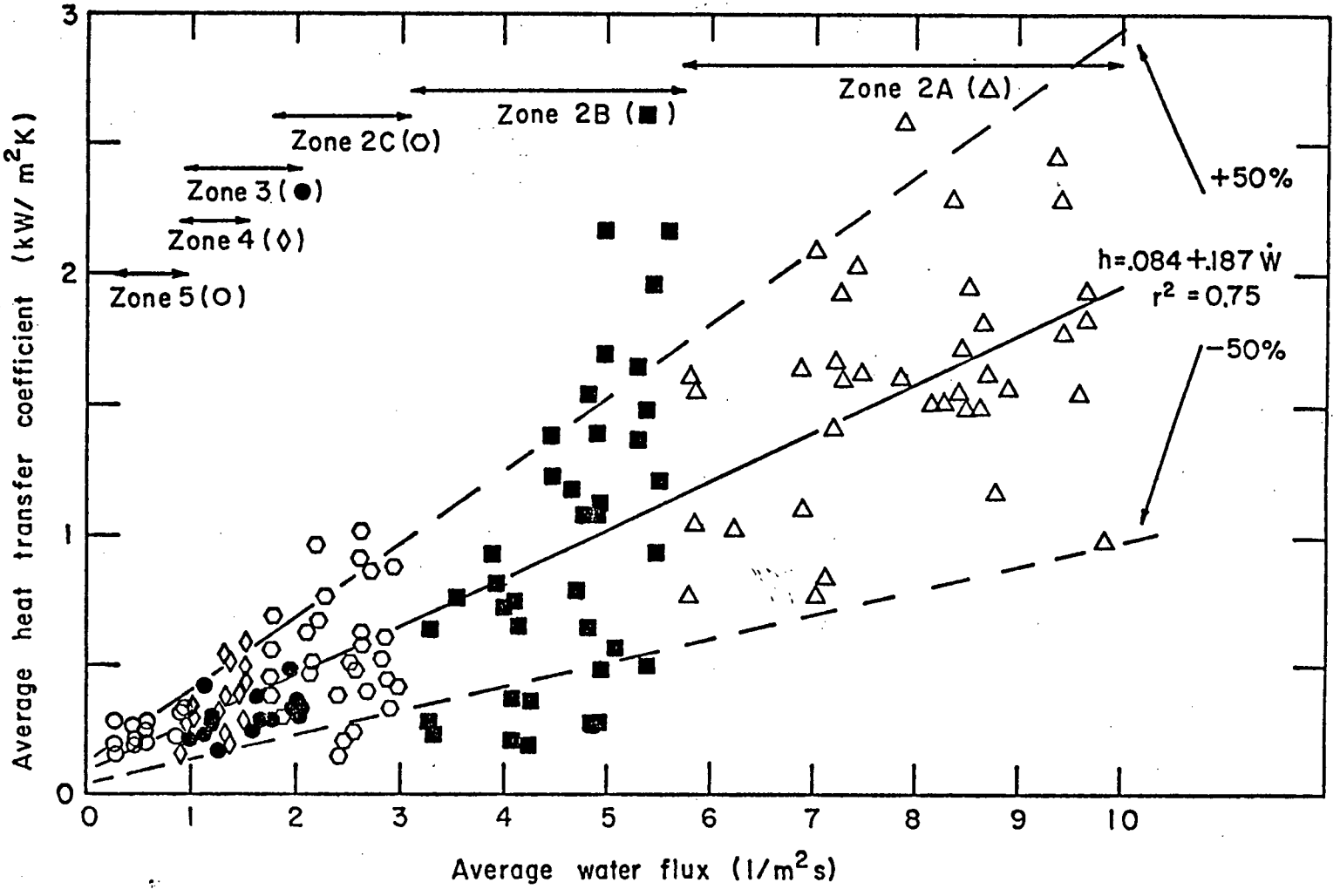

Figure 29 Variation of the average heat-transfer coefficient with average water flux for all zones.

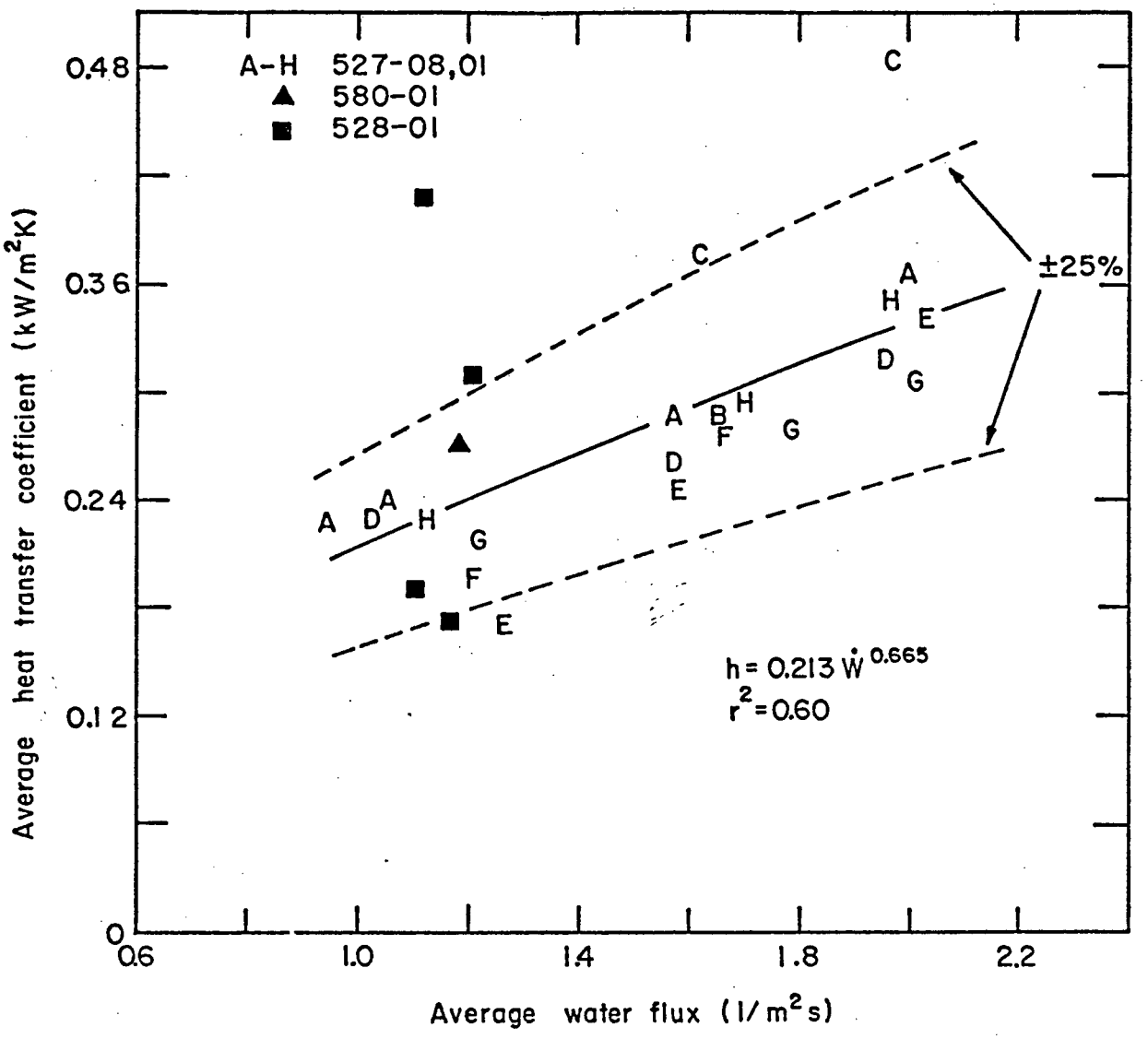

Figure 30 Variation of the average heat-transfer coefficient with average water flux in Zone 3. Plotted letters refer to individual casts.

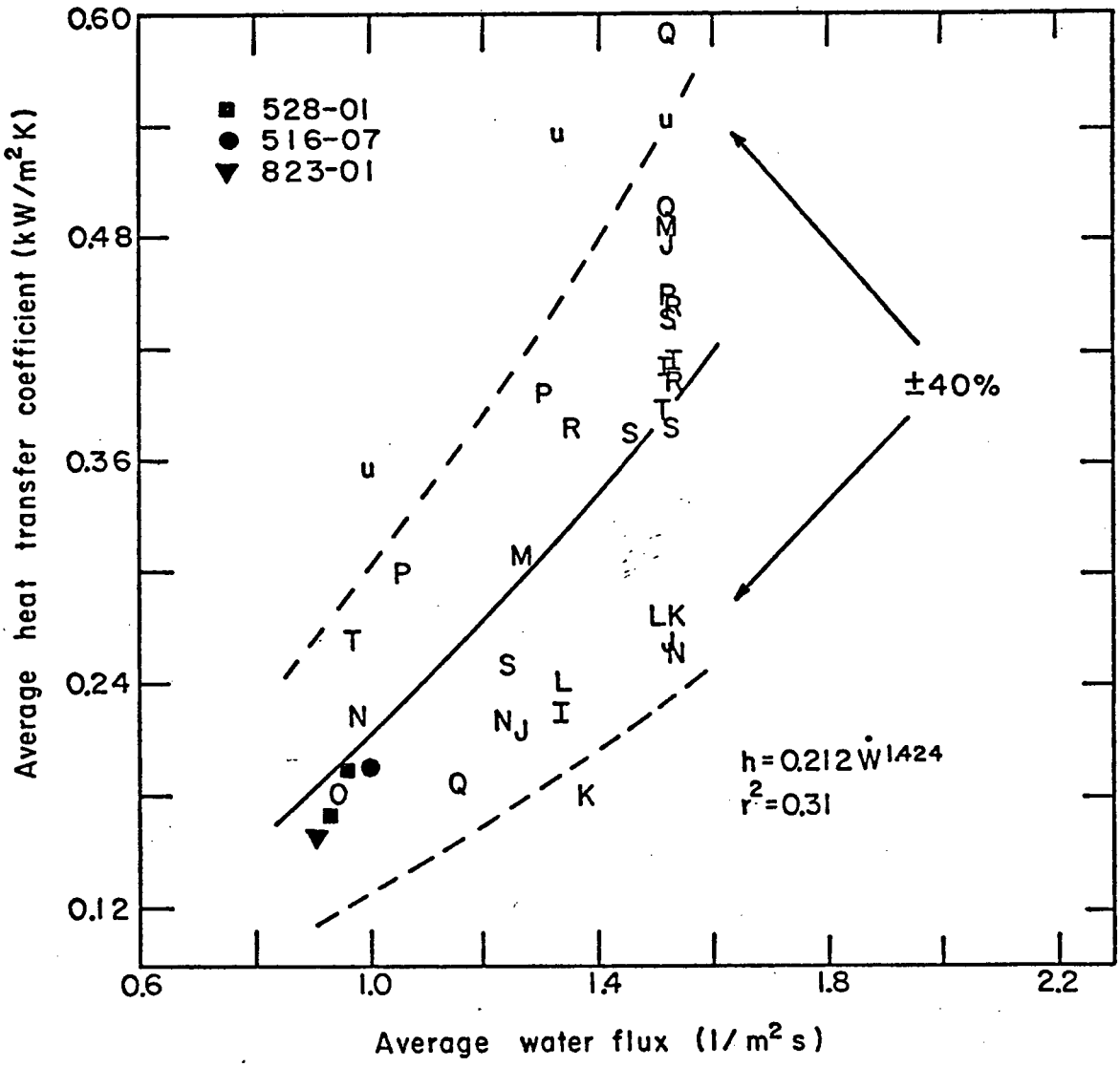

Figure 31 Variation of the average heat-transfer coefficient with average water flux in Zone 4. Plotted letters refer to individual casts.

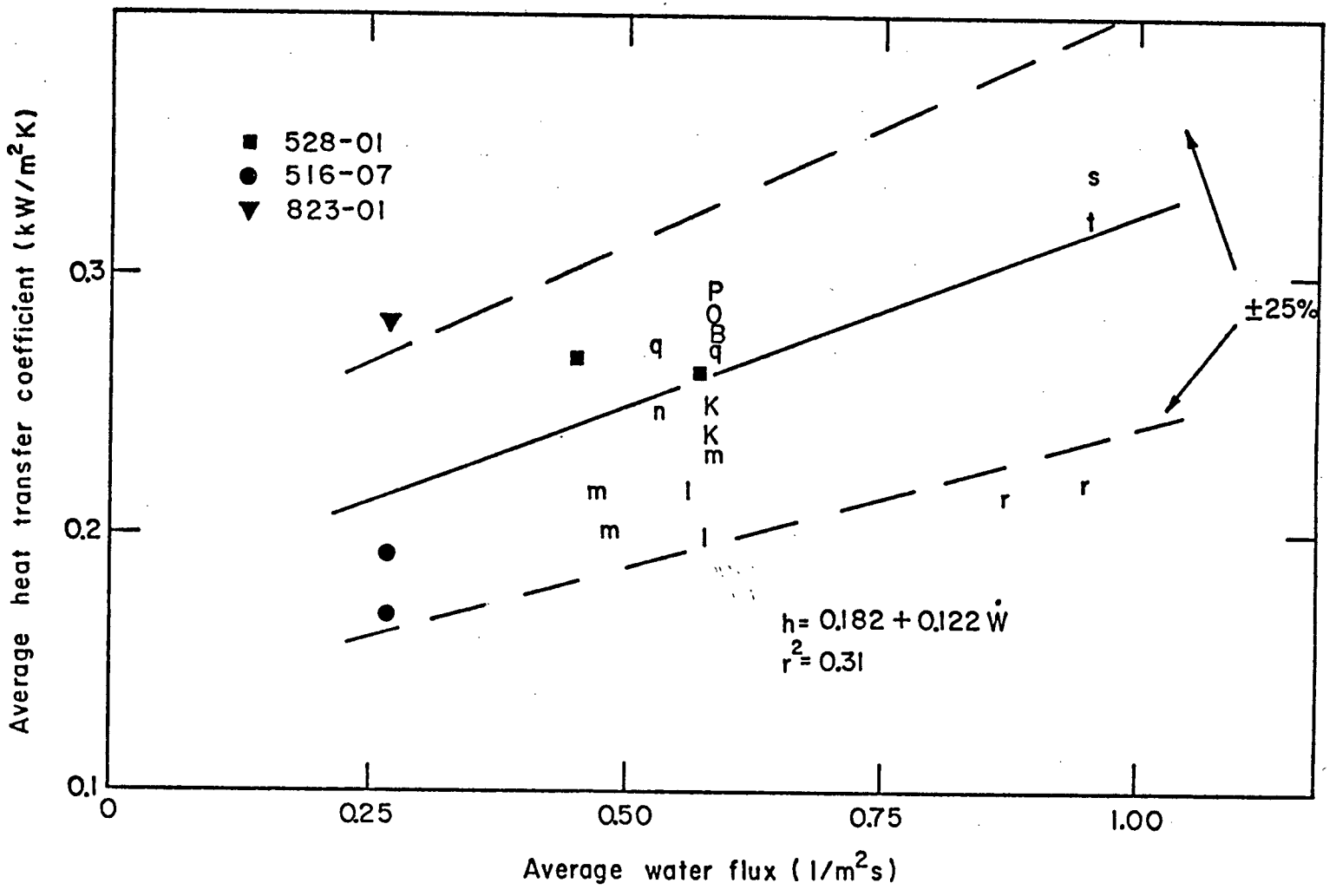

Figure 32 Variation of the average heat-transfer coefficient with average water flux in Zone 5. Plotted letters refer to individual casts.

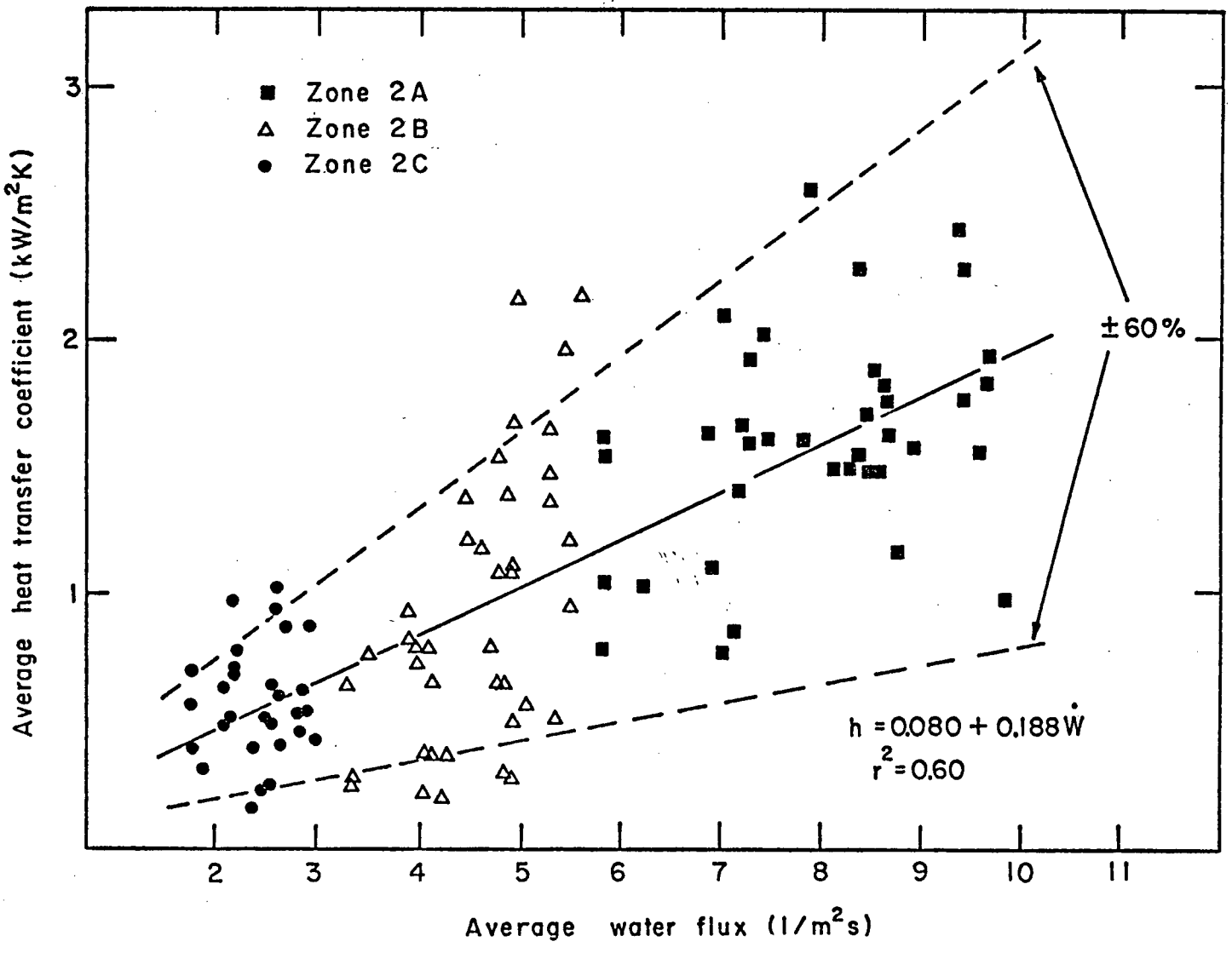

Figure 33 Variation of the average heat-transfer coefficient with average water flux in Zones 2A, 2B, and 2C.

The equations given above refer to average values of heat-transfer coefficient and water flux for each zone. The values of heat-transfer coefficient reported are exclusive of radiation.

The local heat-transfer coefficients that were obtained in the spray-impingement areas of Zone 2 were also plotted versus local water flux. Figure 34 shows the result, from which it is evident that no correlation was found.

The heat-transfer model also enabled determination of the average heat flux in the zone for each run that was made. The heat flux incorporates the effect of all heat-transfer mechanisms. This was correlated to the average water flux in the experiments by the equation:

$$Q = 0.187 + 0.139\,\dot{W} \pm 35\% \;,\; r^2 = 0.79 \qquad (34)$$

The data and regression line are shown in Figure 35.

It should be noted that the convention of adopting error bands in this work rather than confidence limits is not without mathematical justification. One of the standard assumptions in conventional analysis of regression equations is that the residual error of the dependent variable is independent of the value of the independent variable.[80] On the basis of this assumption, standard errors of the regression coefficients,

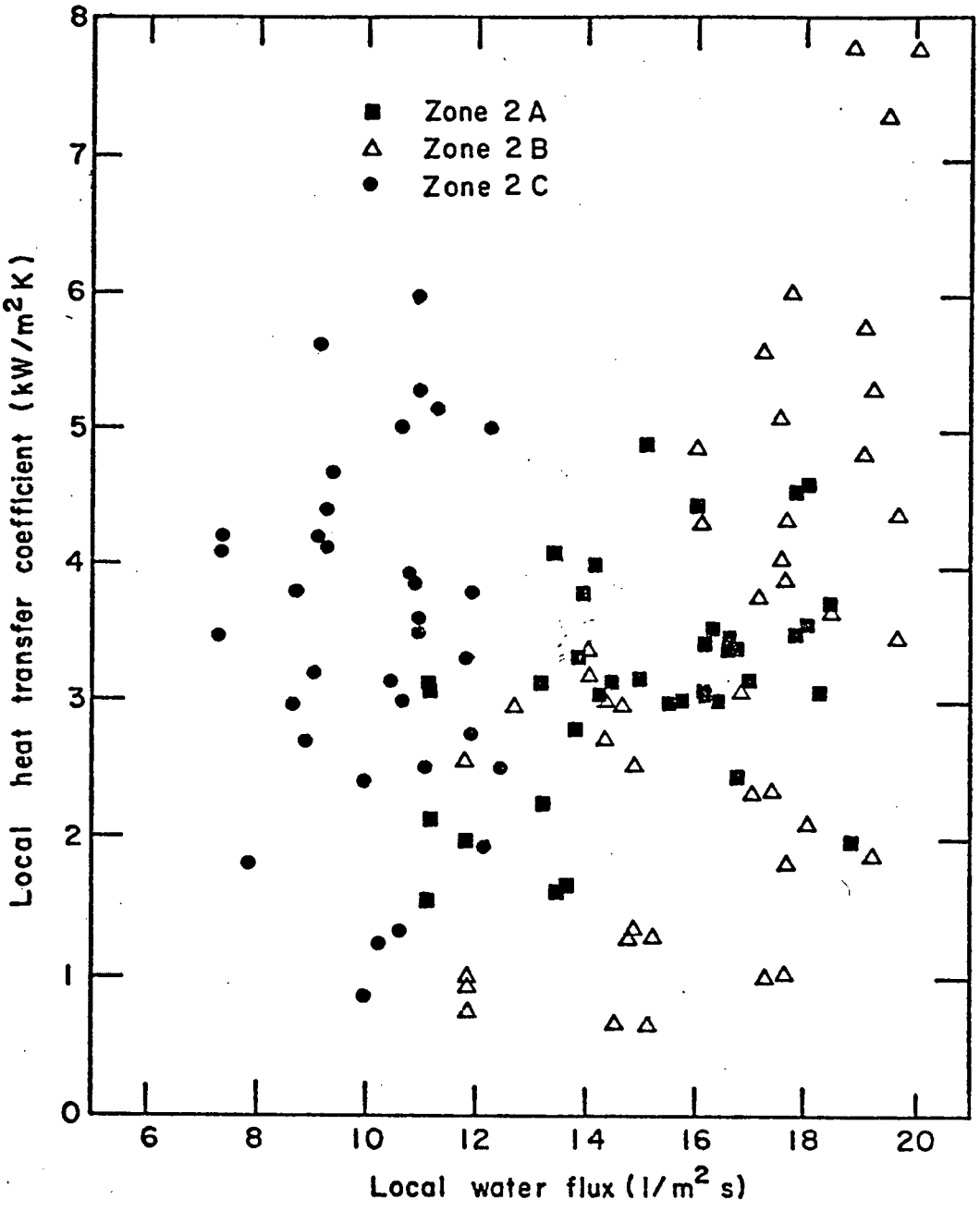

Figure 34 Variation of the local heat-transfer coefficient with local water flux in Zones 2A, 2B, and 2C.

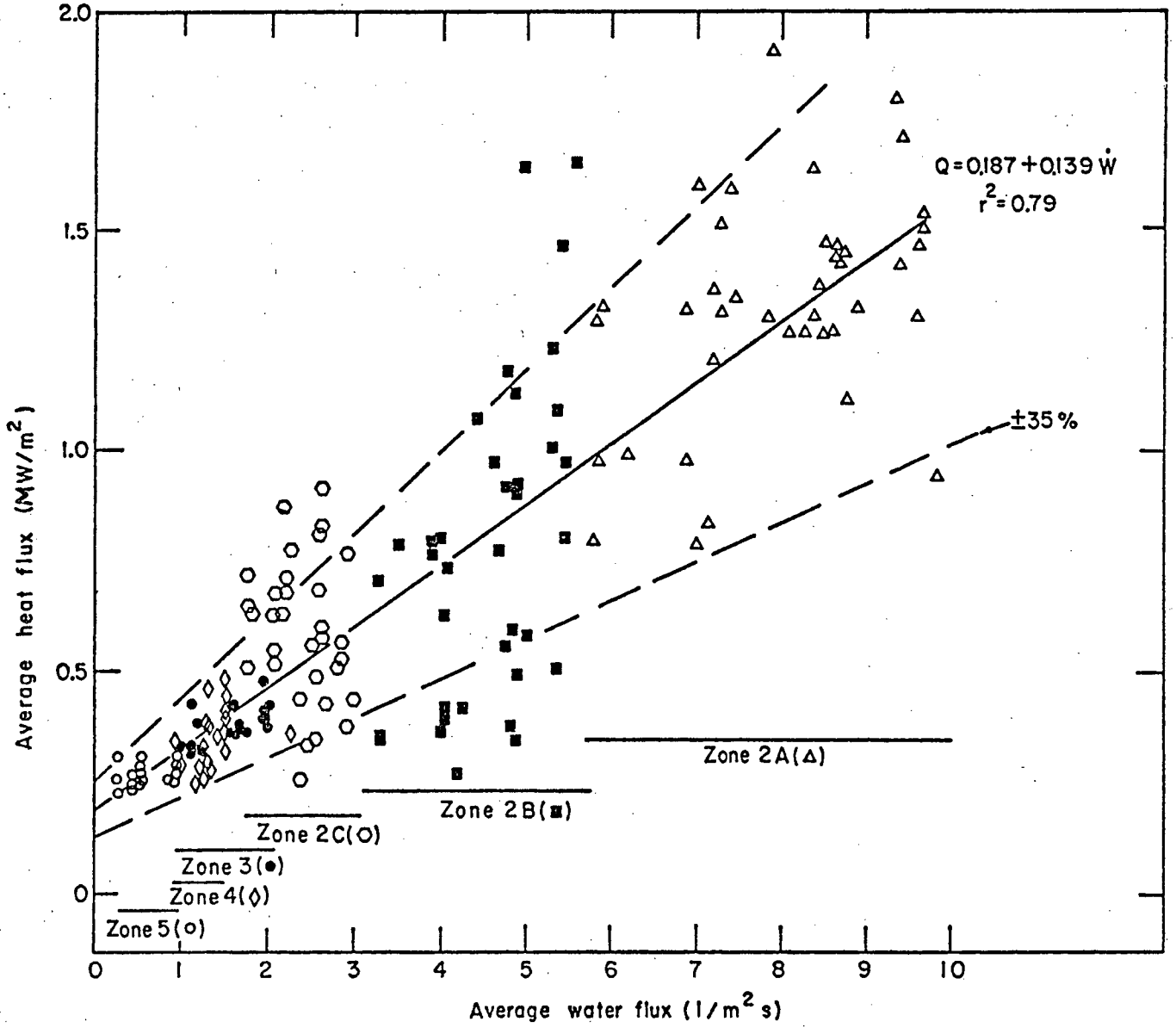

Figure 35 Variation of the average heat flux with average water flux for all zones.

confidence intervals, F-tests, etc., may be calculated. Observation of Figure 29 indicates that this assumption is not valid in this study. The Durbin-Watson d-statistic enables statistical tests for serial correlation to be performed. A Durbin-Watson test of the present data set at a 5 per cent level of significance gave significant evidence of positive serial correlation. Thus the use of confidence intervals is not justified.

6.5 Adequacy of the Regression Equations

Although several regression equations have been derived, no indication has yet been given of the "best" representation of the real behaviour of the secondary cooling system. The r^2 value of the overall regression equation is a good criterion, but a matter of concern is the ability of the overall equation to predict the heat-transfer coefficients and temperatures of the slab in the individual zones. A further point of concern is the ability to rationalize the scatter that was observed in the data. Valuable information may be extracted if the characteristics of each equation are considered. The first point to note is that the scatter resulting from the measurements is different in each zone. Secondly, the overall regression equation appears to predict the behaviour of individual zones accurately only under certain water flow-rate conditions.

The latter point can be seen by comparing plots of the individual and overall regression equations, Figure 36. In some instances the magnitudes of the predicted heat-transfer coefficients agree (Zones 2A, 2C and 2B at higher flow rates, Zone 4 at high flow rates). In other cases, the response of the heat-transfer coefficient to changes in water flux approximately agrees for the individual and overall equations (Zones 2A, 3). The difference between the overall and individual equations possibly results from the statistical analysis. Figure 29 shows that over 80% of the range of water flow rates obtained was for Zone 2. Consequently, the results from Zone 2 have a proportionately large effect on the overall regression equation. This may obscure the results obtained for Zones 3, 4 and 5. The behaviour of these zones, however, is very important because they comprise a large part of the secondary cooling system. Thus the individual regression equations and scatter corresponding to each may have real significance, and require further attention.

In order to check the ability of the overall regression equation to predict the real behaviour of the secondary cooling system, the surface temperatures measured during the experiments were compared to the predicted values and the expected scatter ($\pm$ 50%). Figure 37 shows the calculated surface-temperature profile for a slab cast under standard operating conditions at 1.52 m/min, as well as the maximum expected

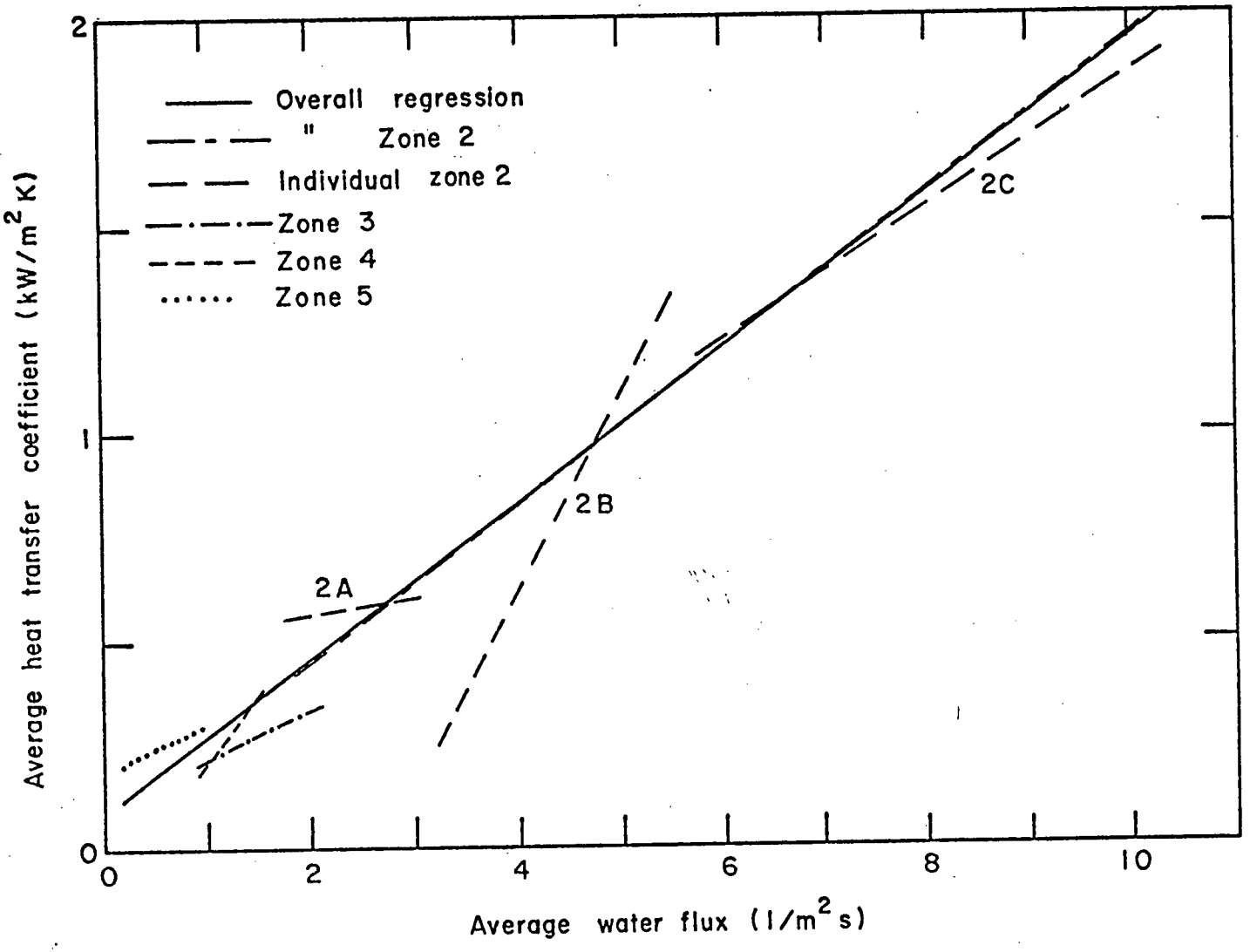

Figure 36 Comparison of the overall regression equation with the regression equations of individual zones.

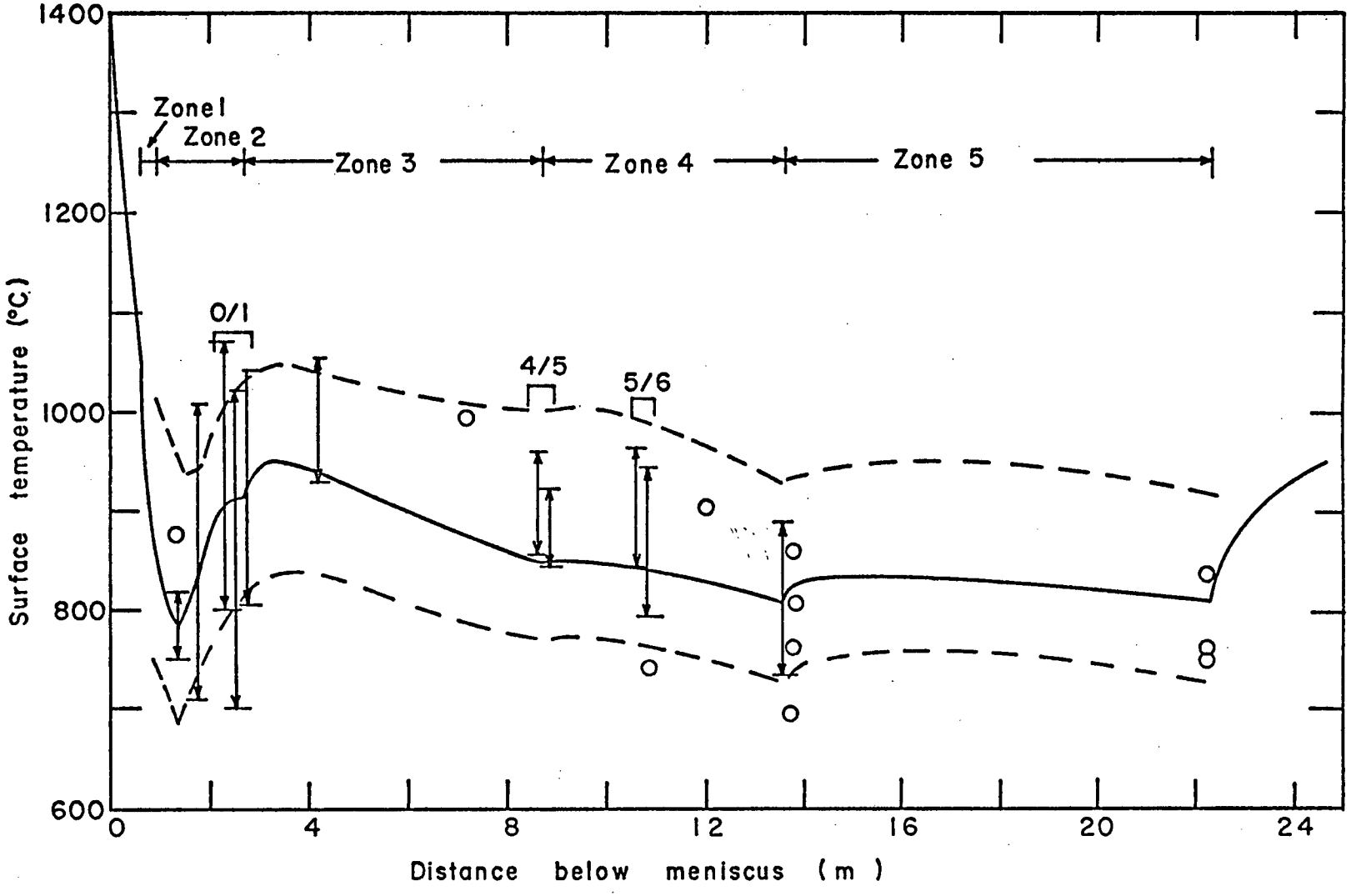

Figure 37 Comparison of temperatures measured during normal operating conditions with the temperature profile predicted by the overall regression equation.

deviation due to the ± 50% scatter associated with the overall regression equation. It is seen that the magnitude of the expected error in temperature measurement is approximately uniform, despite the fact the magnitude of the expected error in the heat-transfer coefficient is larger at larger values of heat-transfer coefficient. This is because the sensitivity of the temperature to heat-transfer coefficient is less in Zone 2, as Figures 23 to 28 indicate. In Zone 2, a larger temperature gradient obtains through the solidified shell, because the slab surface is closer to the solidification front. Therefore heat is transferred to the slab surface at a greater rate and more heat must be removed from the surface to obtain a given reduction in surface temperature. However, the predicted scatter band is still large (about 200°C). The range of measured temperatures in Zones 3, 4 and 5 is also shown in Figure 37 and evidently is not as large as the range predicted. It should be noted that two scatter bands are shown at the 4/5 and 5/6 positions,* which correspond to the measurements in Zone 3 (left side) and Zone 4 (right side). Three scatter bands are shown at the 0/1 position. These correspond to calculated 0/1 temperatures determined from temperatures measured in the spray-impingement region in Zone 2 (left), actual 0/1 measurements in Zone 2 experiments (centre), and

*Notation of the form 4/5 indicates a position between segments. For example, 4/5 refers to the position between Segment 4 and Segment 5.

Zone 3 experiments (right). The predicted temperatures in Zone 2 are seen to lie in the centre of the actual scatter bands and the actual and the regression - predicted scatter bands approximately correspond. However in Zone 3 and much of Zone 4, actual temperatures lie above the predicted values, and the scatter is much less than predicted. Similarly, in Zone 5 the measurements exhibit less scatter and are equal to or slightly less than those predicted by the overall regression equation. These findings agree with the observations made earlier about the locations of the individual regression equations with respect to the overall equation (Figure 36).

Therefore it seems clear that the overall regression equation cannot accurately predict the behaviour of the individual secondary cooling zones. If there is a real difference in the behaviour of each zone, there should be a phenomenological cause. Because the range of water flow rates obtained in Zones 3 and 4 overlap, it is possible, for a given water flow rate, to test if the differences in heat-transfer coefficient obtained in each zone are statistically significant. A t-test was performed and it was found that the mean value of heat-transfer coefficient at the highest water fluxes in Zone 4 is significantly different than the mean value in Zone 3 at the same water flux. This result, and the comments associated with the predicted and

measured temperatures of Figure 37, lead to the conclusion that the individual regression equations for each zone provide the best representation of heat extraction in the secondary cooling system. Because the scatter was large and the correlation poor for Zones 2A, 2B and 2C, a single equation has been used to represent the overall behaviour of Zone 2.

Figure 38 shows the predicted temperature profile for normal operating conditions using the individual regression equations for each zone. The expected scatter predicted by the regression equations and the scatter of measured temperature is also indicated. The real behaviour is more adequately predicted in this figure than in Figure 37. It is therefore concluded that Equations 28, 29, 30 and 33 are the best representation of the behaviour of the secondary cooling system of the Inland Slab Caster.

The fact that the heat-transfer coefficients are affected differently by water flux in each secondary cooling zone points to the possible existence of a phenomenological difference in the spray-cooling mechanism. A dissimilar heat-flow mechanism may also explain the difference in scatter that was obtained in each zone. In order to obtain an estimate of the possible phenomenological contribution to the total scatter observed in individual zones it is useful to account systematically for the error caused by known error sources.

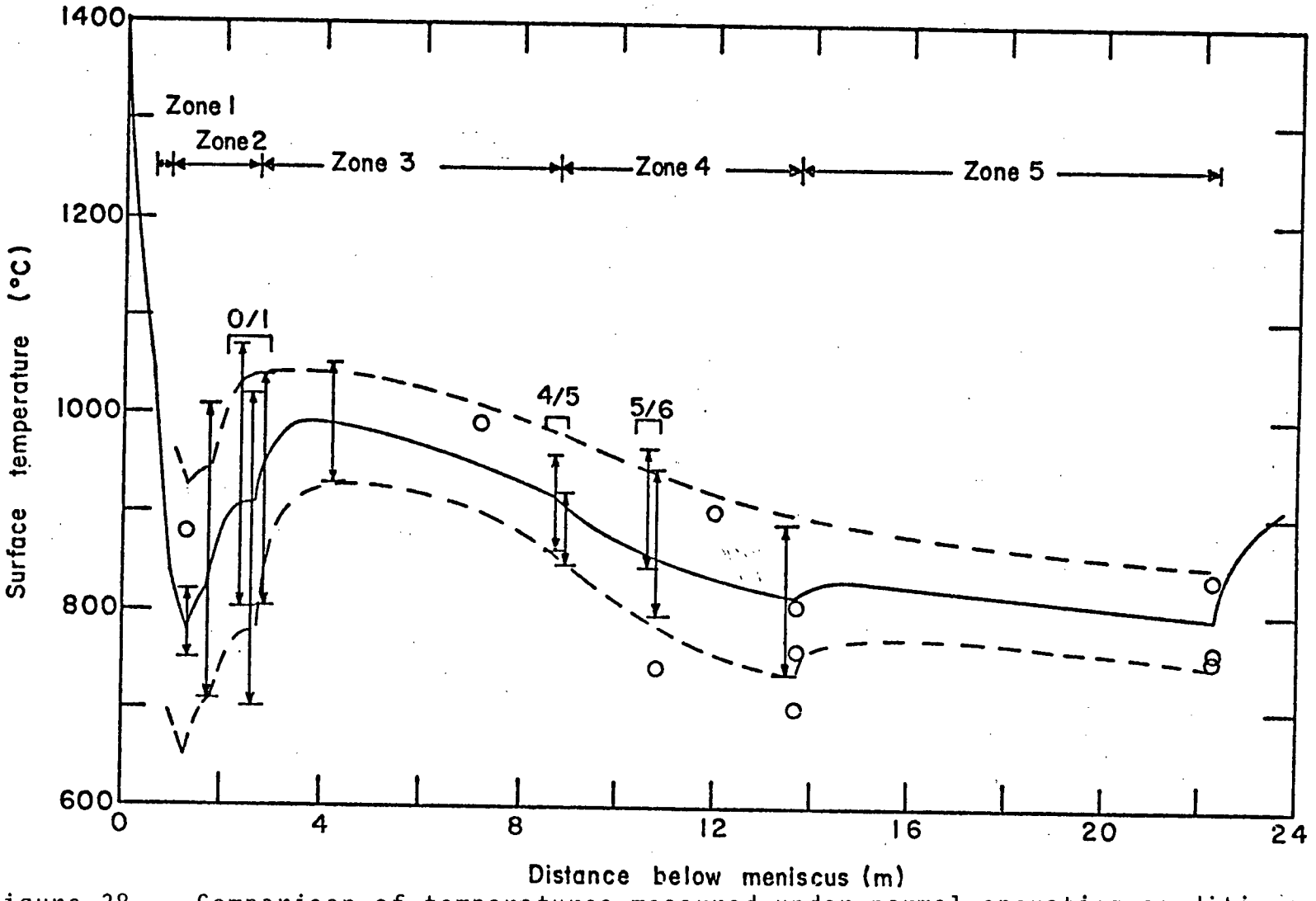

Figure 38 Comparison of temperatures measured under normal operating conditions with the temperature profile predicted by using individual regression equations for each zone.

6.6 Analysis of Experimental Error

6.6.1 Sources of Scatter

Surface-temperature measurements such as those reported here are subject to numerous sources of experimental error. A resultant error in a calculated heat-transfer coefficient is a manifestation of the error in the temperature measurement from which it was obtained. The possible causes of measurement error are:

i) Error in the Vanzetti measurement system.

ii) Presence of semi-detached scale on the slab surface.

iii) Inaccuracy of water flowrate determination.

iv) Casting speed determination.

Other factors which have been noted to affect the measured values of temperature[81] are temperature distribution across the slab, and unsteady casting operation. However since an effort was made during this work to measure temperatures at the same location with respect to the slab centreline, and at steady-state conditions (i.e., not during process transients or during the first heat of the cast), these are not major influencing factors. Also, there are no inside/outside radius effects since all measurements were obtained on the inner radius.

The actual value of the temperature that is measured

may be influenced by other factors. These are:

i) Machine considerations.

ii) Boiling heat-transfer mechanism.

The first factor includes such problems as bent or plugged spray nozzles, and differences in alignment and resulting roll contact when different segments are in the machine. The geometry of the machine itself, which includes roll size and nozzle setback, may influence heat transfer in complicated ways that are not easily discernable. The second factor is highly variable in nature and is complicated further by the local temperature fluctuations between sprayed and non-sprayed areas.

6.6.2 Accountability of Error

The maximum expected error in the regressions of the heat-transfer coefficient may be determined from the maximum expected deviation of temperature due to measurement error. A summary of the analysis is presented in Table XVI. The maximum expected errors in temperature measurement are shown for each error source and zone, and are summed and converted to an expected maximum error in heat-transfer coefficient. It should be noted that the maximum error will be propagated such that temperature is reduced, because the effects of calibration drift and scale will be only to reduce the measured temperature. The percentage decrease in calculated h due to accumulated

TABLE XVI Summary of the Estimation of Maximum Expected Errors

Factor	Zone 2A	Zone 2B	Zone 2C	Zone 3	Zone 4	Zone 5
Error in Vanzetti System (T,°C)						
- system accuracy	13	13	13	13	13	13
- calibration drift	15	15	15	15	15	15
Error due to scale (T,°C)	5	5	5	5	5	5
Effect of casting speed resolution error (T,°C)	4	4	4	4	4	4
Effect of water flow rate error associated with casting speed error (T,°C)	7	7	7	6	13	6
Effect of error in water flow-rate determination (T,°C)	17	16	12	8	23	6
Total temperature error (°C)	61	60	56	50	73	49
Total error in h (kW/m^2K)	270	265	150	65	145	70
Percentage error in h						
- low $\dot{W}$	22	38	37	30	-	32
- high $\dot{W}$	14	24	23	19	40	23

measurement error therefore will be less than the percentage increase.

The Vanzetti measurement error is composed of the system accuracy ($\pm$ 1.5%)[70] and the maximum drift between successive calibration checks (Section 3.5.1). The error due to scale presence on Strand 2 is estimated from investigations performed prior to this study[74] and the results of the descaler test (Appendix B). Casting-speed error results from the limitations in resolving the speed accurately on the chart recorders. The expected effect of casting-speed error on the temperature was determined from Figures 23 to 28. The error in casting speed has an error in water flow rate associated with it. The regression equations were used to estimate the effect on the heat-transfer coefficient and Figures 23 to 28 were used to determine the resultant temperature error. The error due to inaccuracies in the water flow-rate determination itself were estimated similarly. The percentage error in h varies according to the actual value of h in these calculations.

The maximum expected scatter due to measurement error can be compared to the scatter actually observed in order to determine the significance of machine factors and boiling heat transfer. The expected scatters of 19-30 per cent, 40 per cent and 23-32 percent agree favourably with the 25

per cent, 40 per cent and 25 per cent actually obtained about the regression lines for Zones 3, 4 and 5 respectively. The actual scatter of up to 60 per cent obtained in Zone 2 is not as easily accounted for by the causes discussed thus far. This would indicate that machine factors or boiling heat transfer are playing an important role in the observed behaviour of Zone 2. The effect of machine considerations is difficult to assess. Because the measurements in Zone 2 were carried out in the local spray impingement area the effect of a plugged nozzle adjacent to the measurement point would be to increase the measured temperature, the extent of which would be determined by the extent of plugging. The heat-transfer coefficient determined therefrom is then much lower and the calculated temperatures and overall heat-transfer coefficients for the entire zone would actually be represenative of a lower overall average flow-rate. This is further complicated by the fact that, although the average heat-transfer coefficients were not determined to be largely affected by previous thermal history for "smoothed" temperature profiles, the effects of local error on the local heat-transfer coefficient are more pronounced. Thus, for example, if a plugged nozzle has resulted in an erroneously high calculation of temperature at the exit of Zone 2A, the resulting local heat-transfer coefficient in Zone 2B will be higher, assuming that the measured temperature in Zone 2B is correct. The effect is then propagated so that

the calculated temperature at the end Zone 2B is erroneously low.

The overall contribution of plugged nozzles to the scatter obtained in Zone 2 is impossible to determine quantitatively. However, nozzle specifications usually indicate the particle size above which the nozzle orifice is susceptible to plugging. It must be presumed that the nozzles have been selected and the plant water quality has been specified to keep nozzle plugging to a minimum. In addition, a test-rig in the maintenance section of the slab-caster complex is used to check for nozzle plugging before the segment is placed in the machine. Furthermore, Figure 33 indicates that the points from the measurements in Zone 2 are uniformly scattered within the $\pm$ 60% range. This might not be expected from nozzle plugging considerations. A large number of these points are above the predicted regression values, which is not easily accounted for by nozzle plugging. Thus the possible effects of boiling heat transfer merit further attention.

6.7 Significance of Boiling Heat Transfer

Overall consideration of the literature and the results presented to this point suggests that the boiling heat-transfer mechanism could be of fundamental importance in explaining the effects observed. The first important point to recall is that the Leidenfrost temperature is known to be a function of

the water flux (Figure 8). The predicted temperature profiles of Figures 37 and 38 indicate that the surface temperature of the slab can be in the vicinity of the critical temperature if sufficiently high water flow-rates are obtained. The smoothed temperature profiles and average water fluxes would indicate that this is not the case. However, these do not give a true picture of events in the regions of spray impingement. It may be recalled that the secondary cooling system is arranged such that water is sprayed between rolls at high fluxes or narrow transverse strips of the slab surface. Thus the local water flux in the spray-impingement area is higher than the average water flux over the entire zone. This should already be evident from the results of Zone 2 shown in Figures 33 and 34. Secondly, this behaviour results in temperature fluctuations as the slab passes through the various cooling regions illustrated in Figure 12. This behaviour has been verified by thermocouple measurements,[59,65] and was in fact used in performing the Zone 2 calculations.

A further rationalization of the observed behaviour of the secondary cooling system may be accomplished by studying these effects in detail. In order to do this, smoothed profiles were predicted using Equations 28, 29 and 33. The approach was to determine a detailed "real profile" approximation that would predict the same temperature at the end of a

particular zone as predicted by the smoothed profile. This is complicated by the necessity of characterizing the heat-transfer rate in the non-sprayed areas. The exact behaviour is difficult to assess because of the variable effects of water accumulation on the rolls and roll contact. However, it is clear that the heat-transfer coefficients in the non-sprayed areas will be considerably less than those in the sprayed areas. Thus the approach has been to apply a local spray heat-transfer coefficient in the sprayed area and an approximate combined coefficient in the non-sprayed area to account for roll contact and water drainage and accumulation. The latter has been estimated from the works of Etienne et al.[48] and Diener et al.[66] (see Table IV and Figure 14). Fortunately, the exact value of the coefficient in the non-sprayed area is not significant.

The results of these calculations are shown in Figure 39 for the case of Zone 3. The casting speed is 1.52 m/min and two possible average heat-transfer coefficients have been selected. The temperature at the entrance of the zone is on the lower range of those actually measured at the O/1 location. Both the estimated detailed and smoothed profiles are shown. That the smoothed profile corresponds to the peaks of the predicted detailed profile is a consequence of having the spray nozzles capped. A check under both conditions

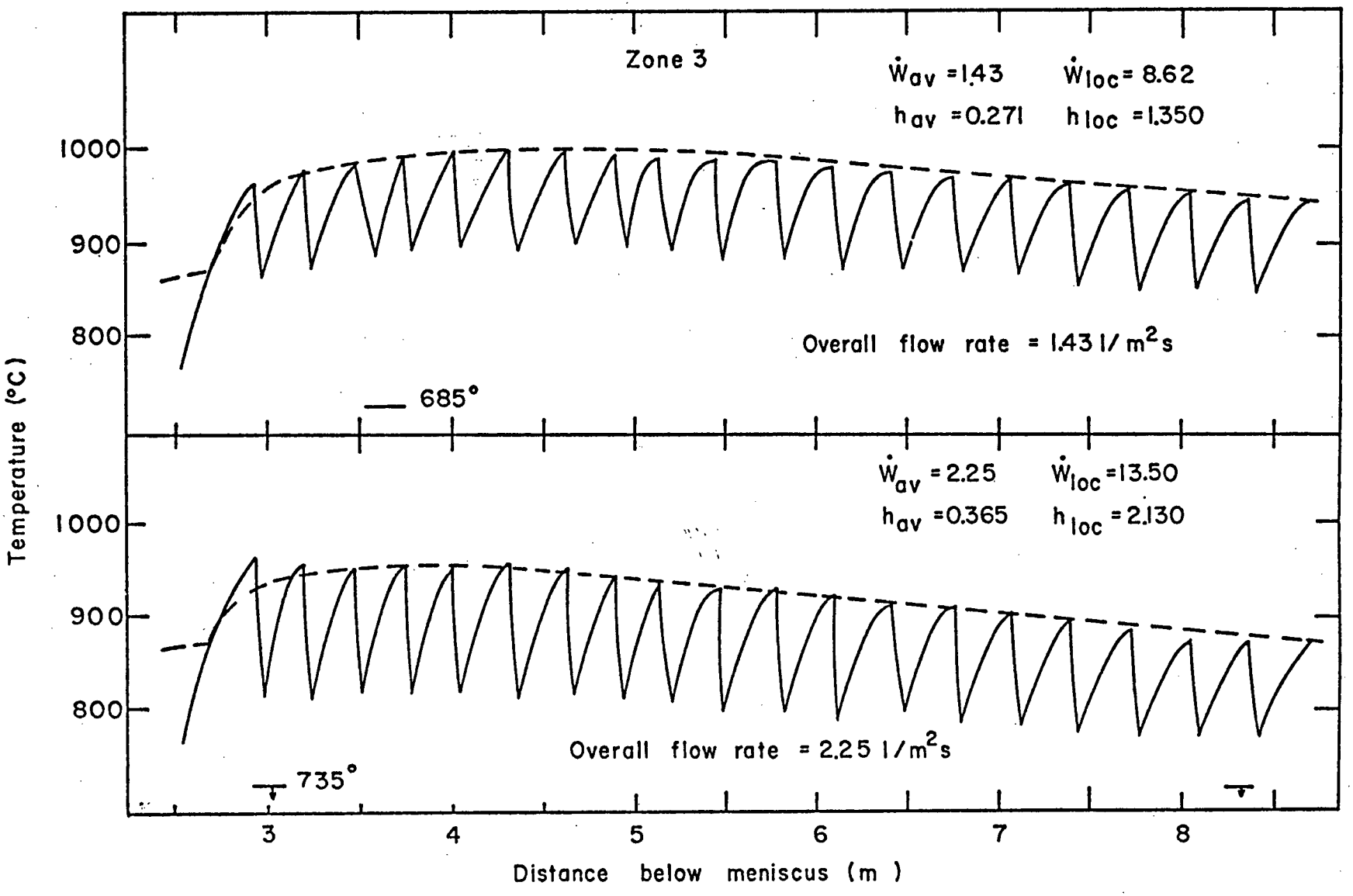

Figure 39 Estimate of the real temperature profile during various water flowrate conditions in Zone 3. Indicated temperatures are the critical temperatures for the water fluxes indicated.

showed that the overall heat extracted in the zone was only 4 per cent greater in the case of the detailed profile. In order to investigate the possible presence of unstable film boiling heat transfer, an estimate of the Leidenfrost temperature at the local spray water flux obtained is indicated. This has been determined from the results of Hoogendoorn et al.,[44] which is the only work that specifically studied the effect of spray water flux on the critical temperature (Figure 8). The spray characteristics (.1 - 1 mm droplet diameter and 15 m/sec spray velocity) of Hoogendoorn's study are representative of the spray variables on the slab caster. The influence of surface characteristics is difficult to ascertain, as noted in Chapter 2, but the only possible effect would be to increase the temperature below which unstable film boiling occurs.[30] In the absence of detailed knowledge of the surface effects, it is worthwhile to make comparisons based on the results of Hoogendoorn. It is seen that even at an average heat-transfer coefficient slightly above the maximum predicted by the regression equation for Zone 3, the lowest temperature obtained in the spray-impingement area (770°C) is higher than the Leidenfrost temperature predicted from Hoogendorn's results at the local spray water flux obtained (735°C). Three general effects of the water flux should furthermore be noted. Firstly, the effect of increasing the average (and local) water flux both decreases the "trough" temperature and raises the critical temperature.

Thus there are dual effects which tend to increase the possibility of the onset of unstable film boiling if, for example, higher water flow rates than expected are obtained. Secondly, the minimum temperatures predicted are actually much lower (up to 150°C) than the peak temperature corresponding to the "smoothed" profile. Thirdly, the effect of decreasing water flux is also to decrease the magnitude of the local oscillations. For example, the effect of decreasing average water flux from 2.25 to 1.43 ℓ/m^2s is to decrease the total fluctuation from approximately 150°C to 110°C.

Figure 40 shows profiles for Zone 4 which have been obtained similarly. It is seen that the minimum temperature obtained (725°C) is again higher than the predicted critical point (700°C) at the highest flow rates obtainable. The magnitude of the local temperature oscillation ranges from 120°C at 1.52 ℓ/m^2s to 100°C at 1.36 ℓ/m^2s. Attainable water fluxes in Zone 4 as low as 0.9 ℓ/m^2s were not investigated. The local oscillations in Zone 5 were not investigated either, but since water fluxes are generally lower it is assumed that the temperature fluctuations are less and well above the estimated critical point.

The calculations for Zone 2 lead to different conclusions. Figure 41 shows that only at the lowest flow rates obtainable are the minimum temperatures above the estimated Leidenfrost

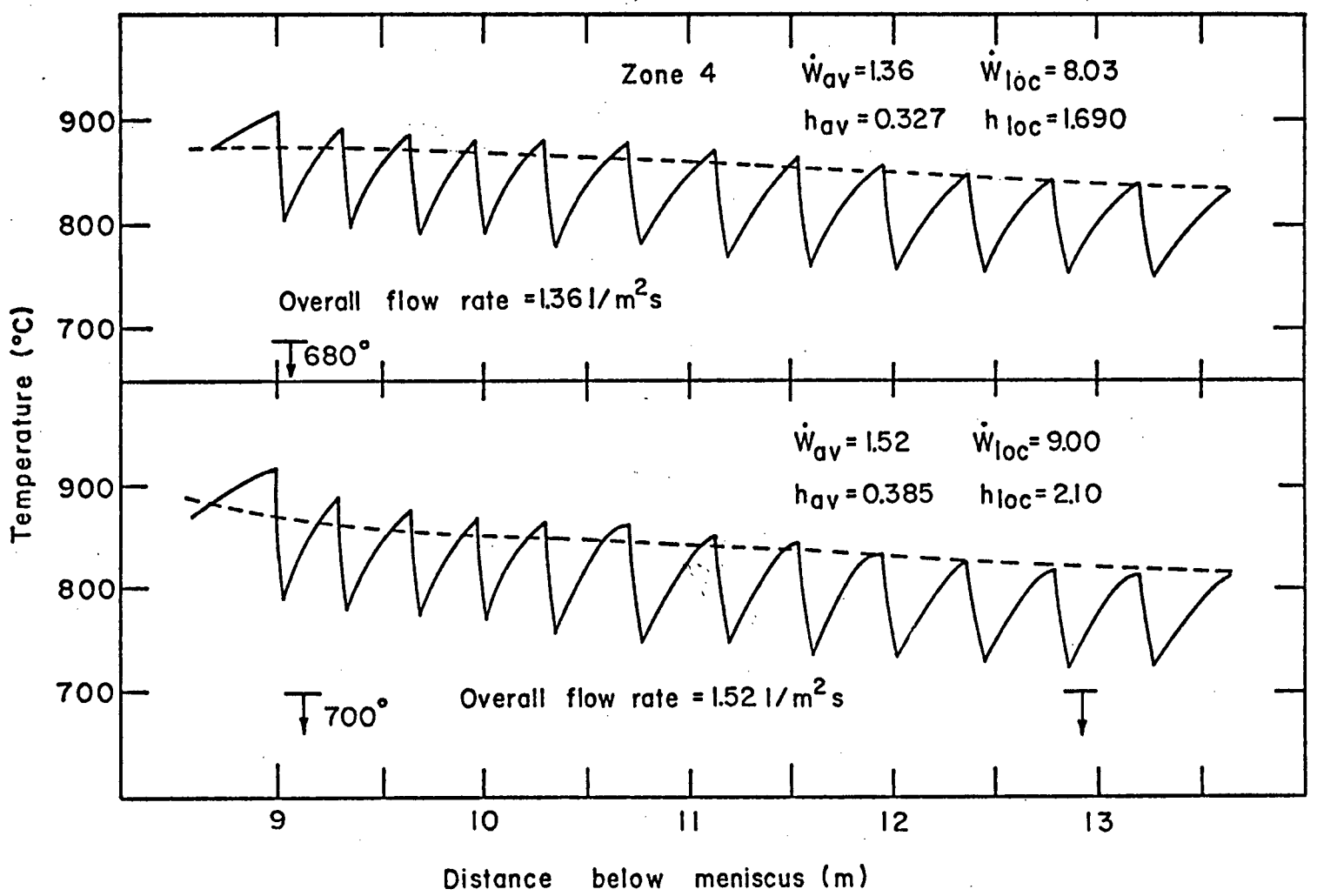

Figure 40 Estimate of the real temperature profile during various water flowrate conditions in Zone 4. Indicated temperatures are the estimated critical temperatures for the specified water fluxes.

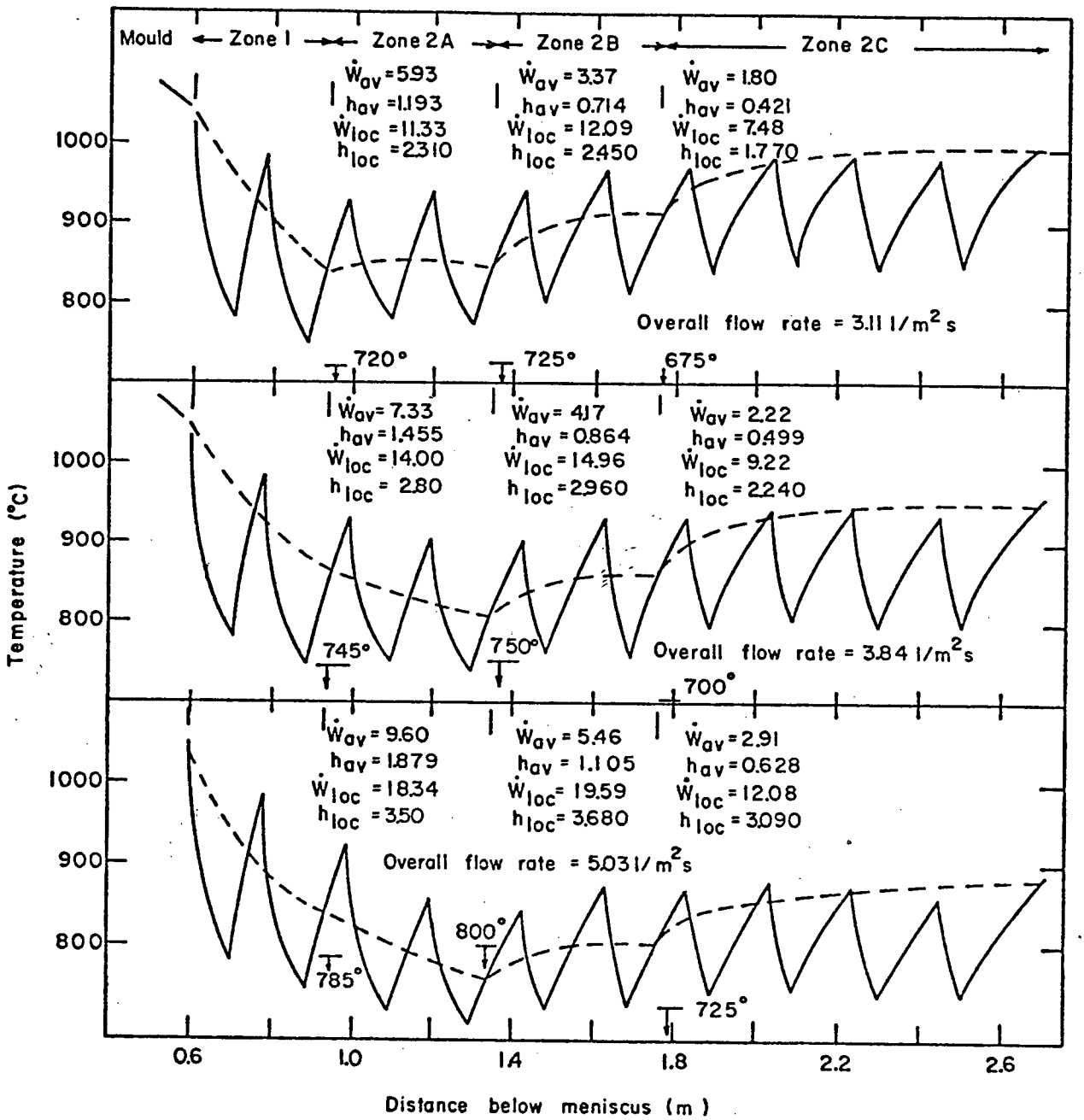

Figure 41 Estimate of the real temperature profile during various water flowrate conditions in Zone 2. Indicated temperatures are the estimated critical temperatures for the specified water fluxes.

point. This is because of the very high local water fluxes in the spray-impingement areas. The high predicted values of Leidenfrost temperature produce strong evidence for the existence of unstable film boiling at overall water fluxes in Zone 2 in excess of 3.84 ℓ/m^2s. Once this boiling mode commences, erratic temperature profiles are to be expected because spray cooling is effectively "out of control." This is because at the lower surface temperatures, the heat extraction rate increases rapidly with decreasing temperature (Figure 9), and is also more strongly influenced by local surface conditions. All predictions would therefore be invalidated due to the uncertain nature of the boiling phenomenon. The predicted temperature oscillations in Figure 41 are also seen to be as high as 200°C in the upper portion of Zone 2.

A theoretical analysis of the real behaviour of the secondary cooling system is now possible. It must be realized that this is dependent on the validity of certain assumptions, such as the correlations of Hoogendoorn, being applicable. However, under operating conditions for the casting of normal grades, it seems fairly certain that unstable film boiling and large local temperature fluctuations are occurring in Zone 2. The large amount of scatter obtained in Zone 2 can perhaps be rationalized on this basis, keeping in mind the other considerations which have been mentioned (i.e. nozzle plugging or roll misalignment). The fact that the observed scatter in

Zone 3 is totally accountable by assuming maximum measurement error, is in agreement with the calculated profile which shows stable film boiling to be prevalent throughout the zone. The results from Zone 4 are more difficult to explain. Although the total scatter obtained is in agreement with that predicted, this is partly a consequence of the large predicted temperature measurement error due to errors in determination of water flow-rate (see Table XVI). The reason for this large effect is the higher sensitivity of the heat-transfer coefficient for Zone 4 to water flux, as indicated by Equation 29. The large slope of the regression equation for Zone 4 is mainly due to the upward spread of data points at higher flow-rates in Zone 4 (see Figure 31). The fact that this behaviour occurs is perhaps indicative of the onset of unstable film boiling in Zone 4 at the higher flow-rates. Though this is not predicted by Figure 40, the predicted temperature minimum and critical point are close enough at the end of the zone that unexpected irregularities in casting speed or water flow-rate could be sufficient to cause the transition to occur. In particular, a lack of uniformity in spray water distribution from the fan spray nozzle will certainly result in a higher real local water flux in the vicinity of the slab centreline where the measurements were made (see Figure 10). The actual Leidenfrost temperature will be higher in this case than predicted. The presence of oxide on the surface may also increase the critical temperature

sufficiently to be above the measured value. Furthermore these effects may only be sufficient to cause unstable boiling at the lower temperatures near the end of the zone (e.g., under the last two or three spray nozzles) and thus not have as drastic effect on the overall heat-transfer coefficient as in Zone 2. Thus "mixed mode" heat transfer may be possible in Zone 4, in which the mechanism passes from stable film boiling at the start of the zone to unstable film boiling at the end of the zone. The scatter band at the 5/6 position in Figure 38, which tends to be slightly above the smoothed curve predicted by Equation 29 supports this hypothesis. The only other possible explanation of the results in Zone 4 would be the presence of some unexpected measurement error, such as Vanzetti probe misalignment. To complete the analysis, it would appear that Zone 5 experiences stable film boiling at all times.

6.8 Comparison of Results with Previous Works

6.81. Average Heat-Transfer Coefficients

In order to obtain a comparison of the results of the current work with those previously reported, the individual regression equations were plotted with the results previously shown in Figure 13. The result is shown in Figure 42. The agreement with previously reported works for slab casters is good.[6,19,63,64] The results of this study are similarly

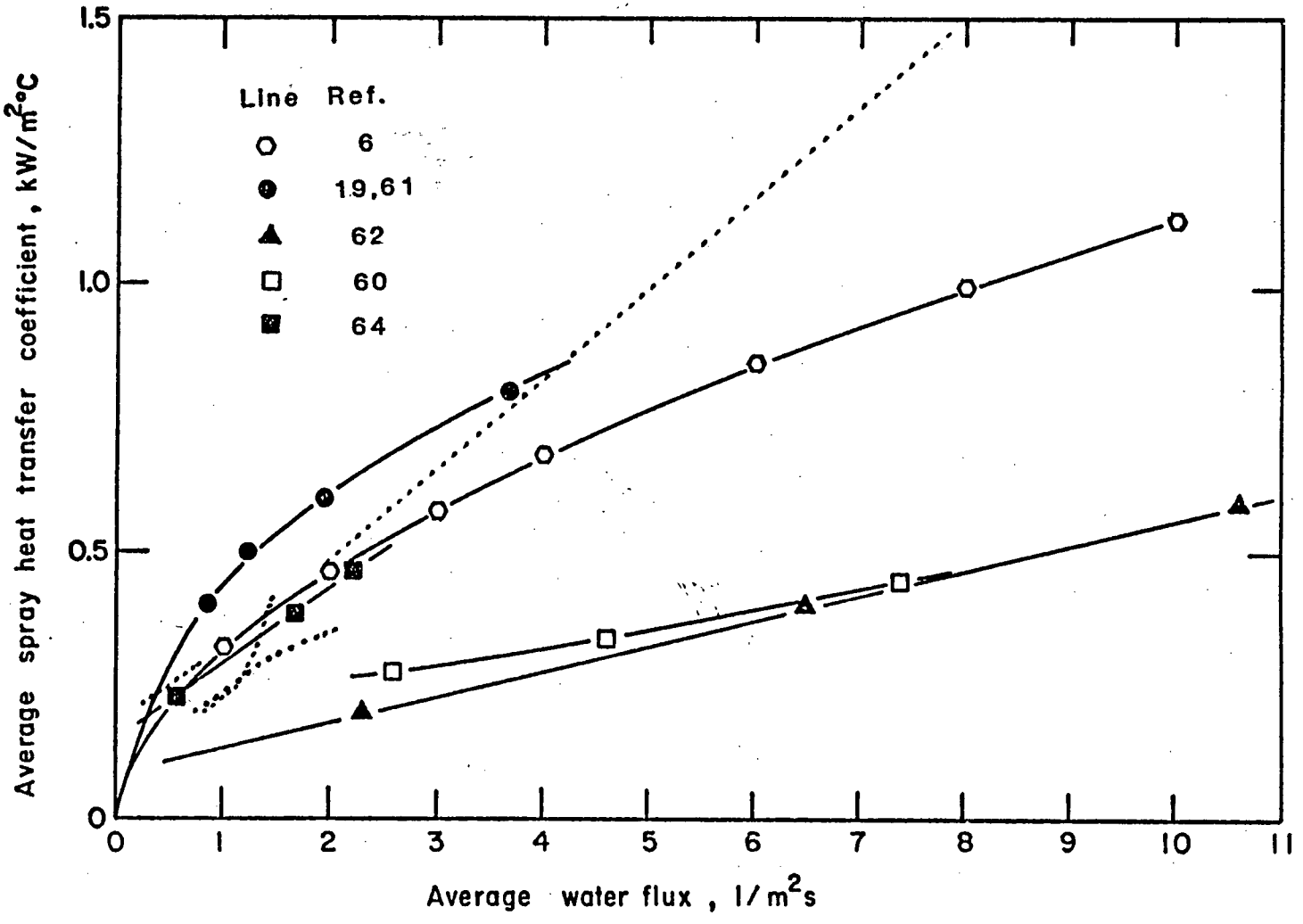

Figure 42 Comparison of the regression equations of the present work (dotted lines) with previous industrial correlations.

above the results reported for centrifugal casters.[60,61,62] Comparison with the latter is difficult because of a lack of information on the spray characteristics in these machines. However it is likely that the centrifugal casters employ lower local water fluxes which are more uniformly distributed over the entire length of the secondary cooling zone. Thus although the overall average water flux is the same, the cooling intensity at a particular location is less and an event such as unstable film boiling is unlikely to occur.

Because good agreement is obtained with the reported works on other slab casters, it is reasonable to suggest that unstable film boiling is a matter of concern in all slab casting operations. Although the results of Nozaki et al.[6] and Alberny et al.[19,63] indicate that h is proportional to water flux raised to a power n, where $n < 1$, their studies do not extend to the very high range of water fluxes. In fact the upper value of water flux is not reported by Nozaki et al., but it is unlikely that very high values were realized since his correlations are for surface temperatures measured only at the straightening point and presumably are correlated to water fluxes averaged over the entire secondary cooling system.

The results of Alberny et al.[19,63] can best be compared to those of the present work. Again, water fluxes exceeding about 4 ℓ/m^2s were not investigated. This is perhaps because

coefficients in the upper spray zones were correlated to the average water flux over the entire upper part of the machine within 3.3 m of the meniscus. Average water fluxes over the entirety of Zone 2 in the present study did not exceed about 5 ℓ/m^2s. If this were the case, the slightly higher results of Alberny could be due to unstable film boiling, discussed earlier, if the water fluxes were "averaged" to lower values over the upper spray zones. However, it is not clear why the heat-transfer coefficients reported by Alberny are higher even at very low water fluxes. The geometry of the continuous casting machine (i.e., nozzle and roll characteristics) must be a consideration. The fact that the present work predicts higher heat-transfer coefficients at the high water fluxes than an extrapolation of Alberny's results would provide, may again be rationalized as a consequence of the unstable film boiling behaviour. Birat[19] has indicated that decreasing surface temperature below 800°C increases the heat-transfer coefficient, but the effect is not large and the location of measurement of the surface temperature referred to is not given. No indication of the scatter obtained or the extent of replicate measurements is provided.

The results of Samoilovich et al.[64] cover a narrow range of water fluxes, but are in good agreement with the present correlation.

6.8.2 Local Heat-Transfer Coefficients

Comparison of the local spray heat-transfer coefficients determined in Zone 2 (Figure 34) with laboratory investigations of secondary cooling (Figure 6) indicates that with the exception of Mitsutsuka,[46] the results obtained in the present study are much higher. The scatter band is in fact between the upper limit of the majority of previously reported investigations and the results of Mitsutsuka. If unstable film boiling is the operating heat-transfer mode in Zone 2, this behaviour is to be expected, particularly if the slab is passing in and out of the transition boiling regime as Figure 41 suggests. The observations of Hoogendoorn et al.,[44] that the heat-transfer coefficient ranged from 0.25 to 1.50 above and from 4.00 to 6.00 kW/m^2K below the critical temperature, support this statement. In fact, most of the actually observed scatter in the local coefficients of Zone 2 is from 0.80 to 6.00 kW/m^2K. That the upper limit approximately corresponds to the results of Mitsutsuka at 15-20 ℓ/m^2s local water flux is interesting because Mitsutsuka is the only worker to have used a plain carbon steel plate for the laboratory study. This plate would be susceptible to scaling, as noted in Chapter 3, and is perhaps more representative of the real behaviour of a continuously cast carbon steel slab. The comments presented in Chapter 3 concerning the effect of surface oxide layers on the stability of film boiling and peak heat flux obtained[29,30] should be kept in mind. Very recent work, also by Mitsutsuka and Fukuda,[82] has attempted to delineate the effects of surface properties

on the boiling mechanism. Three specimens having different surface properties were compared for their heat-transfer characteristics. The pertinent conclusions that they reached are:

i) The surface temperature corresponding to the maximum value of heat-transfer coefficient increases as the amount of surface scale increases.

ii) The heat-transfer coefficient in the transition boiling region increases as the amount of scale deposit increases. The maximum value of h, is less, however.

iii) The heat-transfer coefficient in the film boiling region seems to be little influenced by the surface properties of the specimen.

An estimate of the mean local heat-transfer coefficient in the various zones may be obtained from the detailed temperature profiles corresponding to the profiles predicted with the regression equation (Figures 39 to 41). The local heat-transfer coefficients determined in this way for Zone 2 are of the order of 3.0 kW/m^2K when unstable film boiling is predicted. This value is in approximate agreement with the values expected in the unstable film boiling region, indicated in Figure 9. The local coefficients in the present case may be slightly higher than seen in Figure 9 because the heat-transfer coefficients are necessarily correlated here to

average local water fluxes rather than peak local water fluxes. The discussion presented with respect to Figures 10 and 11 indicates that when correlating heat-transfer coefficients to average rather than peak water fluxes the h-water flux relationships are effectively shifted upwards. The effects of scale just mentioned in points i) to iii) would also be to shift the present relationships upwards, since the results presented in Figure 9 are mainly for scale-free surfaces. Thus the conclusion that unstable film boiling prevails under most conditions in Zone 2 is further justified and the observed scatter of the measured local coefficients is not unexpected.

The local heat-transfer coefficients calculated for Zones 3 and 4 are in the range 1.3 to 2.1 kW/m^2K. Comparison of these values with Figure 9, considering the probable upward shift due to spray water distribution, is inconclusive. It is unlikely that a coefficient of 1.3 kW/m^2K is associated with transition boiling, but at the high water fluxes in Zones 3 and 4 the calculated local heat-transfer coefficient may be representative of transition boiling behaviour.

6.9 Overall Characterization of Heat Transfer in the Secondary Cooling System

Knowledge of the significance of each secondary cooling zone in the overall heat transfer may be useful in estimating the control capability of each zone through changes in spray

water flux. In particular, it is interesting to note the relative contribution of each zone to the total heat transfer, and the relative significance of the different heat-transfer mechanisms.

Figure 43 shows the average heat flux in and fraction of heat extracted by each secondary cooling zone under normal operating conditions at 1.52 m/min. The thickness of the solidified shell is also shown for conditions corresponding to Figure 38. It is seen that although large heat fluxes are obtained in the upper spray zones, the contribution of these zones to the total heat removal is relatively small.

The contribution of direct spray heat transfer to the total heat removed can also provide an understanding of control capability through water flow adjustments. The results of calculations pertaining to normal operating conditions are shown in Table XVII. It is observed that the contribution to the total heat transfer of direct spray impingement varies from 95 per cent high in the machine to 43 per cent low in the machine. This is important because it means that thermal events (i.e. heat flux, surface temperatures, shell thicknesses) are determined more directly by spray cooling practice high in the machine. Thus the ramifications of spray cooling phenomena (e.g., unstable film boiling) will be more visible in this region. Low in the machine, spray-related phenomena are

TABLE XVII Contribution of the Different Heat-Transfer Modes to the Total Heat Extracted in Each Secondary Cooling Zone Under Normal Operating Conditions

Zone	% Contribution to Total Heat Extracted		
	Direct Spray Impingement	Radiation	Roll Contact and Convection to Draining Water
1	95	4	1
2A	92	4	4
2B	85	7	8
2C	79	10	11
3	56	22	22
4	64	16	20
5	43	21	36
All Zones	61	17	22

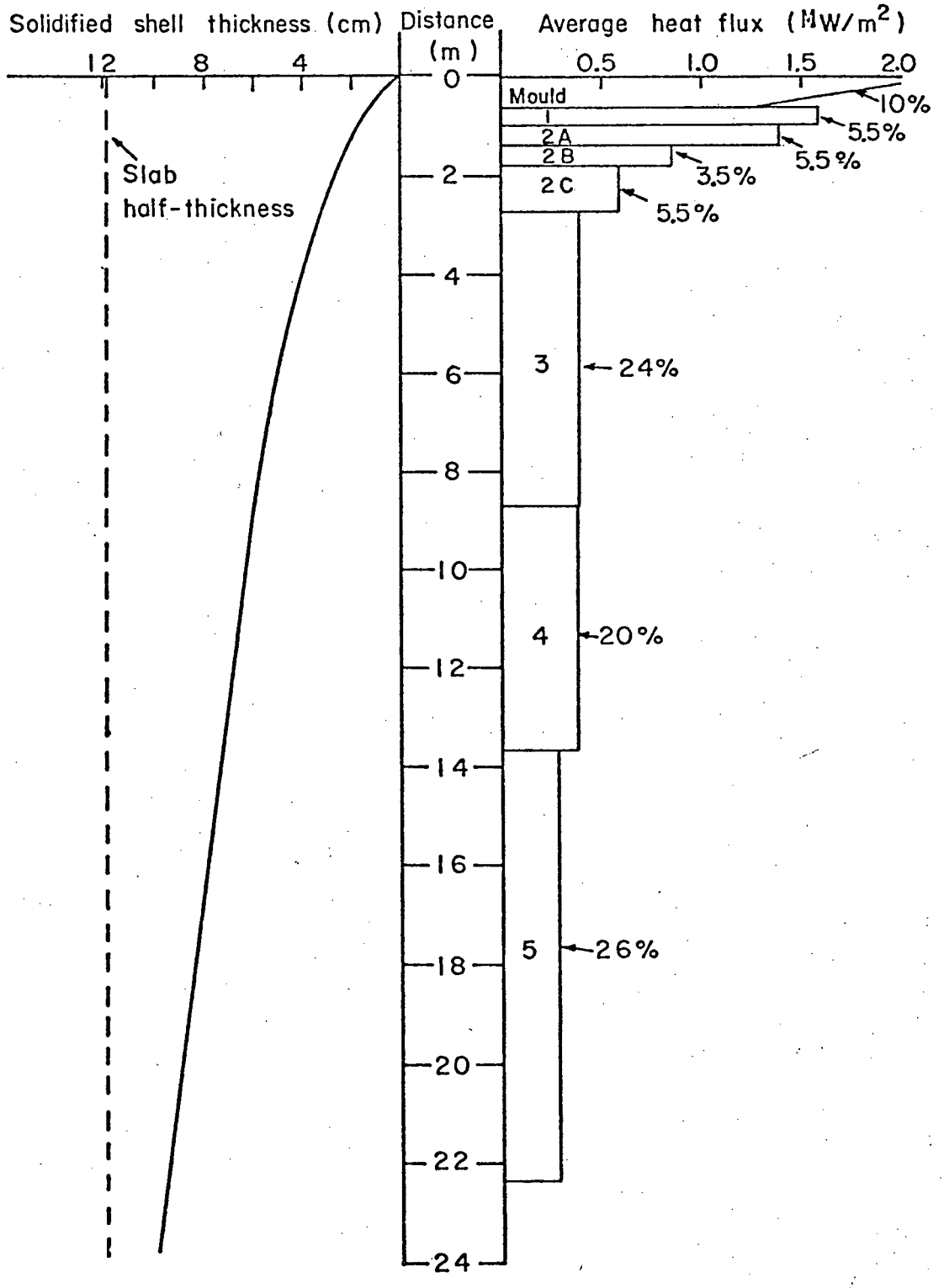

Figure 43 Average heat fluxes and predicted shell thickness for normal operating conditions at 1.52 m/min casting speed.

masked somewhat because of the greater contributions of radiation and roll contact. This explains in part the difficulty in identifying a spray cooling mechanism in Zone 4. It also helps to explain why higher values of heat-transfer coefficient are obtained in slab casters than in other types of continuous casting machine (Figure 13). Because of the increased influence of radiation low in the machine, total heat removal is less influenced by local spray heat transfer. Thus, for example, if spray water flux is reduced in an attempt to obtain film boiling heat transfer and better temperature control, the overall heat removal is "buffered" by the increased importance of radiation heat transfer at higher temperatures.

A further observation pertaining to the total heat flux may be made with respect to Figures 14 and 35. Extrapolation of the total heat flux equation (Equation 34) to zero average water flux gives a heat removal of about 0.187 MW/m^2 in the absence of spray cooling. Radiative heat fluxes calculated beyond Zone 5 during the present work are about 0.090 MW/m^2. The difference of 0.097 MW/m^2 may be attributed to roll contact. This is in good agreement with the results of Diener et al.[66] (Figure 14) for rolls which are not internally water cooled. Since this type of containment roll is employed in Zone 5 and beyond, application of an average heat flux of this amount in roll-contained areas beyond the spray chamber is suggested. Predicted surface-temperature profiles, when this average heat flux is applied, are compared in Figure 44 to predictions in

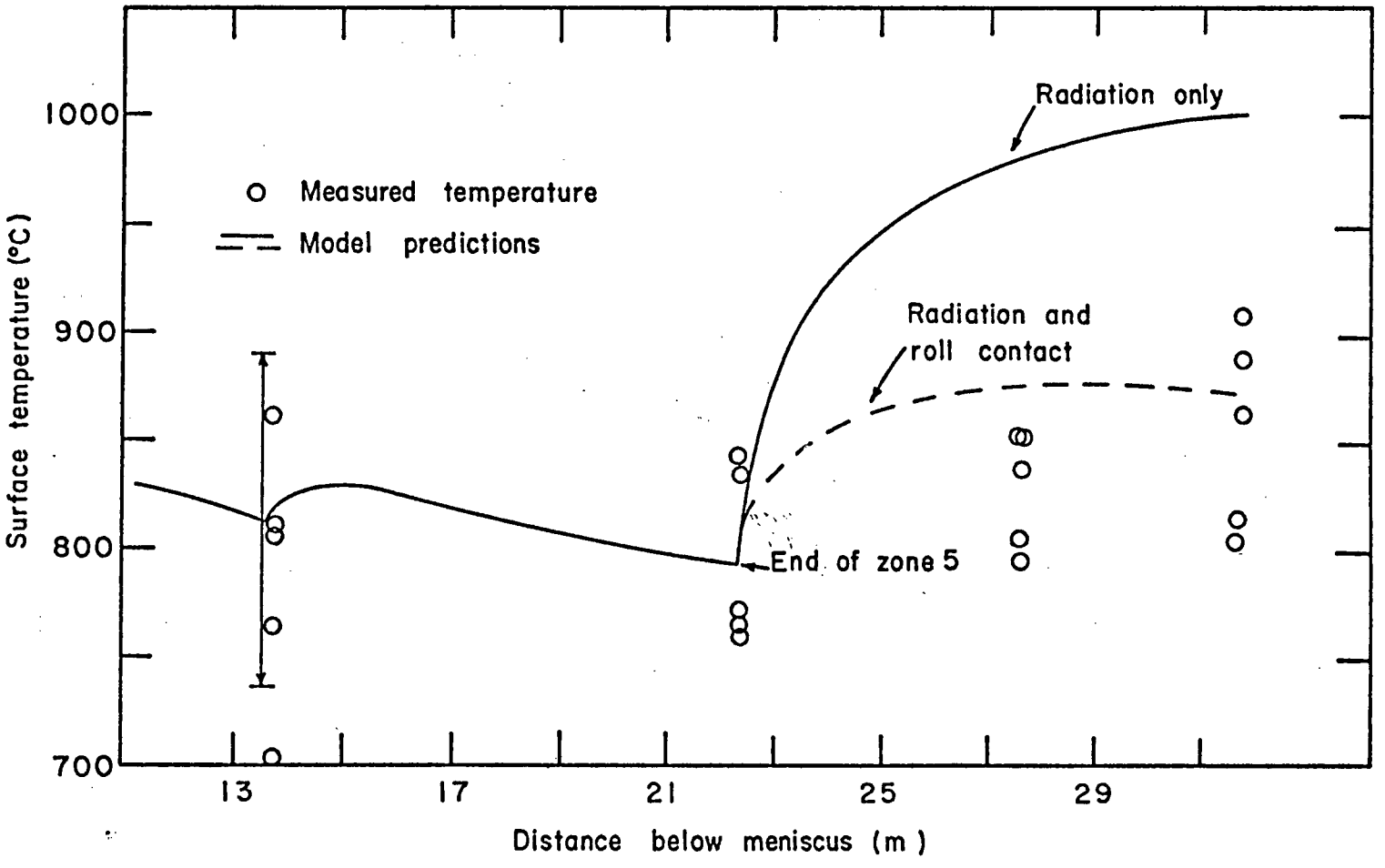

Figure 44 Comparison of predicted and measured temperatures beyond the secondary cooling zones, with and without accounting for roll contact.

which the contribution of the rolls is not included. Measured temperatures outside the secondary cooling system (prior to extension of Zone 5) are in better agreement with predicted temperatures when the average heat flux due to roll contact is included. The significant effect of roll-contact heat transfer low in the machine supports the finding that the heat-transfer coefficient in Zone 5 has a relatively low sensitivity to the spray water flux.

6.10 Application of the Results to Spray Chamber Design and Control

The results reported in this study will assume greater significance if they can be used to solve quality and operating problems in continuous casting operations. The ultimate objective in terms of spray chamber design and control must be to achieve the desired temperature-time profile, mentioned in Chapter 1, on a consistent basis.

Based on the results of this study it does not appear that accurate prediction of slab surface temperatures is possible. The heat-transfer model can be used with the regression equations only to predict a probable mean temperature at a given location. Because of the error sources outlined in Table XVI the predicted temperature may deviate by as much as 70°C from

the temperatures desired, under "ideal" spray-cooling conditions. Thus it would appear that if more accurate control of surface temperature is required, on-line surface-temperature monitoring is necessary. It should be noted that, although this technique would be capable of providing accurate control of measured temperatures, the measured values can still be as great as 25 to 30°C less than the actual temperature, due to pyrometer error (and assuming no surface scale). This error furthermore is based on the assumption that care equivalent to that of the current work would be taken in maintaining pyrometer calibration. Feedback control could be used to make water flow-rate changes which would result in a desired surface temperature, by employing the heat-transfer model and the regression equations (Equations 28, 29, 30 and 33).

The ability of the heat-transfer model to predict surface temperatures accurately is further reduced by unstable film boiling phenomena. However this problem can be overcome by reducing the spray water flow rate so that stable film boiling occurs throughout the secondary cooling system. This would be a significant benefit in that the slab surface temperature would be more easily controlled. The reduction of spray water flux necessary to achieve this objective is not large. Figures 39 to 41 indicate that this may be accomplished if the lowest temperatures obtained in the spra

spray-impingement areas are kept above about 750°C. This would require keeping "smoothed" temperatures normally predicted by the heat-transfer model above about 850°C in Zones 1, 2, 3 and 4. This result is possible using the present spray system.

Figure 45 shows the predicted temperature profiles and shell thicknesses under current and modified spray practices. The modified spray practice is such that surface temperatures will be maintained above the estimated critical point for the onset of unstable film boiling. This requires water flow rate reductions of 6 per cent in Zone 1, 31 per cent in Zone 2 and 13 per cent in Zone 4. Predicted shell thicknesses are nearly identical with both practices. From this consideration alone it would appear that the risk of breakouts will not be substantially increased. However at higher temperatures the shell may be more susceptible to bulging and therefore the risk of breakouts might be increased in Zone 2. However spray water fluxes of the prescribed magnitude were used in the current work during the tests on Zone 2, without adverse effect. Furthermore, Figure 3 indicates that other slab casters operate at lower water fluxes in the upper spray zones than with normal practice at the Inland Slab Caster. Thus it would appear that breakouts are not likely under the modified conditions.

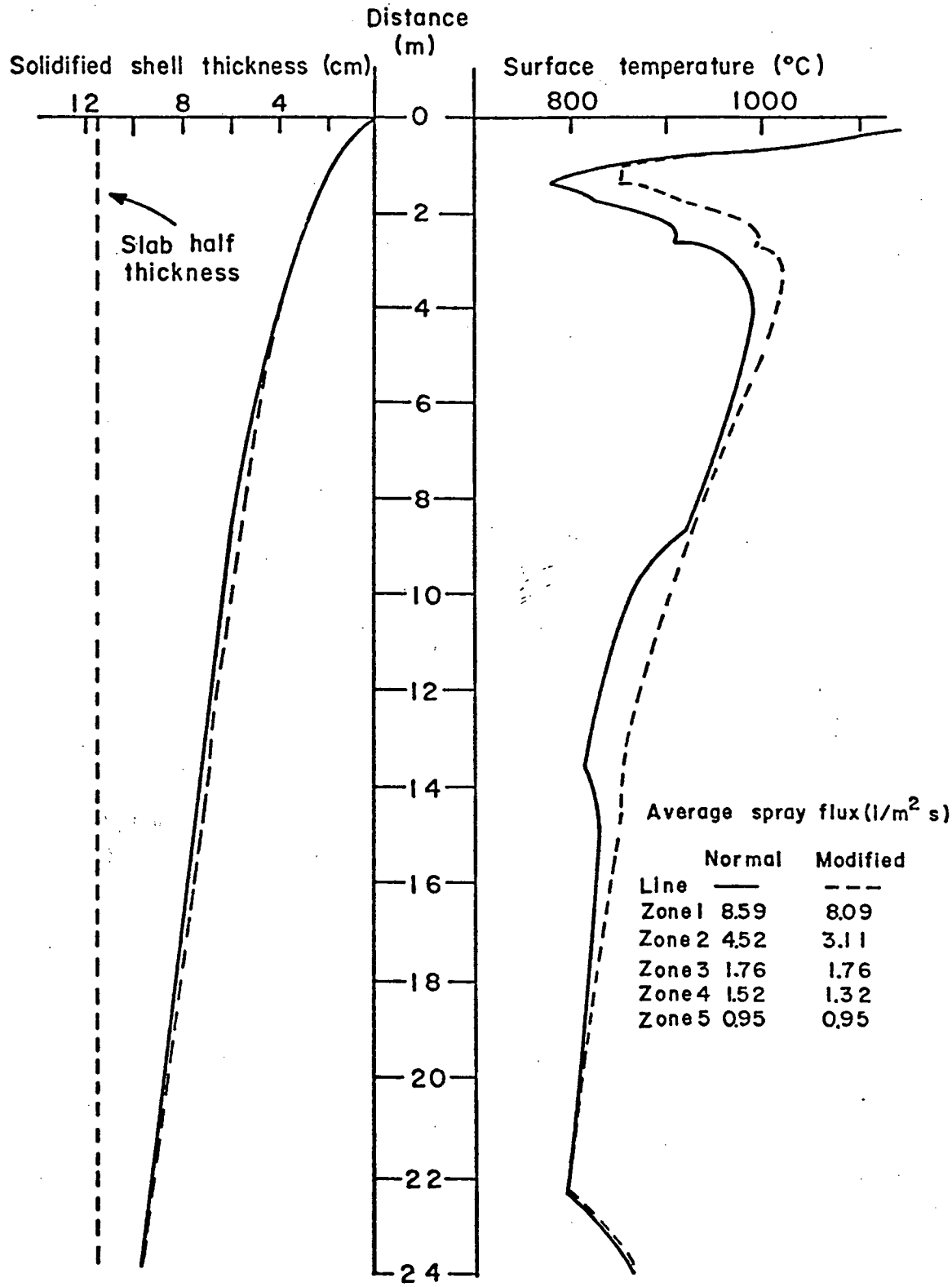

Figure 45 Predicted temperature profiles and solidified shell thicknesses under current and modified spray conditions.

Even with reduced water fluxes in Zones 1 and 2 the cooling intensity is quite high. Longitudinal midface cracking problems that may occur are possibly caused or aggravated by the high cooling intensity in Zones 1 and 2A. The rates of cooling in the local spray-impingement areas are much higher than the smoothed profiles indicate. Calculations based on the results at high flow rates indicate that the cooling rate in the local spray-impingement areas of Figure 41 can be as high as 2000°C/m. Temperature gradients of this magnitude create large tensile stresses at the slab surface which are likely to exacerbate longitudinal midface cracking problems. Reduced spray cooling in the upper spray zones, within practicable limits, would thus appear essential for the improvement of slab surface quality. Thus the modified spray pattern is desirable not only in terms of obtaining reproducible caster operation, but in reducing thermally induced stresses that can lead to cracking.

The above discussion is directly applicable to plain low-carbon grades of steel but similar considerations apply to the casting of microalloyed steels.

In Chapter 1 it has been mentioned that these steels are particularly susceptible to transverse surface cracking. Two considerations are important for the prevention of this type

of crack: minimize precipitation of nitrides or carbonitrides, and straighten the slab with surface temperatures outside of the low ductility range of 700 to 900°C. Although a heat-transfer model is capable of predicting spray conditions necessary to obtain the latter criterion for either a low-temperature or high-temperature strategy, it would appear that the high-temperature strategy is preferable. This is because surface temperatures may be easier to control at higher temperatures under conditions of stable film boiling. However this must be accomplished without causing mechanical problems due to bulging. Furthermore, transverse cracks are often observed at the corners of the slab where the temperature is lower due to two-dimensional heat flow. A two-dimensional heat-transfer model may be necessary in this case to predict spray conditions which will avoid the low ductility region at the slab corners.

Avoidance of nitride precipitation must also be concerned with the local surface temperature fluctuations in Zones 1 and 2. In particular, Brimacombe et al.[9] have noted that A&N precipitation does not proceed during cooling to as low as 800°C but can take place rapidly during heating over the temperature range 700 to 1000°C. Consequently the repeated heating and cooling which are obtained should enhance A&N precipitation and concomitant low ductility. Thus it would appear that greater reductions in cooling rates than those already mentioned are necessary to avoid the embrittling effect of A&N

precipitation. Nozaki et al.[6] applied these considerations to minimize transverse cracking by the "plateau cooling" philosophy, which maintains an average cooling rate of less than 83°C/m in the upper part of the continuous casting machine. The cooling rate of 200°C/m in Zones 1 and 2A of the Inland Slab Caster is far from obtaining such a desired cooling rate. Since Nozaki also mentions that longitudinal midface cracks are reduced when employing this practice, such a spray cooling philosophy may be desirable for all steel grades.

The ability to obtain reduced cooling rates, particularly in Zone 2 at the Inland Slab Caster is limited by the current spray system design. Because of the water flow distribution in Zone 2 the sharp drop in slab surface temperature is followed by a rapid and large reheating. Obviously operators will be somewhat hesitant to raise the temperature in Zone 2A by reduction of spray water flow rate when the Zones 2B and 2C spray water flow rates are also reduced by this action. The consequence could be an extremely large surface reheating and bulging problems. A change in the spray water distribution high in the machine, in Zone 2 in particular, is necessary to achieve desired surface temperature profiles.

Even if spray water flow-rate reductions can be obtained high in the machine, large temperature fluctuations will still

occur due to spray impingement. At the lower local spray water fluxes obtained in Zones 3 and 4 (Figures 39 and 40) the magnitude of the local surface temperature fluctuations exceeds 100°C. Recent Japanese work [82,83] has studied the use of air-water atomized sprays in the cooling of steel plates. The range of heat-transfer coefficients obtainable by "fog" cooling is much greater than by conventional spray cooling. Other recent work[84] utilizing thermocouples welded to the slab surface during continuous slab casting has indicated that equivalent overall cooling rates are obtained by "mist" cooling while reducing local temperature fluctuations in the spray-impingement area from 150°C to 80°C. This is supposedly possible because the air-water atomized spray can "spread out" and impinge over a greater slab surface area than in the case of normal sprays. The mean droplet diameter is claimed to be reduced from 0.4 to 0.05 mm by air atomization and thus the droplet momentum would be reduced. Quality improvements are claimed, but more extensive testing in industrial environments is necessary in order to reach definite conclusions.

6.11 Some Observations of Unsteady-State Phenomena

Although the results presented and discussed to this point have been concerned solely with "steady-state" operation of the continuous casting machine, the differences between phenomena

occurring during steady-state and unsteady-state operation should be mentioned. The behaviour of the secondary cooling system during start-of-cast and shroud changes is of particular interest.

An example of temperatures measured at various locations in Zones 3 and 4 is presented in Figure 46, from cast 9777. During this cast the steady-state casting speed was attained within 1 or 2 minutes. Figure 46 shows that steady-state temperature measurements were not approached until approximately 20 minutes (or greater) from the start of the cast. During the first 10 minutes of the cast, slab surface temperatures were more than 100°C less than those obtained at steady-state. This behaviour occurs as a result of the time necessary for the mould water temperature, spray water temperature, and machine structure to obtain equilibrium thermal conditions. The temperature-time profiles of Figure 46 are typical of those observed during this study. It was also observed that, as distance below the meniscus increased, greater time is necessary for steady-state temperatures to be obtained. These observations are significant when considered with respect to control of slab surface temperatures. If a specific temperature is required at a certain location below the meniscus, and in the absence of quantification of the unsteady-state phenomena, feedback control based on on-line monitoring of surface temperatures may be necessary to obtain quality during

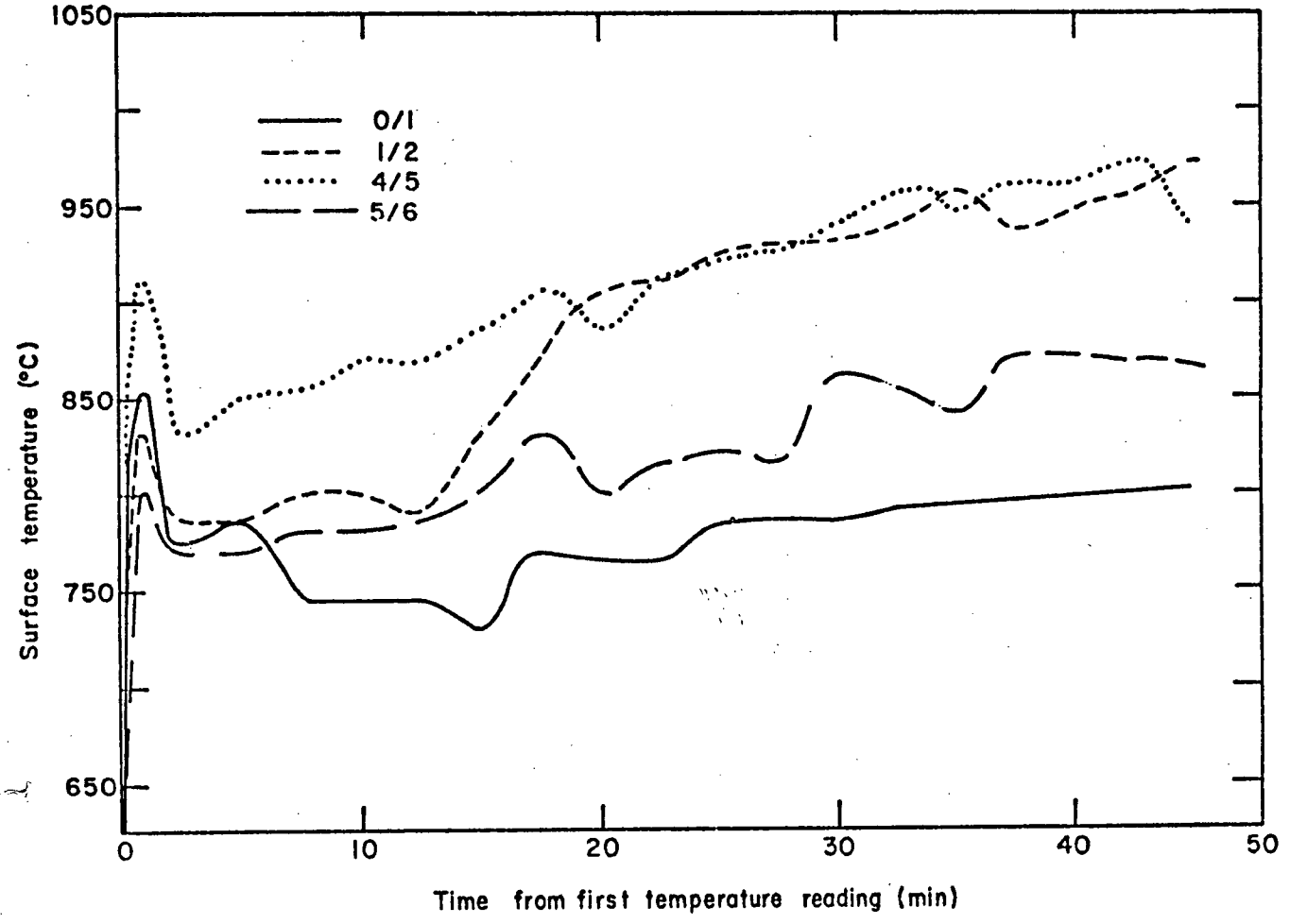

Figure 46 An example of unsteady-state temperature measurements in Zones 3 and 4 after start-of-cast. (Cast 9777).

the first 20 minutes of the cast.

During some casts, the chart speed was increased and the peak-picking feature of the Thermal Monitor System was not used during shroud changes, in order to record unsteady-state temperature fluctuations. Casting speed and temperatures measured at the 0/1 position by this procedure are presented in Figure 47. A steady-state casting speed of 1.40 m/min was reduced to zero during the shroud change. After restart of the cast, casting speeds of 0.6 m/min were employed for several minutes before steady-state was again achieved. During these transients, water flows are controlled in proportion to casting speed, but cannot be reduced below a certain minimum flow rate. Thus when the casting speed is zero, the same areas of the slab surface are sprayed at the minimum flow rate for the duration of the shroud change, while the unsprayed areas may reheat. The effect on slab surface temperatures is clearly shown in Figure 47. Temperature drops corresponding to the spray-impingement areas pass through the measurement point following restart of the cast. This is verified by the fact that the number of temperature drops observed upon cast restart (10) is equal to the number of spray rows above the 0/1 position. Furthermore, a calculation showed that the distance between successive troughs corresponds to the distance between successive spray-impingement areas in Zone 2.

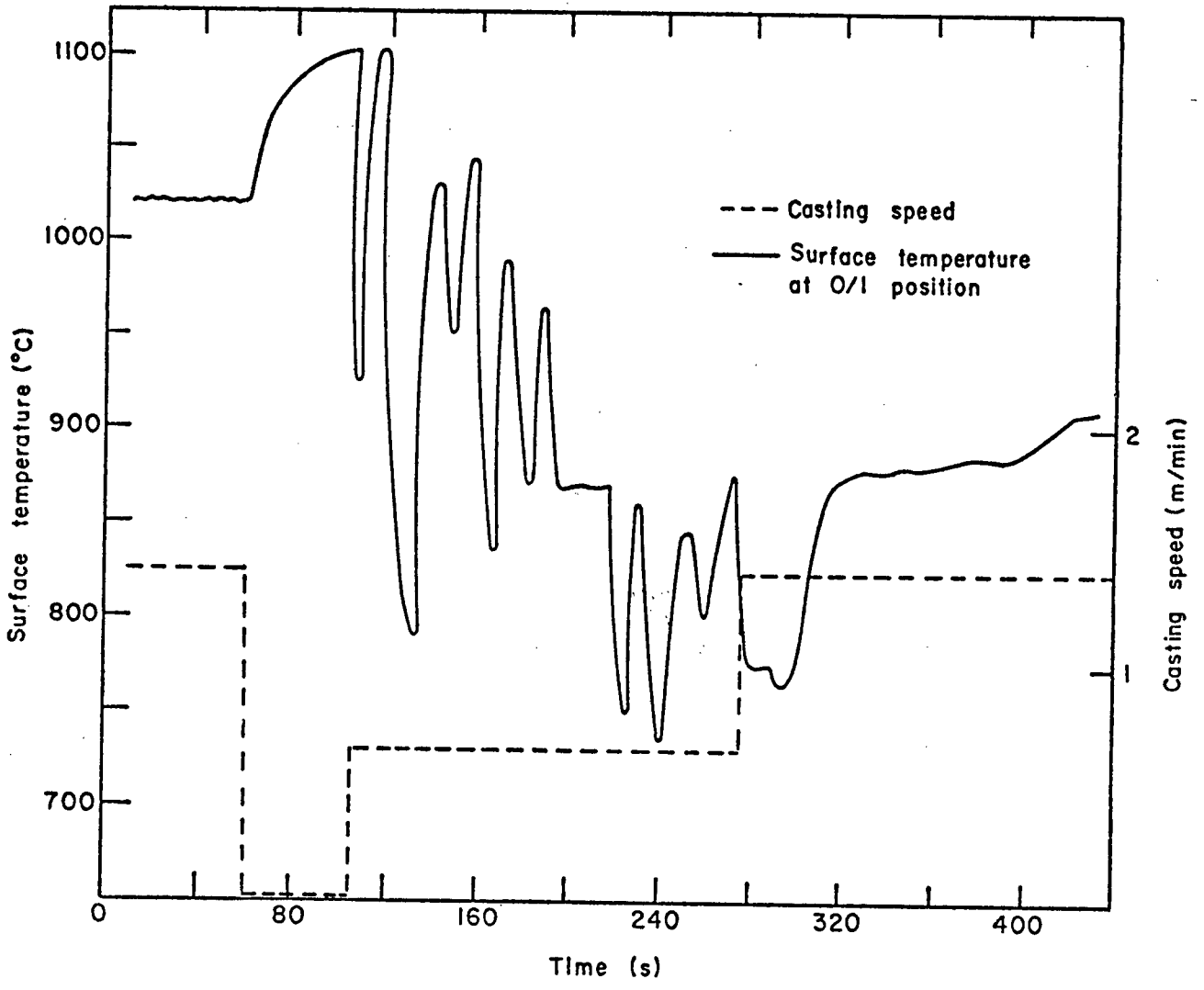

Figure 47 An example of temperatures measured at the O/I position during and after a shroud change. (Cast 9763).

The magnitude of the largest fluctuation (300°C) is greater than the model-predicted fluctuations of Figure 41, which is to be expected if a slab surface element occupied the spray-impingement area for an extended time. These observations are significant in terms of surface temperature control during shroud changes. For example, the ability of a "cooling-with-time" model to obtain desired surface-temperature-time profiles during process transients is limited by the physical construction of the secondary cooling system. Regardless of water flow-rate changes accomplished by a cooling-with-time model, when the casting speed is zero, some areas of the slab surface will be directly under the spray nozzles, and non-sprayed areas will reheat. The only solution is then to keep process transients to a minimum, such as by increasing shroud life.

Chapter 7

SUMMARY AND CONCLUSIONS

This study has been undertaken in an effort to obtain increased understanding of the heat-transfer processes which occur in the secondary cooling system of a continuous slab-casting machine. The experimental work has involved in-plant trials during which slab surface temperatures were measured with radiation pyrometers in the secondary cooling system. Controlled experiments were performed in which temperatures were measured in each zone under normal and modified spray water cooling practices.

A one-dimensional heat-transfer model of the casting process was developed, based on the implicit finite-difference method. The model has been used to convert the measured temperatures into average spray heat-transfer coefficients for each experiment. The average coefficients were determined to be insensitive to the thermal history of the slab prior to entering the zone under study. In Zones 3, 4 and 5 the average heat-transfer coefficients were determined directly from the measured temperatures. In Zone 2 temperatures were measured in the spray-impingement regions, and thus local heat-transfer coefficients in these regions were determined first. The local

coefficients were used to determine a "real" temperature profile and the temperatures at the entrance and exit of Zones 2A, 2B and 2C. These calculated temperatures were then used to determine the average heat-transfer coefficients.

The results have been quantified by means of regression equations which provide relationships between the average spray heat-transfer coefficients and average spray water fluxes obtained during the experiments. The regression equations obtained are:

for Zone 2

$$h = 0.080 + 0.188\,\dot{W}\ , \quad 1.66 \leq \dot{W} \leq 9.85\ \ell/m^2s\ ;$$

for Zone 3

$$h = 0.213\,\dot{W}^{0.665}\ , \quad 0.94 \leq \dot{W} \leq 2.03\ \ell/m^2s\ ;$$

for Zone 4

$$h = 0.212\,\dot{W}^{1.424}\ , \quad 0.91 \leq \dot{W} \leq 1.52\ \ell/m^2s\ ;$$

and for Zone 5

$$h = 0.182 + 0.122\,\dot{W}\ , \quad 0.27 \leq \dot{W} \leq 0.95\ \ell/m^2s\ .$$

In roll-contained regions outside the secondary cooling system, an average heat flux, due to roll contact, of 0.097 MW/m^2 was employed to obtain better agreement between calculated and measured temperatures than when the calculated heat flux was due to radiation only. Direct impingement of the water spray on the slab surface has been calculated to account for between 95 per cent (Zone 1) and 43 per cent (Zone 5) of the total heat extracted in the individual zones. In the entire secondary-cooling system, the contribution of the

different heat-transfer mechanisms to the total heat extracted has been calculated to be

61% direct spray impingement

17% radiation

22% contact with rolls and convection to draining water.

Predictions by the heat-transfer model indicate that, under normal operating conditions, a sharp reduction of slab surface temperature occurs in Zones 2A and 2B, which is followed by a large reheating (of the order of 200°C) in Zones 2C and 3. A comparison of calculations performed in this study to previous laboratory investigations of the Leidenfrost phenomenon indicates that unstable film boiling occurs in the spray-impingement areas of Zone 2. This boiling mechanism may also occur under certain circumstances in Zone 4. These observations are substantiated by the large scatter and high heat-transfer coefficients that obtain in this study when unstable film boiling is predicted.

Consideration of the mechanisms of crack formation in continuous slab casting has indicated that the current spray-cooling practices may exacerbate longitudinal midface and transverse cracking. Transverse cracking may be caused by the cooling/reheating cycles that occur in Zone 2 and by straightening in the 700 to 900°C range. Longitudinal midface cracking may be

exacerbated by thermal stresses on the broad face during the rapid cooling in Zone 2.

In order to avoid unstable film boiling and minimize cracking a reduction of spray water flux in Zone 2 is recommended. Control of slab surface temperatures will be easier if stable film boiling is obtained. Unstable film boiling may be avoided by maintaining "smooth" temperature profiles above 850°C throughout the secondary cooling system. Based on the results of Nozaki et al.,[6] further reductions in cooling rates in Zone 2 are necessary to maximize quality. This may require changing the spray water distribution between Zones 2A, 2B and 2C so that large reheating and concomitant bulging are avoided. Air-water atomised spray systems should receive further attention for obtaining "soft" cooling practices.

Considerable variation of slab surface temperatures is still possible if unstable film boiling is avoided. In this study, the heat-transfer model has been as much as 70°C in error due to known error sources. If more accurate control of slab surface temperatures is required, feedback control based on on-line monitoring of surface temperatures is recommended. This may be necessary particularly during process transients such as occur shortly after the start of a cast.

These measurements of this study have been confined to the

vicinity of the centreline of the broad slab face on the inner radius of Strand 2. It is not known whether the results are applicable to Strand 1 or the outside radii. If accurate knowledge is desired of the heat extraction from Strand 1 or the outside radii, temperature measurements should be carried out at those locations.

REFERENCES

1. Lankford, W.T., "Some Considerations of Strength and Ductility in the Continuous Casting Process," Met. Trans., Vol. 3, June 1972, pp. 1331-1357.

2. Wray, P.J. and Holmes, M.F., "Plastic Deformation of Austenitic Iron at Intermediate Strain Rates," Met. Trans., Vol. 6A, June 1975, pp. 1189-1196.

3. Adams, C.J., "Hot Ductility and Strength of Strand Cast Steels Up to Their Melting Points," Open Hearth Proc., TMS-AIME, Vol. 54, 1971, pp. 290-302.

4. Weinberg, F., "The Ductility of Continuously Cast Steel Near the Melting Point - Hot Tearing," Met. Trans., Vol. 10B, June 1979, pp. 219-227.

5. Weinberg, F., "The Strength and Ductility of Continuously Cast Steels Above 800°C," Met. Trans. Vol. 10B, Dec. 1979, pp. 513-522.

6. Nozaki, T., Matsuno, J., Murata, K., Ooi, H. and Kodama, M., "A Secondary Cooling Pattern for Preventing Surface Cracks of Continuous Casting Slab," Trans. ISIJ, Vol. 18, 1978, pp. 330-338.

7. Offerman, C., Dacker, C.-A. and Enstrom, C., "A Way to Avoid Transverse Cracking by Surface Temperature Control," Scand. J. Met., Vol. 10, 1981, pp. 115-119.

8. Schmidt, L. and Joseffsson, A., "On the Formation and Avoidance of Transverse Cracks in Continuously Cast Slabs from Curved Mould Machines," Scand. J. Met., Vol. 3, 1974, pp. 193-199.

9. Brimacombe, J.K. and Sorimachi, K., "Crack Formation in the Continuous Casting of Steel," Met. Trans., Vol. 8B, Sept. 1977, pp. 489-505.

10. Brimacombe, J. K., Weinberg, F. and Hawbolt, E.B., "Formation of Longitudinal Midface Cracks in Continuously-Cast Slabs," Met. Trans., Vol. 10B, June 1979, pp. 279-292.

11. Brimacombe, J.K., Agarwal, P.K., Baptista, L.A., Hibbins, S. and Prabhakar, B., "Spray Cooling in the Continuous Casting of Steel," Presented at NOH-BOS Conf., Washington, 1980.

12. Ozeki, R.K. and Duke, J.D., "Casting of High Quality Plate Steel Slabs at Texas Works," Proc. Int. Conf. on Continuous Casting of Steel, Biarritz, France, 1976, The Metals Society/ IRSID, pp. 292-299.

13. Duke, J.D. and Ozeki, R.K., "Casting Slabs for Plate Application at U.S. Steel's Texas Works," Iron and Steelmaker, Oct. 1977, pp. 21-27.

14. Myoshi, S., "Influence of Operating Conditions and Mechanical Factors on Centre Segregation of Slabs," Proc. Int. Conf. on Continuous Casting of Steel, Biarritz, France, 1976, The Metals Society/IRSID, pp. 286-291

15. Fujii, H., Ohashi, T. and Hiromoto, T., "On the Formation of Internal Cracks in Continuously Cast Slabs," Trans. ISIJ, Vol. 18, 1978, pp. 510-518.

16. DiCandia, A., "Metallurgical Problems in Continuous Casting of Low-Alloy C-Mn Steel Slabs at Taranto," Proc. Int. Conf. on Continuous Casting of Steel, Biarritz, France, 1976, The Metals Society/IRSID, pp. 135-145.

17. Ichikawa, H., Yamazaki, I., Kimura, T. and Tozaki, Y., "Progress of Quality Steel Slab Casting at Kashima Steel Works," Proc. NOH-BOS Conf., Vol. 60, Pittsburgh, 1977, pp. 243-256.

18. Miyazawa, K. and Schwerdtfeger, K., "Computation of Bulging of Continuous Cast Slabs with Simple Bending Theory," Ironmaking Steelmaking, Vol. 6, No. 2, 1979, pp. 68-74.

19. Birat, J.P., Larrecq, M., LeBon, A., Jeanneau,M.,Poupon,M.and Senaneuch,D., "Control of Secondary Cooling in the Continuous Casting of Plate Grades," Presented at 64th Steelmaking Conf., Toronto, 1981.

20. Brimacombe, J.K., "Design of Continuous Casting Machines Based on a Heat-Flow Analysis : State-of-the-Art Review," Can. Met. Quart., Vol. 15, No. 2, 1976, pp. 163-175.

21. Etienne, A., Mairy, B. and Dauby, B., "Metallurgical Control and Automation for Continuous Casting Operation," Proc. Int. Meeting on Iron and Steelmaking," Brussels-Dusseldorf, May, 1976, Vol. 1B, p. 4.2.3.

22. Foussal, J., "Modèle Pratique de Gestion et de Commande du Refroidissement Secondaire en Calculateur à la Coulée Continue de SOLMER, à Fos-sur-Mer," Rev. Met., Vol. 75, Juin 1978, pp. 404-414.

23. Baptista, L.A., "Control of Spray Cooling in the Continuous Casting of Steel," M.A.Sc. Thesis, University of British Columbia, 1979.

24. Readal, G.J., "Controlling a Continuous-Continuous Casting Operation," Iron and Steelmaker, April, 1977, pp. 36-41.

25. Iida, Y., Kodama, M., Suzuki, K., Yamazaki, J. and Kojima,S., "Development of Surface Temperature Control in Slab Caster," Kawasaki Steel Tech. Report, Vol. 11, No. 3, 1979, pp.121-133.

26. Mairy, B. and Ramelot, D., "'Descatherm', a New Pyrometer for Measuring Strand Surface Temperature in Continuous Casting," Ironmaking Steelmaking, Vol.8, No.2, 1981, pp. 91-94.

27. Kreith, F., "Principles of Heat Transfer," Harper and Row, 1973.

28. Bell, K.J., "The Leidenfrost Phenomenon : A Survey," Chem. Eng. Prog., Symp. Series, No. 79, 1967, p. 73.

29. Moreaux, F., Chevrier, J.C. and Beck, G., "Hydrodynamic and Thermal Study of the Stability of Boundary Layer in the Case of Film Boiling," from "Heat Transfer and Turbulent Buoyant Convection, Vol. II," D.B. Spalding and N. Afgan, eds., Hemisphere Publishing, 1977, pp. 615-623.

30. Diesselhorst, T., Grigull, U. and Hahne, E., "Hydrodynamic and Surface Effects on the Peak Heat Flux in Pool Boiling," from "Heat Transfer in Boiling," E. Hahne and U. Grigull, eds., Hemisphere Publishing, 1977, pp. 99-135.

31. Wachters, L.H.J., Boone, H. and Van Nouhuis, H.J., "The Heat Transfer from a Hot Horizontal Plate to Sessile Water Drops in the Spheroidal State," Chem. Eng. Sci., Vol. 21, 1966, pp. 923-936.

32. Gottfried, B.S., Lee, C.J. and Bell, K.J., "The Leidenfrost Phenomenon : Film Boiling of Liquid Droplets on a Flat Plate," Int. J. Heat Mass Transfer, Vol. 9, 1966, pp. 1167-1187.

33. Moriyama, A., "Heat Transfer from Hot Steel Surface to a Water Droplet," Trans. ISIJ, Vol. 14, 1974, pp. 285-289.

34. Wachters, L.H.J. and Westerling, N.A.J., "The Heat Transfer from a Hot Wall to Impinging Water Drops in the Spheroidal State," Chem. Eng. Sci., Vol. 21, 1966, pp. 1047-1056.

35. Wachters, L.H.J., Smulders, L., Vermuelen, J.R. and Kleiweg, H.C. "The Heat Transfer from a Hot Wall to Impinging Mist Droplets in the Spheroidal State," Chem. Eng. Sci., Vol. 21, 1966, pp. 1231-1238.

36. McGinnis, F.K. and Holman, J.P., "Individual Droplet Heat Transfer Rates for Splattering on Hot Surfaces," Int. J. Heat Mass Transfer, Vol. 12, 1969, pp. 95-108.

37. Pedersen, C.O., "An Experimental Study of the Dynamic Behaviour and Heat Transfer Characteristics of Water Droplets Impinging Upon a Heated Surface," Int. J. Heat Mass Transfer, Vol. 13, 1970, pp. 369-381.

38. Toda, S., "A Study of Mist Cooling (1st Report - Investigation of Mist Cooling)," Heat Transfer, Japanese Research, Vol. 1, No. 3, 1972, pp. 39-50.

39. Bolle, L. and Moreau, J.C., Unpublished Research, Université Catholique de Louvain, Belgium, 1979.

40. Gaugler, R.E., "An Experimental Study of Spray Cooling of High Temperature Surfaces," Ph.D. Thesis, Department of Mechanical Engineering, Carnegie Institute of Technology, 1966.

41. Corman, J.C., "Water Cooling of a Moving, High Temperature Metal Strip," Ph.D. Thesis, Department of Mechanical Engineering, Carnegie Institute of Technology, 1966.

42. Auman, P.M., Griffiths, D.K. and Hill, D.R., "Hot Strip Mill Runout Table Temperature Control," Iron and Steel Engineer, Sept. 1967, pp. 174-179.

43. Lambert, N. and Economopoulos, M., "Measurement of the Heat Transfer Coefficients in Metallurgical Processes," J. Iron Steel Inst., Vol. 10, Oct. 1970, pp. 917-928.

44. Hoogendoorn, C.J. and den Hond, R., "Leidenfrost Temperature and Heat-Transfer Coefficients for Water Sprays Impinging on a Hot Surface," 5th Intl. Heat Transfer Conf., Tokyo, 1974, Paper B3.12, pp. 135-138.

45. Shimada, M. and Mitsutsuka, M., "On Heat Transfer Coefficient by Forced Water Cooling to Carbon Steel," Tetsu-to-Hagane, Vol. 52, 1966, pp. 1643-1645.

46. Mitsutsuka, M., "Study on the Water Spray Cooling of Steel Plate at High Temperature," Tetsu-to-Hagane, Vol. 54, 1968, pp. 1457-1471.

47. Sugitani, Y., Takashima, K. and Kawasaki, S., "Study of Secondary Cooling in Continuous Casting," Tetsu-to-Hagane, Vol. 59, No. 11, Lectures 12 and 13, 1973, pp. 5388-5389 [HB Translation No. 9236].

48. Etienne, A. and Mairy, B., "Heat Transfer in Continuously Cast Strands," C.R.M. Report No. 55, November, 1979.

49. Mizikar, E.A., "Spray Cooling Investigation for Continuous Casting of Billets and Blooms," Iron and Steel Engineer, Vol. 47, June, 1970, pp. 53-60.

50. Sasaki, K. Sugitani, Y. and Kawasaki, M., "Heat Transfer in Spray Cooling on Hot Surface," Tetsu-to-Hagane, Vol.65, 1979, pp. 90-96.

51. Bamberger, M., Jeschar, R. and Prinz, B., "Untersuchung des Wärmeübergongs beim Kühlen von Nichteisenmetallen durch Wasser," Z. Metallkde., Vol. 70, No. 9, 1979, pp. 553-560.

52. Junk, J., "Heat Transfer Investigations in a Simulated Secondary Cooling Zone for the Continuous Casting of Steel," Neue Hütte, Vol. 17, No. 1, 1972, pp. 13-18 [HB Translation No. 8740].

53. Müller, H. and Jeschar, R., "Untersuchung des Wärmeübergans an Einer Simulierten Sekunddärkühlzone beim Strangiessverfahren," Arch. Eisenhüttenwes, Vol. 44, No. 8, 1973, pp. 589-594.

54. Bolle, L. and Moreau, J.C., "Spray Cooling of Hot Surfaces: A Description of the Dispersed Phase and a Parametric Study of Heat Transfer Results," from "Two Phase Flows and Heat Transfer," S. Kakac and T.N. Vezirocu, eds., Proc. NATO Advanced Study Institute, 1976, pp. 1327-1346.

55. Bolle, L. and Moreau, J.C., "Experimental Study of Heat Transfer by Spray Cooling," Int. Conf. Heat and Mass Transfer Metallurgical Processes, Dubrovnik, Yugoslavia, 1979.

56. Prabhakar, B., "An Investigation of Heat Transfer in Spray Cooling," Ph.D. Thesis, University of British Columbia, 1981.

57. Akimenko, A.D., Kazanovich, L.B., Skvortsov, A.A. and Slutskii, B.I., "Investigating Heat Transfer in the Secondary Cooling Zone in a Continuous Casting Plant," Steel in the USSR, June 1972, pp. 448-449.

58. Urbanovich, L.I. et al., "Experimental Research into Hydrodynamics and Heat Transfer During the Spray Cooling of Continuously Cast Billets," Izv. VUZ Chernaya Metall., Vol. 9, 1980, pp. 145-149 [BISI Translation No. 19662].

59. Kojima, S., Matsukawa, T. and Kodama, M., "Condition of Internal Cracks in Continuous Casting of Steel Slabs," Kawasaki Steel Tech. Report, Vol. 12, No. 3, 1980, pp. 101-109.

60. Alberny, R., Leclercq, A. and Basilis, J., "Etude Thermique due Refroidissement Secondaire d'une Machine de Coulée Continue," Circulaire d'Informatio-techniques, Vol. 3, No. 315, 1973, pp. 763-776 [BISI Translation No. 11633].

61. Alberny, R., "Heat Transfer and Solidification in Continuous Casting," from "Casting and Solidification of Steel, Vol. 1," Comm. of European Economic Communities, Inf. Symposium, IPC Science and Technology Press, 1977, pp. 278-335.

62. Benoit, P., Rouzier, M. Perroy, A. and Petegnief, J., "Refroidissement Secondaire en Coulée Continue D'acier par Atomisation Air-eau," Rev. Met., Juin 1978, pp. 363-373.

63. Alberny, R., Perroy, A., Amary, D. and Lahousse, M., "Optimisation du Refroidissement Secondaire en Coulée Continue de Brames D'acier Extra-Doux," Rev. Met., Juin 1978, pp. 353-362.

64. Samoilovich, Y.A., Kolpakov, S.V., Kabakov, Z.K., Emel'Yanov, V.A. and Ermakov, O.N., "Heat Exchange in Secondary Cooling Zone in Curved Mould Continuous Casting Machines," Steel in the USSR, Dec. 1980, pp. 134-135.

65. Weisinger, H.A., Schwaha, K.L. and Kriegner, O., "Mathematical Analysis of the Solidification Process in High Speed Continuous Casting at Various Cooling Conditions," Proc. 2nd Process Technology Conf., Vol. 2, ISS-AIME, Chicago, 1981, pp. 86-94.

66. Diener, A. and Drastik, A., "Heat Exchange Between Strands and Guide Rollers in the Secondary Cooling Zone of a Slab Continuous Casting Machine," Proc. 4th Japan-Germany Seminar, ISIJ, Tokyo, Nov. 1980, pp. 262-275.

67. Vanzetti, R., "Practical Applications of Infrared Techniques," John Wiley and Sons, 1972.

68. Warnke, G.F., "Commercial Pyrometers," from "Temperature - Its Measurement and Control in Science and Industry," Vol. 4, Instrument Society of America, 1972, pp. 503-517.

69. Instruction Manual No. 5043, Infrared Thermal Monitor, Model TM-2, Vanzetti Infrared and Computer Systems, Inc., Canton, Ma., 1980.

70. Pelc, R.E., Unpublished Research, Inland Steel Co., August 1978.

71. Cramb, A.W., Unpublished Research, Inland Steel Co., January 1980.

72. Mairy, B. and Ramelot, D., "Sensor for Measuring the Surface Temperature of the Strand in a Continuous Casting Machine, C.R.M. Reports, No. 46, March 1976, pp. 23-28.

73. Mairy, B. and Ramelot, D., "'Descatherm', a New Pyrometer for Measuring Strand Surface Temperatures in Continuous Casting," Presented at 64th Steelmaking Conf. Toronto, 1981.

74. Cramb, A.W., Unpublished Research, Inland Steel Co., March 1980.

75. Cramb, A.W., Unpublished Research, Inland Steel Co., July 1980.

76. Bindokas, A.J., Unpublished Research, Inland Steel Co., 1981.

77. Carnahan, B., Luther, H.A. and Wilkes, J., "Applied Numerical Methods," John Wiley and Sons, Inc., 1969.

78. Lait, J.E. Brimacombe, J.K. and Weinberg, F., "Mathematical Modelling of Heat Flow in the Continuous Casting of Steel," Ironmaking Steelmaking, Vol. 1, No. 2, 1974, pp. 90-97.

79. Samarasekera, I.V., "Thermal and Mechanical Behaviour of Continuous Casting Moulds," Ph.D. Thesis, University of British Columbia, 1981.

80. Guttman, I., Wilkes, S. and Hunter, S., "Introductory Engineering Statistics," John Wiley and Sons, Inc., 1971.

81. Cramb, A.W., Unpublished Research, Inland Steel Co., April 1980.

82. Mitsutsuka, M. and Fukuda, K., "Cooling Characteristics and Heat Transfer Coefficients during Fog Cooling of Hot Steel Plates," Trans. ISIJ, Vol. 21, 1981, pp. 689-697.

83. Mitsutsuka, M. and Fukuda, K., "Water Atomization Characteristics in Crossflow Type Fog Nozzle and Water Flux Distribution of Fog Flow Ejected From It," Trans. ISIJ, Vol. 21, 1981, pp. 596-602.

84. Unpublished Research, Nippon Steel Corp., 1981.

Appendix A

DATA FROM IN-PLANT MEASUREMENTS

TABLE A.I Results of In Plant Measurements - Zone 3

Date	Cast	Steel Grade	Mould Powder	Slab Width (mm)	Casting Speed (m/min)		Average Water Flux (ℓ/m^2s)		Temperature, °C							
									Seg. 0/1		Seg. 1/2		Seg. 4/5		Seg. 5/6	
					Mean	Std Dev.	Mean	±	Mean	Std. Dev.	Mean	Std Dev.	Mean	Std. Dev.	Mean	Std. Dev.
30/9/80	9732	527-08	C994	1372	1.34	.11	0.94	.00	917	23	1013	10	964	7	-	-
					1.27	.13	1.05	.09	891	22	1060	13	945	23	-	-
					1.33	.05	1.57	.10	947	14	1052	11	915	15	-	-
					1.48	.11	2.00	.05	916	11	1007	10	866	10	-	-
2/10/80	9738	580-01	P389	1350	1.52	.00	1.19	.07	1050	11	1000	8	950	5	980	7
	9737	527-01	P327	1321	1.42	.10	1.65	.10	1041	17	985	13	926	13	919	11
8/10/80	9756	527-08	P327	1422	1.40	.09	1.62	.10	994	18	987	8	854	9	918	5
					1.40	.13	1.97	.05	1000	17	985	8	800	18	967	9
	9757	528-01	P389	1168	1.44	.07	1.17	.06	1003	13	1041	7	1024	2	972	19
9/10/80	9760	527-01	C994	1270	1.25	.12	1.03	.04	920	19	1019	12	949	7	985	6
					1.35	.06	1.57	.10	946	24	983	11	934	6	962	11
	9763	527-03	C994	1270	1.57	.10	1.26	.06	1043	19	1075	7	1045	3	1044	7
					1.36	.08	1.58	.10	1038	19	953	11	953	11	958	10
					1.56	.08	2.03	.04	1047	21	964	14	903	6	968	7
13/10/80	9774	527-08	P327	1575	1.49	.06	1.21	.06	819	14	994	6	993	5	877	8
					1.44	.08	1.66	.10	832	11	943	14	926	8	903	10
14/10/80	9777	527-08	P327	1422	1.51	.04	1.22	.06	825	14	1024	7	981	5	909	8
					1.55	.06	1.79	.10	803	17	929	16	934	11	848	11
					1.51	.09	2.01	.04	814	19	882	12	911	4	851	5
15/10/80	9781	527-08	C994	1524	1.39	.11	1.13	.06	857	19	1012	10	962	7	907	9
					1.47	.09	1.70	.10	881	20	942	18	918	9	875	6
					1.40	.07	1.97	.05	821	13	905	12	862	8	897	9
17/10/80	9786	528-01	P389	1422	1.38	.05	1.12	.06	839	14	967	9	827	9	961	14
	9787	528-01	P389	1372	1.49	.04	1.21	.06	824	9	929	5	906	4	969	2
	9788	528-01	P389	1372	1.37	.06	1.11	.06	839	5	964	12	993	4	944	3

TABLE A.II Results of In Plant Measurement - Zone 4

Date	Cast	Steel Grade	Mould Powder	Slab Width (mm)	Casting Speed (m/min)		Average Water Flux (ℓ/m^2s)		Temperature, °C							
									Seg. 4/5		Seg. 5/6		Seg. 6/7		End Seg. 7	
					Mean	Std. Dev.	Mean	±	Mean	Std. Dev.	Mean	Std. Dev.	Mean	Std. Dev.	Mean	Std. Dev.
23/10/80	9810	527-08	C994	1422	1.52	.05	1.33	.08	882	13	877	10	903	11	905	7
					1.52	.06	1.52	.08	785	13	776	6	826	9	778	10
					1.73	-	1.52	.08	812	13	789	6	868	10	795	9
5/11/80	9851	527-08	C994	1422	1.42	.09	1.27	.08	857	14	976	9	-	-	898	7
					1.33	.08	1.52	.08	903	11	929	10	-	-	748	16
					1.46	.10	1.52	.08	868	11	941	8	-	-	866	12
	9856	516-07	P389	1270	1.52	.00	1.00	.08	942	5	940	3	-	-	942	2
	9857	527-08	C994	1372	1.60	.08	1.38	.08	898	11	852	9	-	-	951	10
					1.56	.09	1.52	.08	923	3	906	4	-	-	877	5
6/11/80	9858	527-08	C994	1422	1.52	.04	1.33	.08	896	7	912	6	-	-	896	5
					1.54	.04	1.52	.08	912	4	904	3	-	-	873	6
	9859	527-08	C994	1422	1.42	.10	1.27	.08	860	10	862	7	-	-	835	7
					1.49	.10	1.52	.08	842	3	819	9	-	-	751	9
	9860	528-01	P389	1168	1.45	.03	0.96	.08	945	4	871	2	-	-	937	4
	9861	528-01	P389	1118	1.40	.04	0.93	.08	958	2	899	2	-	-	955	2
7/11/80	9862	527-08	C994	1422	1.48	.12	0.98	.08	897	8	887	7	-	-	907	4
					1.35	.10	1.23	.08	922	8	873	8	-	-	900	8
					1.57	.04	1.52	.08	928	4	868	2	-	-	894	3
	9863	823-01	P389	1499	1.38	.08	0.91	.08	927	6	887	3	-	-	957	4
17/11/80	9901	527-08	C994	1321	1.44	.12	0.95	.08	814	6	890	16	-	-	914	15
	9902	527-08	C994	1473	1.60	.07	1.05	.08	849	11	875	11	-	-	851	14
					1.48	.13	1.30	.08	872	11	865	11	-	-	796	17
					1.73	.06	1.52	.08	861	6	871	8	-	-	788	11
	9903	527-08	C994	1676	1.22	.08	1.15	.08	844	6	859	11	-	-	900	4
					1.63	.06	1.52	.08	872	8	797	4	-	-	763	10
19/11/80	9906	527-08	P327	1753	1.56	.06	1.35	.08	888	8	842	4	-	-	811	8
					1.59	.08	1.52	.08	877	5	809	5	-	-	783	9
					1.60	.06	1.52	.08	905	4	845	3	-	-	805	5
(19/11/80)	9907	527-08	C994	1626	1.38	.08	1.24	.08	850	6	867	11	-	-	862	9
					1.30	.11	1.46	.08	831	5	796	9	-	-	786	14
					1.65	.08	1.52	.08	890	5	874	7	-	-	819	9
21/11/80	9910	527-01	C994	1270	1.46	.07	0.97	.08	1018*	4	936	13	-	-	895	10
					1.43	.11	1.27	.08	1022*	4	977	7	-	-	858	10
					1.49	.05	1.52	.08	1016*	2	946	4	-	-	819	2
	9911	527-08	C994	1270	1.52	.06	1.00	.08	755	7	786	10	-	-	802	7
					1.52	.06	1.33	.08	846	5	745	0	-	-	734	10
					1.47	.06	1.52	.08	912	5	750	6	-	-	736	6

*Spray Connection Hose to Segment 4 was broken.

TABLE A.III Results of In Plant Measurements - Zone 2

Date	Cast	Steel Grade	Mould Powder	Slab Width (mm)	Casting Speed (m/min)		Average Water Flux (ℓ/m^2s)		Temperature, °C							
									Rolls 2/3		Rolls 4/5		Rolls 6/7		Rolls 10/11	
					Mean	Std. Dev.	Mean	±	Mean	Std. Dev.	Mean	Std. Dev.	Mean	Std. Dev	Mean	Std. Dev.
4/12/80	9950	528-01	P389	1422	1.32	.09	4.13	.13	766	22	723	8	821	7	991	8
	9951	528-01	P389	1372	1.33	.11	4.16	.13	741	12	725	7	790	8	1020	11
		527-08	C994		1.57	.07	4.62	.17	844	15	731	15	747	11	863	21
5/12/80	9954	823-01	P389	1499	1.55	.08	4.58	.16	821	22	742	13	865	9	1011	8
8/12/80	9966	527-08	P327	1753	1.46	.08	4.41	.15	710	13	739	14	-	-	-	-
					1.53	.07	5.09	.10	758	12	752	25	-	-	837	7
					1.40	.11	3.70	.16	737	10	763	10	-	-	-	-
	9967	527-01	C994	1219	1.66	.06	3.27	.39	848	14	877	18	922	14	840	6
					1.47	.09	3.79	.16	793	12	804	14	792	26	773	9
					1.53	.11	4.55	.16	761	8	761	8	775	23	756	6
9/12/80	9969	527-08	C994	1727	1.40	.06	4.28	.14	786	12	768	9	847	7	794	5
					1.46	.07	4.92	.11	761	7	720	10	-	-	-	-
	9970	527-08	P327	1702	1.34	.06	3.63	.16	798	4	807	9	791	13	752	9
					1.47	.06	4.42	.15	787	11	773	8	849	8	816	6
					1.48	.09	4.97	.11	731	15	702	18	731	4	711	7
	9971	527-08	C994	1575	1.51	.07	3.84	.16	780	14	806	10	798	13	778	4
					1.43	.08	4.35	.15	788	8	795	15	807	13	768	6
					1.46	.07	4.92	.11	737	12	710	14	743	5	748	6
10/12/80	9972	527-08	C994	1524	1.47	.05	3.08	.29	782	7	873	9	845	14	826	10
					1.49	.09	3.80	.16	772	12	842	16	780	18	781	13
					1.50	.09	4.49	.16	744	15	788	15	768	7	763	6
	9973	527-08	C994	1702	1.33	.06	3.62	.16	768	8	770	3	789	12	740	7
					1.53	.06	4.55	.16	765	13	765	10	773	6	722	7
					1.52	.06	5.05	.10	788	11	715	10	750	6	670	10
11/12/80	9974	527-08	C994	1727	1.45	.06	3.06	.27	865	17	894	15	858	15	778	11
					1.40	.08	3.70	.16	854	14	877	17	869	8	782	8
					1.48	.07	4.45	.15	766	12	718	9	754	6	701	7
11/12/80	9976	527-08	P327	1778	1.52	.00	4.53	.16	790	11	762	12	750	11	-	-
					1.57	.00	5.18	.11	835	10	742	18	749	11	-	-
	9977	527-08	P327	1524	1.70	.10	3.94	.16	787	12	865	22	798	23	873	12
					1.60	.07	4.68	.17	793	7	839	19	776	20	846	13
					1.53	.07	5.09	.10	756	12	768	23	753	9	842	17
12/12/80	9978	527-08	P327	1524	1.45	.09	3.06	.27	776	9	860	25	847	12	914	9
					1.51	.07	3.84	.16	755	11	817	26	809	17	886	13
					1.54	.07	4.66	.16	767	7	818	27	780	16	807	22
	9980	527-08	C994	1422	1.44	.07	3.76	.16	849	12	990	9	938	13	995	1
					1.49	.06	4.47	.16	789	8	886	14	853	8	939	7
					1.48	.05	4.97	.11	763	17	809	13	857	14	926	8
	9982	527-08	C994	1372	1.47	.08	3.08	.29	827	17	957	15	906	10	1022	6
					1.57	.07	3.91	.16	750	7	838	13	826	18	933	9
					1.54	.05	4.57	.16	770	10	849	35	789	22	916	9

TABLE A.IV Results of In Plant Measurements - Zone 5

Date	Cast	Steel Grade	Mould Powder	Slab Width (mm)	Casting Speek (m/min)		Average Water Flux (ℓ/m²s)		Temperature, °C							
									Rolls 43/44		Rolls 63/64		Rolls 68/69 Rolls 71/72*		Rolls 78/79	
					Mean	Std. Dev.	Mean	±	Mean	Std. Dev.	Mean	Std. Dev.	Mean	Std. Dev.	Mean	Std. Dev.
9/3/81	0288	527-08	C994	1753	1.45	.08	0.87	.06	862	8	844	6	853*	11	865	5
					1.44	.07	0.95	.05	807	16	835	9	838*	9	-	-
12/3/81	0299	527-08	C994	1727	1.55	.09	0.95	.06	811	7	771	1	854*	2	911	4
					1.52	.06	0.95	.05	764	8	762	3	807*	5	890	5
17/3/81	0314	527-08	C994	1321	1.53	.08	0.95	.06	696	3	761	2	865*	5	816	4
					1.57	.06	0.95	.05	687	2	760	1	797*	27	806	4
	0317	528-01	P389	1219	1.30	.08	0.45	.07	779	6	787	3	835*	14	831	7
					1.45	.05	0.57	.07	779	11	807	6	845*	3	860	7
9/4/81	0401	516-07	P389	1270	1.30	.03	0.27	.04	843	8	865	9	-	-	-	-
10/4/81	0403	527-08	C994	1270	1.60	.10	0.58	.04	807	9	836	4	-	-	-	-
					1.46	.06	0.58	.03	797	7	818	7	-	-	-	-
	0404	527-08	C994	1270	1.51	.08	0.57	.04	789	7	857	4	-	-	-	-
					1.34	.11	0.56	.03	783	10	825	4	-	-	-	-
	0406	521-02	C994	1524	1.57	.08	0.47	.04	754	7	841	3	-	-	-	-
					1.37	.13	0.48	.04	765	14	838	5	-	-	-	-
					1.61	.08	0.58	.03	775	9	836	4	-	-	-	-
13/4/81	0417	521-08	P327	1575	1.45	.05	0.53	.04	768	5	815	3	803	5	-	-
					1.49	.05	0.58	.03	768	4	798	5	771	9	-	-
21/4/81	0449	521-02	P327	1473	1.61	.06	0.58	.04	853	3	819	11	757	5	-	-
					1.45	.06	0.58	.03	808	5	796	3	768	8	-	-
	0451	527-08	P327	1422	1.61	.07	0.58	.04	870	3	810	4	783	8	-	-
					1.60	.05	0.58	.03	813	6	812	4	761	2	-	-
	0452	823-01	P389	1524	1.40	.06	0.27	.04	950	5	807	5	738	4	786	2
					1.44	.05	0.53	.04	769	5	797	4	768	6	736	7
	0453	521-08	P327	1575	1.42	.08	0.58	.03	726	7	787	4	738	2	723	5

Note - The end of Zone was extended from position 61/62 to 71/72 as of 5/4/81.

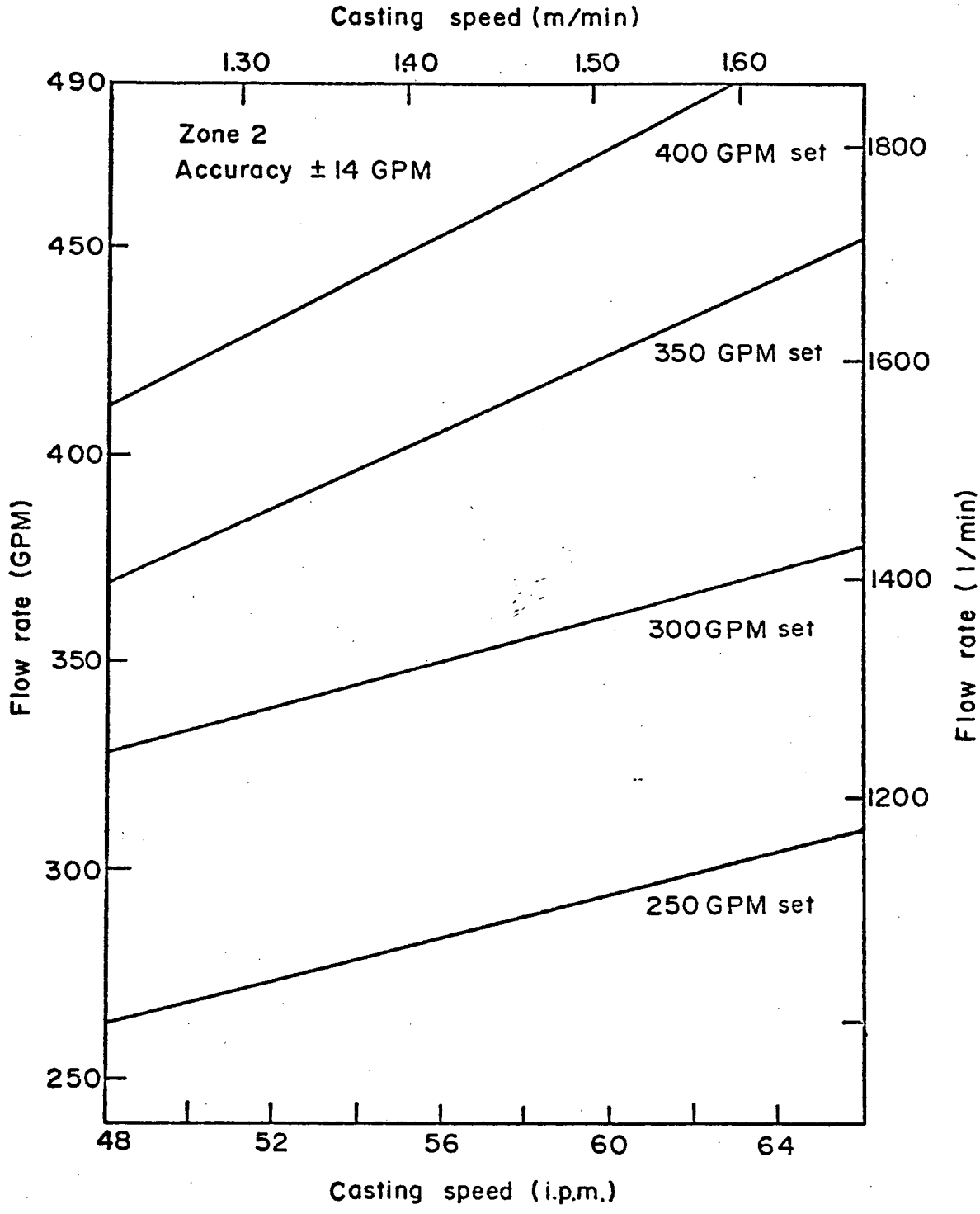

Figure A.1 Water flowrate - casting speed relationships, Zone 2.

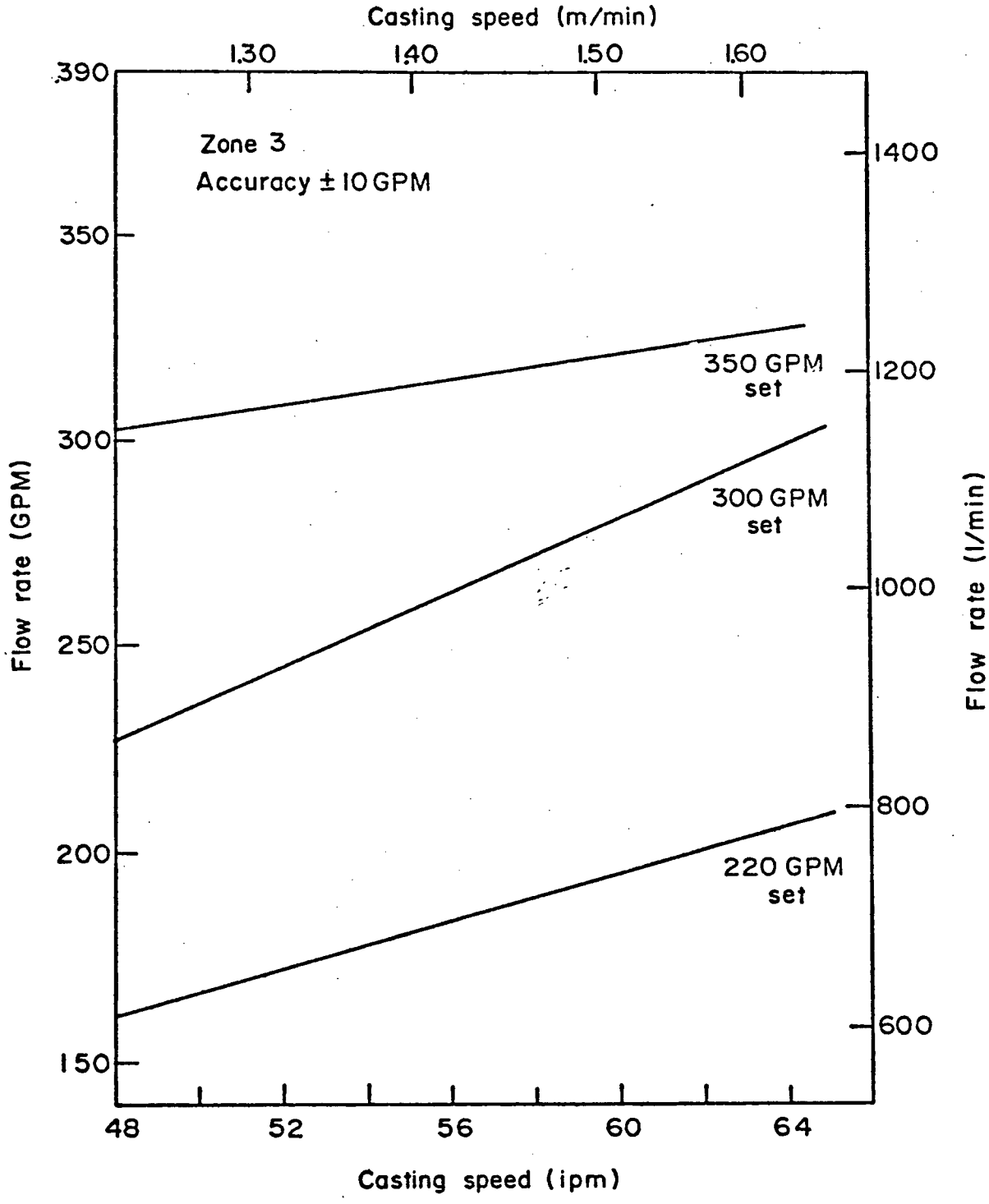

Figure A.2 Water flowrate - casting speed relationships, Zone 3.

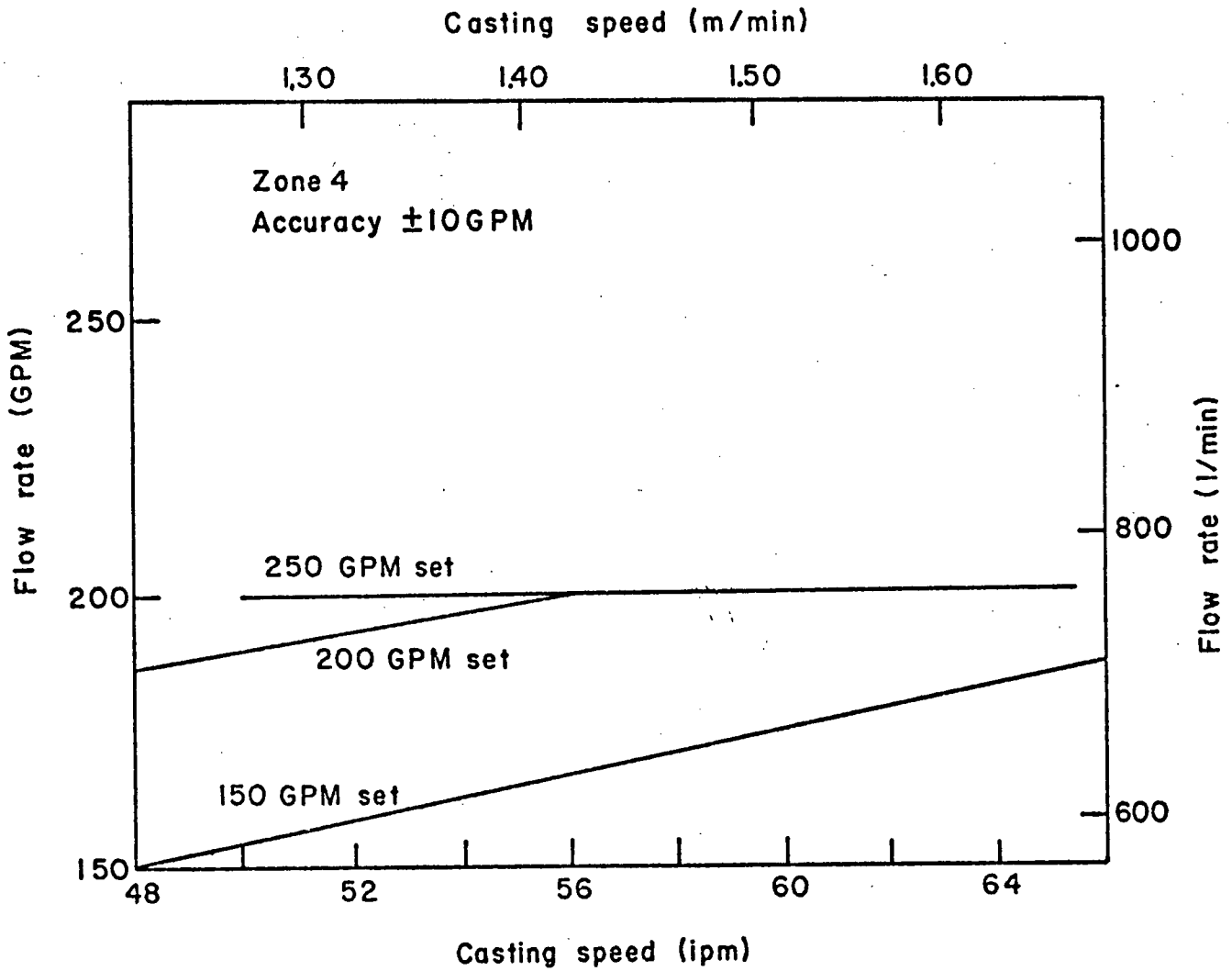

Figure A.3 Water flowrate - casting speed relationships, Zone 4.

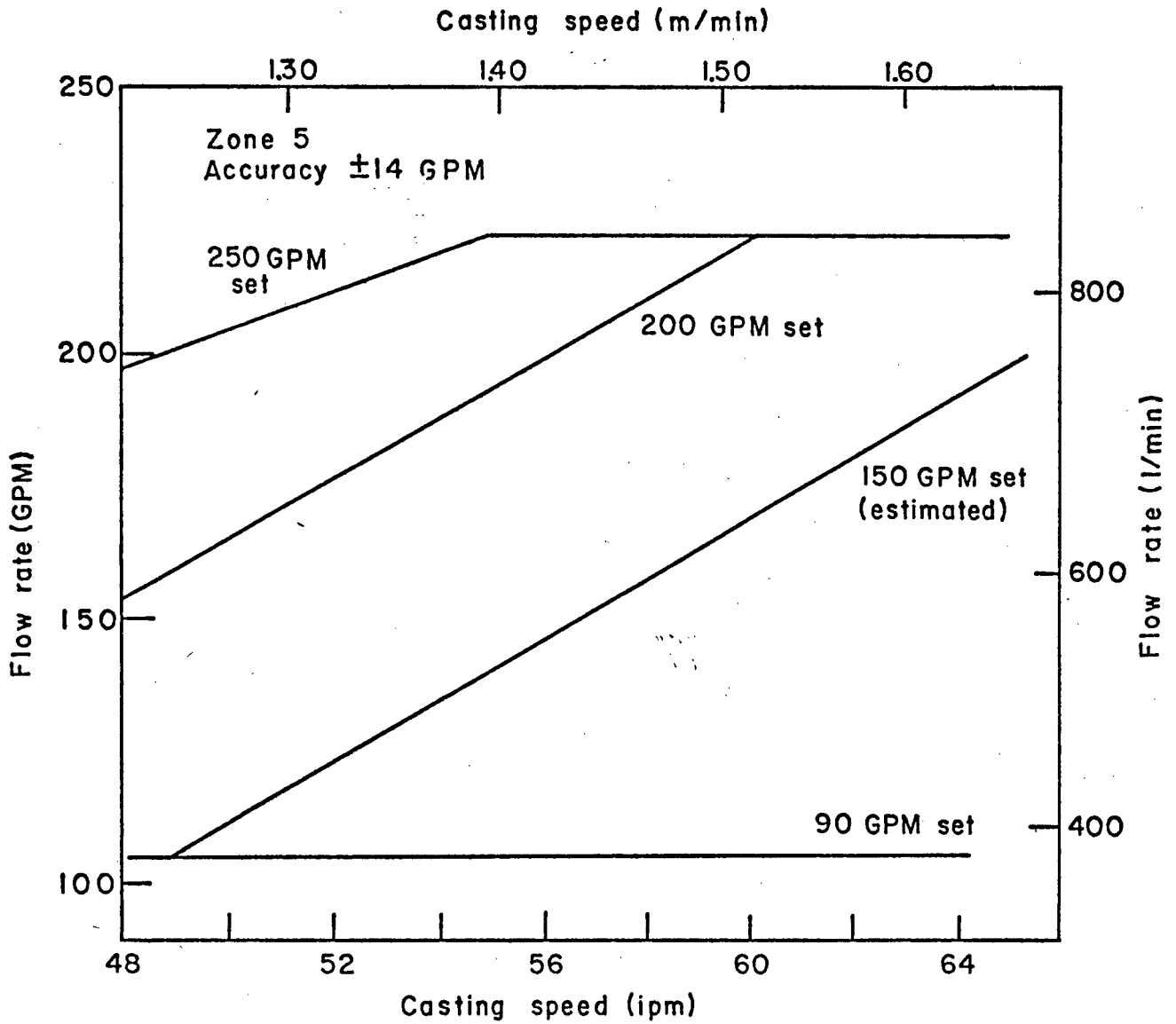

Figure A.4 Water flowrate - casting speed relationships, Zone 5.

Appendix B

RESULTS OF THE DESCALER TESTS

A series of tests was performed at the Inland Steel No. 1 Slab Caster to determine the effect of scale on slab surface-temperature measurements.[76] Data was obtained using the DESCATHERM (Trademark of C.R.M.) and was analyzed statistically to determine whether there was an actual difference between the temperature readings with the descaler on and those with the descaler off.

A summary of the data is presented in Table B.I. The data was collected with the descaler installed on the inner radius of Segment 2 on Strand 2.

The data shows, for each of 60 separate observations: the steel grade that was being cast, whether the descaler was on or off, the mean casting speed, the mean slab surface temperature, and the range of measured temperature. For the range of casting speeds used, it was found that the temperatures are not dependent on the casting speed. Thus the temperatures could be compared even though the casting speeds were not exactly the same.

For grade 527-08, a t-test was used to compare the mean temperature observed with the descaler on and that with the descaler off. It was found that there is no statistically significant difference between the mean temperatures with the descaler on or off. The difference (4.2°C for this grade) was found to be significant at only the 30 per cent confidence level.

TABLE B.I Temperatures Measured During In-Plant Descaler Tests

Steel Grade	Descaler	Casting Speed (in/min)	Temperature (°C)	Range (°C)
527-08	Off	48	970	20
		50	960	40
		50	1020	40
		50	1020	40
		52	980	20
		52	1010	20
		52	1040	20
		54	960	20
		56	960	20
		56	970	20
		56	980	20
		56	990	40
		56	1000	20
		56	1040	20
		58	970	20
		58	1030	20
		64	1030	20
	On	52	1030	20
		54	990	40
		56	970	40
		56	1030	20
		58	970	20
		58	980	20
		58	990	20
		58	990	40
		58	1040	10
		60	1000	40
		60	1020	20
		62	990	20
521-02	Off	52	990	20
		52	990	40
		54	960	20
		54	980	20
		56	960	40
		56	980	20
		56	990	20
		56	990	20
		56	1010	20
	On	52	970	20
		52	1000	20
		54	1000	20
		56	990	40
		60	970	40
		60	1030	20
726-08	Off	56	1020	40
	On	54	1000	40
524-02	Off	64	1020	40
	On	64	1030	40
528-71	Off	58	1030	20
	On	56	1030	20
		58	1020	20
		58	1020	20
		58	1040	20
527-71	Off	54	1040	20
	On	62	1050	20
521-71	Off	56	960	20
		56	970	20
		62	970	40
	On	52	980	20
		56	970	40

A similar analysis was done for grade 521-02. The t-test once again showed there is no statistically significant difference between the mean temperature with the descaler on or off. The difference (10°C for this grade) was found to be significant at only the 67% confidence level.

Overall, it can be concluded for the steel grades and operating conditions used during the test, no statistically significant difference was found in the temperatures measured with the descaler on or off when the DESCATHERM (Trademark of C.R.M.) was installed on the inner radius of Segment 2 on Strand 2 of the No. 1 Slab Caster.